

# **Electrical Wavelength Tuning in Single and Multi-wavelength, Mode-locked Semiconductor Fiber Ring Lasers**

Hong Cao

Department of Electrical and Computer Engineering  
McGill University  
Montréal, Québec, Canada  
December 2004

A thesis submitted to the McGill University in partial fulfillment of the requirements of the degree of Master of Engineering

© Hong Cao, 2004



Library and  
Archives Canada

Bibliothèque et  
Archives Canada

Published Heritage  
Branch

Direction du  
Patrimoine de l'édition

395 Wellington Street  
Ottawa ON K1A 0N4  
Canada

395, rue Wellington  
Ottawa ON K1A 0N4  
Canada

*Your file* *Votre référence*

*ISBN: 0-494-12589-6*

*Our file* *Notre référence*

*ISBN: 0-494-12589-6*

#### NOTICE:

The author has granted a non-exclusive license allowing Library and Archives Canada to reproduce, publish, archive, preserve, conserve, communicate to the public by telecommunication or on the Internet, loan, distribute and sell theses worldwide, for commercial or non-commercial purposes, in microform, paper, electronic and/or any other formats.

The author retains copyright ownership and moral rights in this thesis. Neither the thesis nor substantial extracts from it may be printed or otherwise reproduced without the author's permission.

#### AVIS:

L'auteur a accordé une licence non exclusive permettant à la Bibliothèque et Archives Canada de reproduire, publier, archiver, sauvegarder, conserver, transmettre au public par télécommunication ou par l'Internet, prêter, distribuer et vendre des thèses partout dans le monde, à des fins commerciales ou autres, sur support microforme, papier, électronique et/ou autres formats.

L'auteur conserve la propriété du droit d'auteur et des droits moraux qui protègent cette thèse. Ni la thèse ni des extraits substantiels de celle-ci ne doivent être imprimés ou autrement reproduits sans son autorisation.

---

In compliance with the Canadian Privacy Act some supporting forms may have been removed from this thesis.

Conformément à la loi canadienne sur la protection de la vie privée, quelques formulaires secondaires ont été enlevés de cette thèse.

While these forms may be included in the document page count, their removal does not represent any loss of content from the thesis.

Bien que ces formulaires aient inclus dans la pagination, il n'y aura aucun contenu manquant.

  
**Canada**

# Abstract

The explosive growth in the information technology industry requires high-performance optical sources. In recent years, wavelength-tunable optical pulse sources are of interest for applications in optical instrumentation, communications, and sensing. This thesis demonstrates and analyzes the generation of wavelength tunable, picosecond pulses from mode-locked semiconductor fiber ring lasers. One structure using an intracavity electro-optic modulator and the other an injected optical control signal, are investigated and experimentally characterized. A single or superimposed linearly chirped fiber Bragg gratings are used to provide wavelength selectivity, tunability, and multi-wavelength operation. The semiconductor optical amplifier as the gain media makes it possible to obtain stable simultaneous oscillation of several wavelengths at any wavelength band with very small channel spacing. We have successfully generated picosecond pulses at one or two wavelengths over the reflection bandwidth(s) of the grating(s) by simply changing the modulation frequency.

## Résumé

La croissance rapide de la photonique nécessite des sources optiques de plus en plus perfectionnées. Des lasers pulsés accordables trouvent maintenant une application dans les domaines de l'optique instrumentale, des communications, et de la détection. Nous avons créé, analysé et caractérisé expérimentalement des lasers en anneau accordables produisant des impulsions picosecondes et multifréquences. Une cavité utilisait un modulateur électro-optique pour produire la synchronisation modale et l'autre utilisait un signal optique de contrôle injecté dans la cavité. Un réseau ou une combinaison de réseaux de Bragg glissés linéairement en fréquence furent utilisés pour obtenir l'accordabilité et l'effet laser multifréquence. Le milieu de gain utilisé, soit un amplificateur optique à semi-conducteur, permet d'obtenir un effet laser multifréquences stable avec une faible séparation entre les canaux. Des impulsions picosecondes à une et deux longueurs d'onde furent générées à l'aide d'un réseau de Bragg en réflexion simplement en changeant la fréquence de modulation.

# Acknowledgements

I would like to thank to my supervisor Prof. Lawrence R. Chen for his superb guidance, support and constant encouragement throughout my thesis writing and the whole research work. I deeply appreciated his instructive teaching from theories to experiments and beyond.

I would like to thank all members in Photonic Systems Group at McGill University for their support in the last two years. Special thanks to Aref Bakhtazad for his helpful discussion on setup design and troubleshooting, and Dominik Pudo for his help on lab equipments and experiments. I would like to thank fellow students, Roberto Rotili, Nicolas Bélanger and Bing Xia for their wisdom, patience and teamwork. I would like to give a special word of thanks to Chris Rolston, who tirelessly made sure that our working conditions were second-to-none.

I would also like to thank S. LaRochelle (Université Laval) for providing the superimposed grating.

Finally, I thank my family, for their unconditional love and encouragement.

This research was supported by the Canadian Institute for Photonic Innovations.

# Table of Contents

<b>1. Introduction</b> .....	1
1.1 Motivation.....	1
1.2 Thesis objectives and outline.....	3
References.....	5
<b>2. Overview of fiber ring lasers</b> .....	6
2.1 Introduction to fiber lasers.....	6
2.1.1 Fiber laser basics.....	6
2.1.2 Fiber ring lasers.....	7
2.2 CW vs. pulsed lasers.....	8
2.2.1 Introduction.....	8
2.2.2 Mode-locking in fiber lasers.....	9
2.2.3 Mode-locking techniques.....	12
2.3 SOA vs. EDFA based fiber ring lasers.....	14
2.3.1 Semiconductor and optical fiber amplifiers.....	14
2.3.2 SOA vs. EDFA based fiber ring lasers.....	16
References.....	18
<b>3. Semiconductor fiber ring lasers</b> .....	21
3.1 Semiconductor optical amplifiers basics.....	21
3.1.1 SOAs basic description.....	21
3.1.2 Fundamental device characteristics.....	22
3.2 Survey of different semiconductor fiber ring lasers.....	27
3.2.1 Intracavity mode-locked fiber ring laser configurations.....	28
3.2.2 All-optical mode-locked fiber ring laser configurations.....	35

3.3 Summary.....	46
References.....	47
<b>4. Electrically tunable single wavelength semiconductor fiber ring lasers.....</b>	<b>49</b>
4.1 Brief description of dispersion tuning.....	50
4.2 Mode-locking using an intracavity modulator.....	51
4.2.1 Operation description.....	51
4.2.2 Experiments and results.....	54
4.3 All-optical mode-locking.....	59
4.3.1 Design concept.....	59
4.3.2 Operation description.....	60
4.3.3 Experiments and results.....	61
4.4 Discussion and summary.....	65
References.....	66
<b>5. Electrically tunable multi-wavelength semiconductor fiber ring lasers.....</b>	<b>68</b>
5.1 Brief description of multi-wavelength dispersion tuning.....	68
5.2 Mode-locking using an intracavity modulator.....	69
5.2.1 Operation description.....	69
5.2.2 Experiments and results.....	71
5.3 All-optical mode-locking.....	74
5.3.1 Operation description.....	74
5.3.2 Experiments and results.....	74
5.4 Discussion and summary.....	78
References.....	79
<b>6. Conclusion and future work.....</b>	<b>80</b>
<b>Appendix A.....</b>	<b>83</b>

References.....	90
<b>Appendix B.....</b>	<b>92</b>

# List of Figures

Fig. 2.1 Fiber ring laser scheme.....	8
Fig. 2.2 Longitudinal modes in laser operation. (a) Overall bandwidth of the laser output $\Delta\nu$ . (b) Fine structure of the components showing the different modes. [2.1].....	10
Fig. 2.3 Mode locking to obtain giant pluses of short duration. (a) Frequency distribution of the intensity of a complex of $M$ waves of equal intensity and phase. (b) Time dependence of the complex waves in mode-locking condition. [2.1].....	12
Fig. 3.1 Schematic diagram of an SOA. [3.1].....	21
Fig. 3.2 Principle of operation of the TW-SOA. [3.1].....	22
Fig. 3.3 Typical TW-SOA gain spectrum. [3.1].....	24
Fig. 3.4 Typical SOA gain versus output signal power characteristic. [3.1].....	26
Fig. 3.5 General structure of fiber ring laser [3.10].....	28
Fig. 3.6 Schematic diagram of laser configuration. [3.13].....	29
Fig. 3.7 Optical spectrum of output pulses. [3.13].....	30
Fig. 3.8 Optical waveform of output pulses. [3.13].....	30
Fig. 3.9 Experimental setup for multiwavelength pulse train generation. [3.14].....	31
Fig. 3.10 Output spectrum and simultaneous pulse train for 3 channels at 10 GHz. [3.14].....	32
Fig. 3.11 Experimental setup. [3.15].....	32
Fig. 3.12 Spectrum of multi-wavelength laser in mode-locked operation at 10 GHz. [3.15].....	34
Fig. 3.13 Pulse width and output power against wavelength. [3.15].....	34
Fig. 3.14 The experimental setup. [3.4].....	35

Fig.3.15 Simultaneous pulse train for four wavelengths. [3.4].....	37
Fig. 3.16 (a) Variation of the pulsewidth and pulsewidth–bandwidth product versus wavelength. (b) Variation of the output power versus wavelength. [3.4].....	38
Fig. 3.17 The experimental setup. [3.5].....	39
Fig.3.18 Pulse shape of the mode-locked output pulses at about 5 GHz. [3.5].....	40
Fig. 3.19 Spectrum of the mode-locked output pulses at about 5 GHz. [3.5].....	40
Fig. 3.20 The experimental setup of the fiber ring laser. [3.6].....	41
Fig. 3.21 The wavelength switching characteristics of the laser. [3.6].....	43
Fig. 3.22 Experimental setup of the SOA-based fiber ring laser. [3.8].....	45
Fig. 3.23 Operation principle of the pulse source (i) multiwavelength pulses generated from the SOA; (ii) pulse P1 after the DCF; (iii) pulse P2 after the DCF; (iv) subharmonic driving signal of EOM 2; (v) subharmonic gated optical pulse; (vi) optical pulse obtained after SMF. [3.8].....	46
Fig. 4.1 Experimental setup. [4.10].....	51
Fig. 4.2 Schematic of the mode-locked semiconductor fiber ring laser with intracavity modulator. OC: optical circulator, MOD: electro-optic modulator, PC: polarization controller.....	52
Fig. 4.3 The characteristics of the single LCFBG (a) reflectivity, (b) group delay.....	53
Fig. 4.4 The Avanex A1901 SOA module [4.16].....	53
Fig. 4.5 Output spectral (a) and temporal (b) characteristics under different SOA bias currents.....	55
Fig. 4.6 Output pulse characteristics under different SOA bias currents: (a) 3 dB bandwidth; (b) pulse width; (c) time-bandwidth product; (d) average output power.....	55

Fig. 4.7 Tuning characteristics of the SFRL using the single LCFBG.....	56
Fig. 4.8 Output spectral and temporal characteristics of the SFRL using the single LCFBG for $f_{mod}$ = (a) 5250.894 MHz, (b) 5251.864 MHz, and (c) 5253.764 MHz.....	57
Fig. 4.9 Output pulse characteristics of the SFRL: (a) 3 dB bandwidth, (b) pulse width, (c) time-bandwidth product.....	58
Fig. 4.10 Schematic of all-optically mode-locked semiconductor fiber ring laser. TLS: tunable laser source, BPF: bandpass filter, EOM: electro-optic modulator, PC: polarization controller.....	60
Fig. 4.11 Output pulse characteristics as a function of (a) SOA bias current (with $P_{avg}^{control}$ = 2.9 mw) and (b) control signal average power (with $I_{SOA}$ = 135 mA). In all cases, the control signal wavelength is 1555 nm.....	62
Fig. 4.12 Output spectral characteristics using different control signal wavelengths.....	62
Fig. 4.13 (a) Tuning and (b) output pulse characteristics of the ML-SFRL using the single LCFBG.....	63
Fig. 4.14 Spectral and temporal characteristics of the output pulses for $f_{mod}$ = (a) 5254.842 MHz, (b) 5256.641 MHz, and (c) 5259.335 MHz. Inset: typical auto-correlation trace with $\text{sech}^2$ fit.....	64
Fig. 4.15 Output spectral change under with and without the control signal.....	64
Fig. 5.1 Schematic of the SFRL using SI-LCFBGs.....	69
Fig. 5.2 SI-LCFBGs characteristics.....	70
Fig. 5.3 Tuning characteristics of the laser.....	71

Fig.5.4 Spectral and temporal characteristics of the laser for $f_{mod} =$ (a) 5403.375 MHz, (b) 5404.217 MHz, and (c) 5406.270 MHz. The inset shows the output pulses at each lasing wavelength obtained using a bandpass filter external to the laser.....	72
Fig. 5.5 Output pulse characteristics of the laser: (a) 3 dB bandwidth, (b) pulse width, (c) time-bandwidth product.....	73
Fig. 5.6 Output spectral characteristics under (a) different bias currents, (b) different control signal powers, and (c) different control signal wavelengths.....	75
Fig. 5.7 (a) Tuning and (b) output pulse characteristics of the mode-locked SFRL using SI-LCFBGs.....	76
Fig. 5.8 Typical spectral and temporal characteristics of laser output with dual-wavelength operation for $f_{mod} =$ (a) 5257.426 MHz, (b) 5260.166 MHz, and (c) 5263.939 MHz. The insets show the output pulses at each lasing wavelength obtained using a bandpass filter external to the laser and the output waveform after propagation through 7.44 km of SMF.....	77
Fig. 5.9 Output spectral change under with and without the control signal.....	78
Fig. A.1 Schematic representation and principle of operation of a fiber Bragg grating. [A.1].....	83
Fig. A.2 Diffraction of a light wave by a grating. [A.7].....	84
Fig. A.3 Ray-optic illustration of core-mode Bragg reflection by a fiber Bragg grating. [A.7].....	85
Fig. A.4 A schematic diagram of a chirped grating with an aperiodic pitch. For forward-propagating light as shown, long wavelengths travel further into gratings before being reflected [A.9].....	85

Fig. A.5 (a) Typical transmission and reflection profiles of a chirped Bragg grating [A.12]; (b) Group delay for unapodized and apodized chirped grating [A.13].....87

Fig. A.6 Superimposed multiple Bragg gratings at the same location on photosensitive optical fiber. The plot on the lower shows reflectivities for each of the Bragg gratings, as a function of the number of gratings, superimposed on the same location [A.14].....89

## List of Tables

Table 2.1	Waveshape results of mode-locked lasers. [2.1].....	12
Table 2.2	The comparison between the main features of EDFAs and SOAs. [2.13].....	16
Table 3.1	Desired properties of a practical SOA. [3.1].....	22
Table 3.2	Comparison between different SFRL configurations.....	47
Table 4.1	Characteristics of the A1901 SOA module. [4.16].....	54

# Chapter 1

## Introduction

### 1.1 Motivation

The rapid growth in the information technology industry, like double-digit increases in wireless services, specialized services such as unified communications, video/audio conferencing, services in support of equipments, and high-speed Internet access, leads to continuously explosive growth in bandwidth demand and network traffic [1.1]. More and more data and various types of information need to be transferred over communication networks. It has been well recognized that the only way to adapt this growth in bandwidth demand is to use photonic networks. With the recent slowdown in the telecom industry revenue and equipment spending, it is more important for research to focus on developing technology and systems that will allow industry to offer reliable and cost effective optical solutions.

At present, in order to develop a more cost effective, adept photonic network that can meet developing market needs, many novel network end components, agile network switching and routing technologies are being developed by researchers worldwide. Among network end facilities, optical sources, which are responsible for generating stable and short pulses, receive a primary focus. Currently, the major problems in optical sources used in today's fiber optical networks are their cost and complexity [1.2]. Since semiconductor distributed feedback (DFB) lasers, which are now typically used as optical sources, are only single-wavelength sources, we have to implement one DFB laser per channel in WDM systems. This leads to a very bulky and complicated situation in

network development. The fast growth in the industry has intensified research efforts to demonstrate multi-wavelength and high-speed optical sources and to qualify them in optical transmission systems. The emphasis is on trying to find suitable high-bit-rate optical sources that are compact, multi-wavelength operational, and low in cost. In recent years, a large number of research focuses have been directed towards innovation in DFB laser arrays, vertical cavity surface emitting lasers (VCSELs), and mode-locked fiber lasers. As multi-wavelength light sources, they are all different and have their own advantages. The DFB laser arrays are compact and multi-wavelength operational, but wavelength stabilization is done on a per channel basis, which presents complicated setups in multiple channels systems [1.3]. VCSELs are good candidates as ideal optical sources, but there are still a significant amounts of effort required in their fabrication processes [1.4]. The other approach that has been intensively investigated is where the multi-wavelength signal is obtained directly from mode-locked lasers, like from erbium doped fiber lasers (EDFLs) [1.5] and semiconductor fiber lasers (SFLs) [1.6]-[1.8]. This approach preserves the advantage of relative wavelength stability between all oscillating modes with relatively simple configurations. With this technique, all the mode-locked wavelengths are simultaneously timed to the modulation signal in the laser and they are also synchronized with each other. In comparison with EDFLs, SFLs are not constrained by the homogeneous broadened gain medium nature of the EDF, which limits the spectral separation between the lasing wavelengths to be large enough to minimize gain competition. Since the semiconductor optical amplifier (SOA) is an inhomogeneously broadened gain element, it is possible to obtain stable simultaneous oscillation of several wavelengths with very small channel spacing at the room temperature. Moreover, the use

of SOAs allows for operation at any wavelength band; and as a result, we are not constrained to the C- and/or L-bands as with EDFLs. So, SFLs are very promising as multi-wavelength sources in optical networks. In addition to the above, their merit lies in their compactness, low cost, and compatibility with photonic integrated circuits [1.9].

As SFLs have so many advantages over EDFLs, academia and industry have joined to research and develop this kind of semiconductor optical sources. Besides the applications in telecommunications, like all-optical sources for next generation all-optical network and photonic devices testing and characterization, SOA-based optical sources can be widely applied in optical instrumentation, time-resolved spectroscopy, and optical sensors, etc.

## 1.2 Thesis objectives and outline

In this thesis, we focus on demonstrating novel designs of high performance optical sources that generate short (picosecond) pulses at multiple wavelengths with wavelength tunable capacity. We consider two types of mode-locked semiconductor fiber ring laser (SFRL) structures. The first involves an intracavity modulator, while the second comprises an all-optical control technique. In both cases, linearly chirped fiber Bragg gratings (LCFBGs) work as the key component to sustain operation. The significant contributions of the thesis include the following:

- the design and successful demonstration of electrically tunable, single and multi-wavelength actively mode-locked SFRLs with an intracavity electro-optic modulator,

- the first design and successful demonstration of a tunable, single wavelength all-optically mode-locked SFRL using an LCFBG, and
- the first design and successful demonstration of a tunable, multi-wavelength all-optically mode-locked SFRL using superimposed (SI)-LCFBGs.

The remainder of this thesis is organized as follows. In Chapter 2, we first introduce some basic properties of fiber lasers and details on mode-locking operation. We then describe and compare SFRLs and EDFLs. In Chapter 3, we discuss the basic properties of SOAs. Next, we provide an up-to-date survey on various mode-locked SFRLs. In Chapter 4, two approaches of tunable single wavelength mode-locked SFRLs, one using an intracavity modulator and the other an injected optical control signal, are proposed and experimentally characterized. We investigate the multi-wavelength operation of mode-locked SFRLs in Chapter 5. Finally, in Chapter 6, we summarize our results and discuss future work.

**References:**

- [1.1] Telecommunication Industry Association, 2004 Telecommunications Market Review and Forecast, 2004.
- [1.2] T. Ono and Y. Yano, "Key technologies for Terabit/second WDM systems with high spectral efficiency of over 1 bit/s/Hz," *IEEE J. Quantum Electron.*, 34, 11, pp.2080-2088, 1998
- [1.3] C.E. Zah, M.R. Amersfoort, B. Pathak, P.S. D. Lin, A. Rajhel, N.C. Andreadakis, R. Bhat, C. Caneau, and M.A. Koza, "Wavelength accuracy and output power of multiwavelength DFB laser arrays with integrated star couplers and optical amplifiers," *IEEE Photon. Technol. Lett.*, 8, 7, pp.864-866, 1996.
- [1.4] W. Yuen, G.S. Li, and C. J. Chang-Hasnian, "Multiple-wavelength vertical-cavity surface-emitting laser array," *IEEE J. Selected Topics in Quantum Electron.*, 3, 2, pp.422-428, April 1997.
- [1.5] G. E. Town, L. Chen, and P. W. E. Smith, "Dual wavelength modelocked fiber laser," *IEEE Photon. Technol. Lett.*, 12, pp. 1459-1461, 2000.
- [1.6] K. Vlachos, K. Zoiros, T. Houbavlis, and H. Avramopoulos, "10 × 30 GHz pulse train generation from semiconductor amplifier fiber ring laser," *IEEE Photon. Technol. Lett.*, 12, 1, pp. 25-27, 2000.
- [1.7] J. He and K. T. Chan, "All-optical actively modelocked fiber ring laser based on cross-gain modulation in SOA," *Electron. Lett.*, 38, 24, pp.1504-1505, 2002.
- [1.8] K. Vlachos, C. Bintjas, N. Pleros, and H. Avramopoulos, "Ultrafast semiconductor-based fiber laser source," *IEEE J. Sel. Topics in Quantum Electron.*, 10, 1, pp.147-154, 2004.
- [1.9] M. J. Connelly, Semiconductor optical amplifiers, Kluwer Academic, 2002.

## Chapter 2

### Overview of fiber ring lasers

#### 2.1 Introduction to fiber lasers

##### 2.1.1 Fiber laser basics [2.1]

In general, the fiber laser is a by-product of the fiber amplifier that is used to enhance signal transmission in fiber optical systems. When the right length of fiber is chosen in combination with a resonator, the fiber amplifier can oscillate at specific wavelengths. It is a basic fiber laser and represents an innovative use of optical fibers to produce light beams. The following components are required to build a basic fiber laser:

- (1) a resonant system that can feed back and regenerate the amplified signal to a level that can maintain lasing,
- (2) a pump source to start the laser both in frequency and in power level,
- (3) a coupling section to bring in the pump laser to excite the fiber,
- (4) a modulator to impress the modulation signal to the system if mode-locked operation is desired, and
- (5) a polarization controller if applicable.

Just following the discovery of the erbium doped fiber amplifier (EDFA) in the late 1980s, fiber lasers have been predominantly developed for telecom applications. Short optical pulses at repetition rates of up to 200 GHz have been demonstrated [2.2].

The following show the advantages of fiber lasers:

- (1) relative short length of gain fiber (normally less than 10 meters), then fiber loss is not a concern,

- (2) no special structural design considerations, like waveguiding property, carrier confinement, and mode selection mechanism,
- (3) no special coupling device is needed to couple the light into the fiber, and
- (4) relative low noise, as little extra noise is introduced.

In realizing the many advantages a fiber laser has over its counterparts, academia and industry have collaborated efforts to further increase their development. Significant work has been done to try to limit the environment sensitivity of fiber lasers and make them more stable and desirable for applications [2.3]-[2.7]. To date, besides the traditional applications in telecom industry, researchers recently have developed some new fiber lasers that can be applied in optical sensing, instrumentation, and biophotonics.

### **2.1.2 Fiber ring lasers**

Fig. 2.1 shows the schematic of the simple structure of a fiber ring laser. It consists of a finite length of gain fiber, an optical filter used to set the wavelength of operation, fiber-based wavelength selective couplers (to couple pump and lasing signals), an isolator to ensure unidirectional propagation in the laser cavity, a polarization controller, and if mode-locked, a modulator to serve as the mode-locking element. The laser output is taken from an output coupler. When the pump laser is activated, lasing at the wavelength set by the optical filter occurs when the threshold condition is satisfied. Since the length of the fiber used for the laser is determined by the doping concentration in the fiber core, the fiber length is designed so that the system gain is right enough to compensate the cavity loss. Otherwise, fibers longer than necessary will absorb the laser energy and then reduce the overall efficiency.

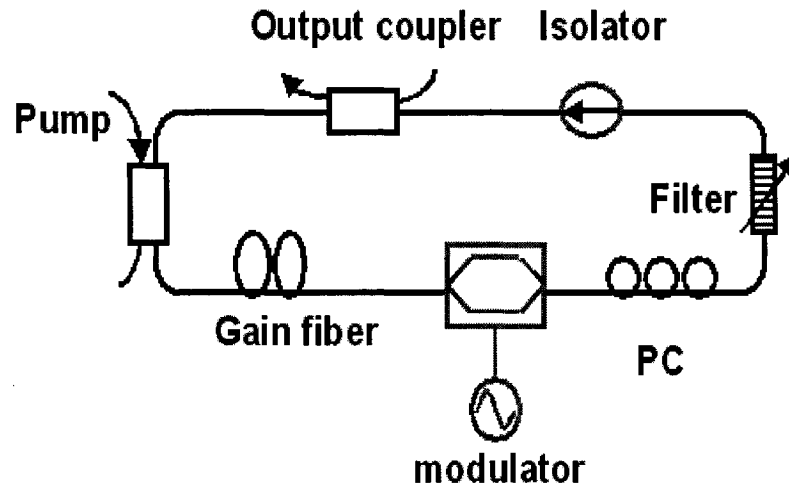


Fig. 2.1 Fiber ring laser scheme

## 2.2 CW vs. pulsed lasers

### 2.2.1 Introduction

When a person thinks of a laser beam, the general perception is of a continuous light beam that transmits over a long distance. This type of light beam occurs when a laser operates in cw (continuous wave) mode. By switching on and off rapidly, lasers can also operate in pulsed modes. In general, there are two reasons why one would wish to pulse a laser: one is high peak power and the other is that a pulsed laser can give information on a very rapidly occurring processes.

In comparison with cw lasers, pulsed operation of lasers is often desirable for signal transmission. There are number of ways to make a laser pulsed. The most direct method of obtaining a pulsed light beam from a laser is to use a cw laser in conjunction with an external switch or modulator that transmits the light only during selected short intervals. The method is very inefficient, and the peak power is limited to the steady power of the cw source. Moreover, by installing a modulator or by using a Q-switch (inserting a

saturable absorber) inside the laser cavity to turn off the laser output periodically, pulsed light can also be achieved too. Furthermore, the mode-locking method is the other method to be used in pulsed operation. Mode-locking can be achieved by locking the phases of each longitudinal mode of a multimode laser together, forcing the laser to form a periodic pulse train.

Among the different methods of pulse generation, mode-locking is perhaps the most complicated method of creating laser pulses. But it is also the most effective and useful one, as it seems to be the only method of generating ultrashort pulses at ultrahigh repetition rates.

Although with the advent of wavelength-division multiplexing (WDM) most of the available fiber capacity was released, the fast evolving ultra high-speed optical time-division multiplexing (OTDM) can offer distinct advantages over the current low-speed WDM channels of equivalent capacity. Furthermore, the two technologies can be combined in a hybrid OTDM/WDM manner with a fewer number of channels at significant higher data rates. Optical sources capable of generating ultrashort pulse trains at high repetition rates [2.8]–[2.10] are key elements for optical networks that combine WDM and OTDM transmission techniques [2.11].

### **2.2.2 Mode-locking in fiber lasers [2.1]**

As is known, a laser can lase on many longitudinal modes, with frequencies that are equally separated by the intermodal spacing frequency  $\nu_F = c/2d$  ( $c$  is the speed of light in the medium, and  $d$  is the cavity length, assuming a standing-wave configuration). If the bandwidth of the spectral distribution is  $B$ , then the number of possible lasing modes

is  $m = B/\nu_F$ , and optical power is divided among the different lasing modes. The distribution of the amplitudes of the modes is centered at a frequency  $\nu_0$  where the gain is the highest and decreases further away to both sides of this frequency; however, the number of modes that actually carry optical power is far less than the number of possible modes. Fig. 2.2 shows the frequency distribution of a multimode laser.

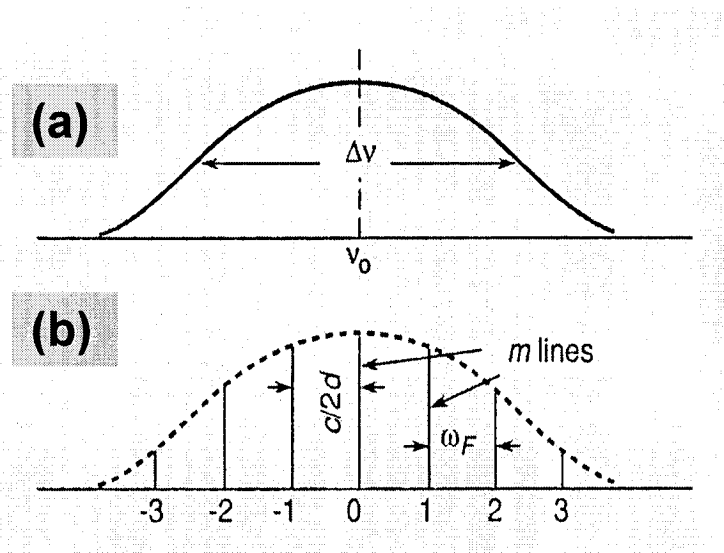


**Fig. 2.2** Longitudinal modes in laser operation. (a) Overall bandwidth of the laser output  $\Delta\nu$ . (b) Fine structure of the components showing the different modes. [2.1]

By introducing an intracavity element to provide sufficient loss to discourage lasing of the undesired modes, a multimode laser can operate on a single mode. Furthermore, to lock all the modes into one single mode, a multimode laser can work on a single mode without loss in the total optical power.

If multiple modes were locked, the waveform and wave amplitude would both change. Consider each laser mode to be represented by a uniform plane wave traveling in the  $z$  direction with speed  $c = c_0/n$ . The general electromagnetic field equation for the total complex wavefunction of the field as a sum of these individual waves is

$$U(z,t) = \sum_q A_q \exp\{i\omega_q(t - z/c)\} \quad (2.1)$$

where

$$\nu_q = \nu_0 + q\nu_F, \quad q = 0, \pm 1, \pm 2, \dots \quad (2.2)$$

and  $\nu_q$  is the frequency of mode  $q$ . Substituting (2.2) into (2.1) and assigning  $\nu_0$  as the center frequency of the laser lineshape at  $q=0$ , (2.1) can be rewritten as

$$U(z,t) = A(t - z/c) \exp\{i2\pi\nu_0(t - z/c)\} \quad (2.3)$$

where

$$A(t) = \sum_q A_q \exp(i2\pi qt/T_F) \quad (2.4)$$

$$T_F = 1/\nu_F = 2d/c \quad (2.5)$$

The complex envelope  $A(t)$  in (2.4) is a periodic function of period  $T_F$  and  $A(t - z/c)$  is a periodic function of  $z$  with period  $cT_F = 2d$ . Then the optical intensity can be expressed as

$$I(t,z) = A(t - z/c)^2 = m^2 A^2 \left\{ \sin^2(t - z/c)/T_F \right\} / \left\{ \sin^2[t - z/c]/T_F \right\} \quad (2.6)$$

where  $m$  is the number of modes and

$$\sin c(\pi x) = \sin(\pi x) / \pi x.$$

Fig. 2.3 (a) shows the frequency distribution of a complex wavefunction  $U_\nu$  that shows the intensity of a complex  $M$  of waves of equal phase. Fig. 2.3 (b) represents the time distribution of the intensity  $I$  when mode-locked.

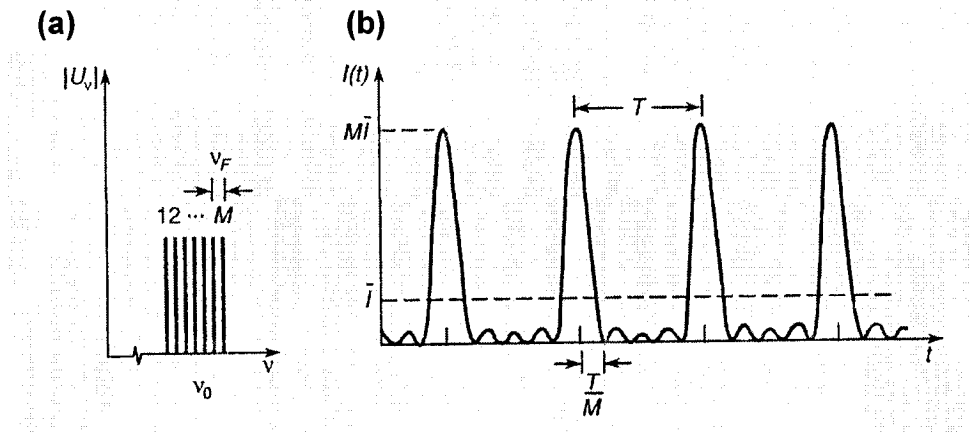


**Fig. 2.3** Mode locking to obtain giant pulses of short duration. (a) Frequency distribution of the intensity of a complex of  $M$  waves of equal intensity and phase. (b) Time dependence of the complex waves in mode-locking condition. [2.1]

The results on waveshape are summarized in the following Table 2.1:

Temporal period	$T_F = 2d / c$ , where $d$ is the cavity length
Pulse width	$\tau = T_F / m = 1 / m\nu_F$
Spatial period	$2d$
Pulse length	$d = c\tau = 2d / m$
Mean intensity	$I = mA^2$
Peak intensity	$I_p = m^2 A^2$

**Table 2.1** Waveshape results of mode-locked lasers. [2.1]

### 2.2.3 Mode-locking techniques

There are two traditional classifications of techniques used to mode-lock lasers: passive or active. The passive mode-locking devices are those that are able to start mode-locking without any time-varying manner. They are normally based on the optical effect in a material. In contrast, active mode-lockers involve the use of some externally modulated media or device. In this thesis, we focus on active mode-locking.

Active mode-locking is one of the key techniques for the generation of ultrashort optical pulses [2.12]. It is especially important when synchronization between optical and electrical signals is required.

Active mode-locking mechanisms are the result of using a time varying optical or electronic exploitation of a material's response. They use electro-optic or acousto-optic switches inside the laser cavity to modulate the phases into mode-locking position. When the switch is activated, it passes light only for the duration of the pulse. So only those modes that have equal phases can lase. Then once the lasing starts, they continue to be locked. Modes of equal phase are accumulated up and form a single giant pulse. Without the phase locking, the individual modes of different phases are dependent on the random conditions at the onset of their lasing and are partially or totally blocked, adding to the cavity loss.

There are three major active mode-locking techniques: AM modulation, FM modulation, and synchronous pumping.

AM modulation is the most commonly used active mode-locking mechanism. In a laser cavity with an AM modulator (like a fiber-based Mach-Zehnder interferometer) that has many random distributed pulses exiting, assuming AM modulator works as a fast shutter, pulses with the right timing will circulate in the laser cavity and all of other pulses will be absorbed by the AM modulator. In fact, the AM modulator works not only to form the pulses in the cavity, but also shapes them.

The difference between the FM modulation and AM modulation is that the FM modulators do not rely on any interference as AM modulators do. FM modulators use the same electro-optic materials as the AM modulator. As is known, by changing the

refractive index of the crystal in a time varying intervention, we can effectively change the cavity length. Thus FM modulation can be formulated by oscillating the position of one of the cavity's mirrors. The mirror is oscillating around a fixed point that it passes twice during a single oscillation period. As the mirror spends more time near each of its maxima, it will generate mode-locked pulses.

Synchronous pumping is another active mode-locking mechanism. It periodically modulates a laser's gain media at a repetition rate corresponding to a harmonic of the fundamental cavity frequency. Since the cavity's gain that is modulated as opposed to AM mode-locking which corresponds to the modulation of the cavity's loss, we can view this kind of mode-locking as a type of inverse AM modulation.

## **2.3 SOA vs. EDFA based fiber ring lasers**

### **2.3.1 Semiconductor and optical fiber amplifiers [2.13]**

The first studies on semiconductor optical amplifiers (SOAs) started at around the time of the advent of the semiconductor laser in the 1960's. These early devices were based on GaAs homojunctions and operated at low temperatures. After the arrival of double heterostructure devices, the use of SOAs in optical communication systems was further investigated in the 1970's. In the 1980's, important advances on SOA device design and modeling concentrated on AlGaAs configurations in the 830 *nm* spectral window. Then in the late 1980's, studies were carried out on InP/InGaAsP SOAs designed to operate in both the 1.3  $\mu m$  and the 1.55  $\mu m$  spectral windows [2.14].

Before 1989, SOA structures were based on anti-reflection coated semiconductor laser diodes and had an asymmetrical waveguide structure. This led to a strongly polarization

sensitive gain. With the developments in anti-reflection coating technology, researchers began the fabrication of traveling-wave (TW) SOAs [2.15]. In 1989, with the use of more symmetrical waveguide structures giving much reduced polarization sensitivities, SOAs began to be designed as devices in their own right [2.16].

The erbium doped fiber amplifier (EDFA) was invented in 1986. It led to a revolution in optical communications as it made possible the replacement of regenerators in links limited by fiber attenuation and leading to the possibility of optically transparent networks. The EDFA has become the major optical amplifier in current long haul networks and multi-channel optical applications at  $1.55 \mu\text{m}$  window. EDFAs are especially attractive as their high gain, low insertion loss, low noise figure and negligible nonlinearities; however, they require an external pump laser.

In fact, EDFAs and SOAs are complementary technologies. Although SOAs have relative low gain and high noise figure as well as nonlinearities, this technology is advancing rapidly. SOA design and development has progressed in correspondence with advances in semiconductor materials, fabrication, antireflection coating technology, packaging and photonic integrated circuits, to the point where reliable low cost devices are now available for use in current fiber optical networks and applications. Moreover, developments in SOA are ongoing with particular interest in functional application such as photonic switching and wavelength conversion. The use of SOAs in photonic integrated circuits is also attracting much research interest. They are compatible with monolithic integration and offer a wide range of applications, including optical signal processing that can not be achieved by fiber amplifiers. SOAs are the most promising

components in evolving optical communication networks. A comparison between the main features of EDFAs and SOAs is given in Table 2.2.

<b>Features</b>	<b>EDFA</b>	<b>SOA</b>
Typical maximum internal gain (dB)	30-50	30
Typical insertion loss (dB)	0.1-2	6-10
Polarization sensitive	No	Weak (< 2 dB)
Pump source	Optical	Electrical
3 dB gain bandwidth (nm)	30	30-50
Nonlinear effects	Negligible	Yes
Saturation output power (dBm)	10-15	5-20
Typical intrinsic noise figure (dB)	3-5	7-12
Photonic integrated circuit compatible	No	Yes
Functional device possibility	No	Yes

**Table 2.2** The comparison between the main features of EDFAs and SOAs. [2.13]

The major current use of SOAs is as basic amplifiers in WDM and other fiber optical networks, and as switching elements in all-optical switching and crossconnection. As shown above, the future for SOAs is bright, and even more applications of the device will arise when the technology matures and manufacturing costs decrease.

### **2.3.2 SOA vs. EDFA based fiber ring lasers**

EDFAs represent an attractive means of generating tunable high power oscillations at a wavelength suitable for long-haul communication systems. At the  $1.55 \mu\text{m}$  working window, several actively mode-locked fiber lasers incorporating EDFs as the gain medium and the production of ultrashort pulses at high-repetition-rate has demonstrated [2.17]–[2.22]. The majority of these systems use lithium niobate electro-optic modulators

(AM modulation) for their large electro-optic coefficient and compact structure. As lithium niobate modulators are polarization-sensitive devices, so laser sources with this kind of modulators either have to be built from polarization preserving components [2.20],[2.21] or with stabilization feedback circuits [2.22],[2.23]. Moreover, the use of lightly or moderately doped EDF for gain results in long cavities, which make fiber lasers sensitive to environmental perturbations, then active stabilization techniques are needed to limit their environment sensitivity.

In recent years, a very promising technique of active mode-locking has been demonstrated with SOAs to provide both gain and modulation in the cavity [2.24]. In addition, mode locking can be achieved via cross gain modulation (XGM) from an external injected optical signal [2.25],[2.26].

As mentioned before, since SOA is an inhomogeneously broadened gain element, the use of SOAs allows for stable simultaneous multi-wavelength oscillation with very small channel spacing at the room temperature and operation at any wavelength band. When compared with EDFAs, SOAs are compact, low-cost devices with photonic integrated circuits compatibility and capable of sustaining multiple wavelength operation. So SOAs are ideal as the gain medium in mode-locked fiber lasers for current and more future applications. In chapter 3, we will provide overview of various SFRLs.

**References:**

- [2.1] C. Yeh, Applied Photonics, Academic Press, 1990
- [2.2] E. Yashida and M. Nakazawa, "80-200 GHz erbium doped fibre laser using a rational harmonic mode-locking technique," *Electronics Lett.*, 32, pp.1370, 1996.
- [2.3] G. Sucha, M. Hofer, M.E. Fermann, F.Haberl, and D. Harter, "Synchronization of environmentally coupled, passively mode-locked fiber lasers," *Optics Lett.*, 21, pp.1570, 1996.
- [2.4] G. Sucha, S.R. Bopltton, S. Weiss, and D.S. Chemla, "Period doubling and quasi-periodicity in additive pulse mode-locked lasers," *Optical Lett.*, 20, pp.1794, 1995.
- [2.5] M. Horowitz, C. R. Menyuk, T. F. Carruthers, and I. N. Duling, III, "Theoretical and experimental study of harmonically mode-locked fiber lasers for optical communication systems," *J. Lightwave Tech.*, 18, pp.1565, 2000.
- [2.6] A. Chandonnet and M. Piche, "Single-mode pulses from a high-pressure CO<sub>2</sub> laser operated below emission threshold," *IEEE J. of Quantum Elect.*, 27, pp. 2226, 1991.
- [2.7] D. Spence, J. Evans, W. Sleat, and W. Slibbett, "Regeneratively initiated self-mode locked Ti:sapphire laser," *Optics Lett.*, 16, pp.1762, 1991.
- [2.8] E. A. Swanson, S. R. Chinn, K. Hall, K. A. Rauschenbach, R. S. Bondurant, and J. W. Miller, "100-GHz soliton pulse train generation using soliton compression of two phase side bands from a single DFB laser," *IEEE Photon. Technol. Lett.*, 6, pp. 1194–1196, Oct. 1994.
- [2.9] K. Sato et al., "High-repetition frequency pulse generation at 102 GHz using modelocked lasers integrated with electroabsorption modulators," *Electron. Lett.*, 34, 8, pp. 790–791, Apr. 1998.
- [2.10] S. Arahira and Y. Ogawa, "Transform-limited 480 GHz colliding-pulse modelocked laser diode," *Electron. Lett.*, 37, 16, pp. 1026–1027, Aug. 2001.
- [2.11] K. Fukuchi et al., "10.92 Tb/s (273x 40 Gb/s) triple-band/ultra-dense WDM optical-repeated transmission experiment," PD24, *Optical Fiber Communications Conf.*, Anaheim, CA, 2001.
- [2.12] L. A. Zenteno, H. Avramopoulos, and G. H. C. New, "Detailed analysis of active mode-locking," *Appl. Phys. B*, 40, 3, pp. 141–146, July 1986.

- [2.13] M. J. Connelly, Semiconductor Optical Amplifiers, Kluwer Academic, 2002.
- [2.14] J.C. Simon, "GaInAsP semiconductor laser amplifiers for single-mode fibre communications," *IEEE/OSA J. Lightwave Technol.*, 5, pp.1286-1295, 1987.
- [2.15] C.E. Zah, C.Caneau, F.K.Shokoohi, S.G. Menocal, F.Favire, L.A.Reith and T.P. Lee, "1.3  $\mu\text{m}$  GaInAsP near-traveling-wave laser amplifiers made by combination of angled facets and antireflection coatings," *Electron. Lett.*, 24, pp.1275-1276, 1988.
- [2.16] N.A. Olsson, R.F.Kazarinov, W.A.Nordland, C.H.Henry, M.G. Oberg, H.G. White, P.A.Gabrbinski and A.Savage, "Polarisation-independant optical amplifier with buried facets," *Electron. Lett.*, 25, pp.1048-1049, 1989.
- [2.17] A. D. Ellis, R. J. Manning, I. D. Phillips, and D. Nesses, "1.6 ps pulse generation at 40 GHz in phase-locked ring laser incorporating highly non-linear fiber for application to 160 Gbit/s OTDM networks," *Electron. Lett.*, 35, 8, pp. 645–646, Apr. 1999.
- [2.18] G. E. Town, L. Chen, and P. W. E. Smith, "Dual wavelength modelocked fiber laser," *IEEE Photon. Technol. Lett.*, 12, pp. 1459–1461, Nov. 2000.
- [2.19] L. Duan, C. Richardson, Z. Hu, M. Dagenais, and J. Goldhar, "A stable smoothly wavelength-tunable picosecond pulse generator," *IEEE Photon. Technol. Lett.*, 14, pp. 840–842, June 2002.
- [2.20] H. Takara, S. Kawanishi, M. Sarawatari, and K. Noguchi, "Generation of highly stable 20 GHz transform-limited optical pulses from actively mode-locked Er-doped fiber lasers with an all-polarization maintaining ring cavity," *Electron. Lett.*, 28, 22, pp. 2095–2096, 1992.
- [2.21] M. Nakazawa, E. Yoshida, and Y. Kimura, "Ultrastable harmonically and regeneratively mode-locked polarization-maintaining erbium fiber laser," *Electron. Lett.*, 30, 19, pp. 1603–1605, 1994.
- [2.22] C. G. Lee, Y. J. Kim, H. K. Choi, and C.S. Park, "Pulse-amplitude equalization in a rational harmonic mode-locked semiconductor ring laser using optical feedback," *Optics Commun.*, 209, pp. 417–425, Aug. 2002.
- [2.23] X. Shan, T. Woddowson, A. D. Ellis, and A. S. Siddiqui, "Very simple method to stabilise mode-locked erbium fiber lasers," *Electron. Lett.*, 32, 11, pp. 1015–1016, May 1996.

[2.24] C. Peng, M. Yao, J. Zhang, H. Zhang, Q. Xu, and Y. Gao, "Theoretical analysis of actively mode-locked fiber ring laser with semiconductor optical amplifier," *Opt. Commun.*, 209, pp.181–192, 2002.

[2.25] J. He and K. T. Chan, "All-optical actively modelocked fiber ring laser based on cross-gain modulation in SOA," *Electron. Lett.*, 38, 24, pp.1504-1505, 2002.

[2.26] K. Vlachos, C. Bintjas, N. Pleros, and H. Avramopoulos, "Ultrafast semiconductor based fiber laser source," *IEEE J. Sel. Topics in Quantum Electron.*, 10, 1, pp.147-154, 2004.

## Chapter 3

### Semiconductor fiber ring lasers

#### 3.1 Semiconductor optical amplifiers (SOAs) basics

##### 3.1.1 SOAs basic description [3.1][3.2]

SOAs are one type of optical amplifiers which can amplify an input light signal under suitable operating conditions. A schematic diagram of an SOA is shown in Fig 3.1. The active region in the device imparts gain, via stimulated emission, to an input signal. An embedded waveguide is used to confine the propagating signal wave to the active region. An external electric current provides the energy to enable gain. The output signal is accompanied by noise. This additive noise, amplified spontaneous emission (ASE), is produced by the entire amplification process. The amplifier facets can be reflective, thus causing ripples in the gain spectrum.

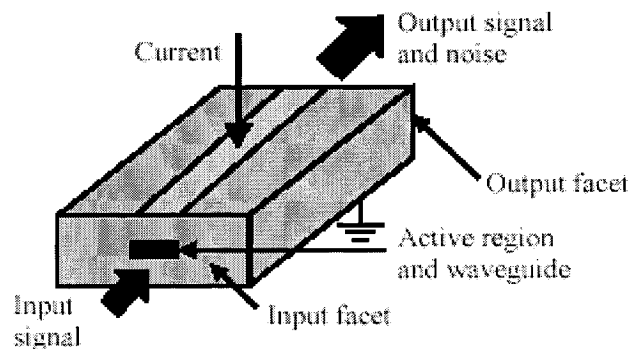


Fig. 3.1 Schematic diagram of an SOA. [3.1]

In general, there are two main types of SOAs: the Fabry-Perot SOA (FP-SOA) and the traveling-wave SOA (TW-SOA). The major difference between the FP-SOA and TW-SOA is that reflections from the end facets are significant in FP-SOA but are negligible

in TW-SOA. As shown in Fig 3.2, anti-reflection coatings in TW-SOA can be used to reduce facet reflectivities to less than  $10^{-5}$ . Moreover, the TW-SOA is not as sensitive as the FP-SOA to environmental fluctuations, like bias current, temperature and signal polarization, etc.

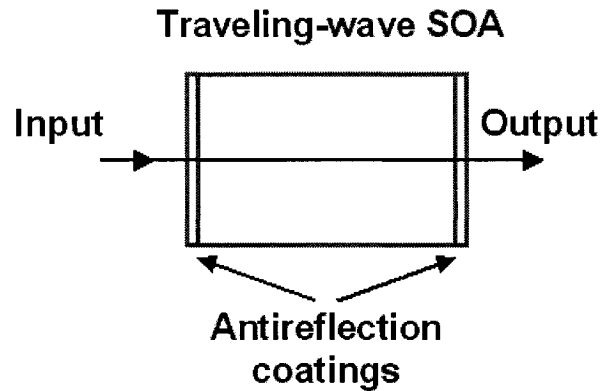


Fig. 3.2 Principle of operation of the TW-SOA. [3.1]

### 3.1.2 Fundamental device characteristics [3.1]

The main use of SOAs is as basic amplifiers in WDM and other fiber optical networks. The following desired properties for this application are listed in Table 3.1.

Desired properties of a practical SOA	
High gain and gain bandwidth	Negligible facet reflectivities
Low polarization sensitivity	High saturation output power
Additive noise near the theoretical limit	Insensitive to the input signal modulation characteristics
Multichannel amplification with no crosstalk	No nonlinearities

Table 3.1 Desired properties of a practical SOA. [3.1]

In tandem with advances in semiconductor materials, device fabrication, antireflection coating technology and packaging, the goal of most SOA research and development is to realize above mentioned properties in practical devices.

### 3.1.2.1 Small-signal gain and gain bandwidth

There are two basic gain definitions for SOAs: intrinsic gain  $G$  and fiber-to-fiber gain. The former is simply the ratio of the signal power at the input and output facets. The latter includes the input and output coupling losses. The gain spectrum of a particular SOA depends on its structure, material and operational parameters. The small-signal internal gain of a FP-SOA at optical frequency  $\nu$  is given by [3.3],

$$G(\nu) = \frac{(1-R_1)(1-R_2)G_s}{(1-\sqrt{R_1 R_2} G_s)^2 + 4\sqrt{R_1 R_2} G_s \sin^2 [\pi(\nu - \nu_0) / \Delta \nu]} \quad (3.1)$$

where  $R_1$  and  $R_2$  are the input and output facet reflectivities,  $\Delta \nu$  is the cavity longitudinal

mode spacing given by  $\Delta \nu = \frac{c}{2Ln_r}$ ,  $n_r$  is the refractive index of the active region, and  $\nu_0$

is the closest cavity resonance to  $\nu$ . Cavity resonance frequencies occur at integer

multiples of  $\Delta \nu$ . The  $\sin^2$  factor in (3.1) is equal to zero at resonance frequencies and

equal to unity at the anti-resonance frequencies. The effective SOA gain coefficient is

$$g = \Gamma g_m - \alpha \quad (3.2)$$

where  $\Gamma$  is the optical mode confinement factor and  $\alpha$  the absorption coefficient. The single-pass amplifier gain is  $G_s = e^{gL}$ .

An uncoated SOA has facet reflectivities approximately equal to 0.32. The amplifier gain ripple  $G_r$  is defined as the ratio between the resonant and non-resonant gains. From (3.1), we get

$$G_r = \left[ \frac{1 + \sqrt{R_1 R_2 G_s}}{1 - \sqrt{R_1 R_2 G_s}} \right] \quad (3.3)$$

From (3.3) the relationship between the geometric mean facet reflectivity  $R_{geo} = \sqrt{R_1 R_2}$  and  $G_r$  is

$$R_{geo} = \frac{1}{G_s} \left[ \frac{G_r - 1}{G_r + 1} \right] \quad (3.4)$$

In general, high gain and wide gain bandwidth are desired for most applications. Moreover, wide gain bandwidth SOAs are especially useful in systems where multi-channel amplification is required such as in WDM networks. A wide gain bandwidth can be achieved in an SOA with an active region fabricated from quantum-well or multiple quantum-well materials. Fig 3.3 shows a typical TW-SOA gain spectrum. The definition of the gain bandwidth  $B_{opt}$  is the wavelength range over which the signal gain is not less than half its peak value.

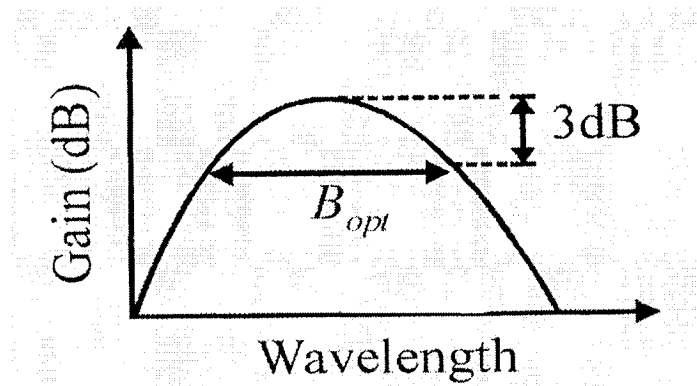


Fig. 3.3 Typical TW-SOA gain spectrum. [3.1]

### 3.1.2.2 Polarization sensitivity

In general, SOAs are polarization sensitive. It is due to a number of factors including the waveguide structure and the gain material. Furthermore, cascaded SOAs accentuate this polarization dependence. Two mutually orthogonal polarization modes, Transverse Electric (TE) and Transverse Magnetic (TM) modes, characterize the amplifier waveguide's polarization. The input signal polarization state usually lies somewhere between these two. The difference between the TE mode gain  $G_{TE}$  and TM mode gain  $G_{TM}$  is

$$G_{TE/TM} = |G_{TE} - G_{TM}| \quad (3.5)$$

The polarization sensitivity can be improved by the use of square-cross section waveguide and strained quantum-well material in practical devices.

### 3.1.2.3 Signal gain saturation

As is known, both the input signal power and internal noise generated by the amplification process influences the gain of an SOA. When the signal power increases, the gain decreases as shown in Fig. 3.4. This gain saturation can cause significant signal distortion. The parameter for quantifying the gain saturation is the saturation output power  $P_{o,sat}$ . The definition of  $P_{o,sat}$  is the amplifier output signal power at which the amplifier gain is half the small-signal gain. In fact, the gain saturation can limit the gain achievable when SOAs are used as multi-channel amplifiers in WDM systems.

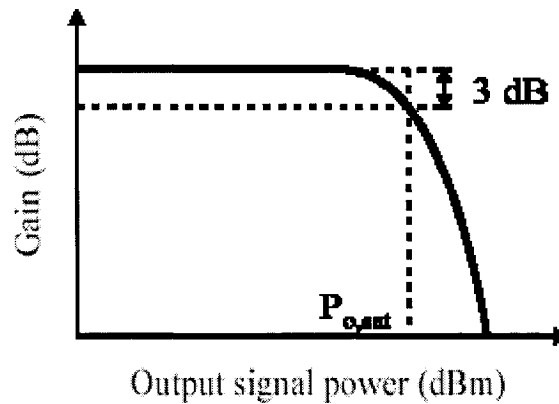


Fig. 3.4 Typical SOA gain versus output signal power characteristic. [3.1]

### 3.1.2.4 Noise figure

The noise figure,  $F$ , defined as the ratio of the input and output ratio

$$F = \frac{(S/N)_i}{(S/N)_o} \quad (3.5)$$

is a useful parameter for quantifying optical amplifier noise. In the limiting case where the amplifier gain is much larger than unity and the amplifier output is passed through a narrowband optical filter, the noise figure is given by  $F = 2n_{sp}$ . The lowest value possible for  $n_{sp}$  is unity, which occurs when there is complete inversion of the atomic medium. In fact, the noise figure is degraded by the amplified input coupling loss, thus adding to the intrinsic noise figure.

### 3.1.2.5 Dynamic effects

When SOAs are used to amplify modulated light signals, gain saturation will occur if the signal power is high. This would not be a serious problem if the gain dynamics were a slow process, such as in doped fiber amplifiers, which have recombination lifetimes of a few milliseconds. However, the carrier recombination lifetime (a few hundred

picoseconds) determines the gain dynamics in SOAs. This means that the gain will react perfectly quickly to changes in the input signal power. Then it can cause signal distortion, which becomes more severe as the modulated signal bandwidth increases. Moreover, these effects are very important in multi-channel systems where the dynamic gain leads to interchannel crosstalk.

### **3.1.2.6 Nonlinearities**

In general, SOAs exhibit nonlinear behavior. These nonlinearities can cause problems such as frequency chirping and generation of second or third order intermodulation products. However, nonlinearities can be of use in using SOAs as functional devices such as wavelength converters.

## **3.2 Survey of different semiconductor fiber ring lasers**

Researchers at different academic institutes have demonstrated the applications of fiber ring lasers that incorporate an SOA as a gain medium and/or a mode locker. Indeed, actively mode-locked laser sources which incorporate SOAs have been demonstrated by several research groups [3.4]–[3.8] for the generation of short optical pulses at various repetition rates. Techniques used fall under of two classifications: using intracavity modulator or all-optical mode-locking. In these experiments, the SOA was used either as the gain in combination with an intracavity intensity modulator [3.9],[3.10] or used to provide both gain and electrically controlled gain modulation [3.11]. Additionally, SOAs have been used also as the mode-locking elements providing gain modulation in storage rings [3.12].

### 3.2.1 Intracavity mode-locked semiconductor fiber ring laser configurations

#### 3.2.1.1 General model [3.10]

The general model of actively mode-locked SFRLs with an intracavity intensity modulator is shown in Fig. 3.5, where there is an SOA as the gain medium in the ring and an amplitude modulator (AM) driven by a frequency synthesizer to modulate the loss of the cavity. The lasing wavelength is chosen by a tunable optical filter. Isolators ensure the unidirectional light propagation in the cavity. To obtain stable pulse trains, the modulating frequency should be nearly a multiple of the fundamental frequency of the cavity,  $c/L$  ( $c$  is the speed of light in the medium, and  $L$  is the cavity length). During stable operation, every pulse in the cavity has the same shape. The pulse shape is modified by the SOA, the filter, and the modulator in the cavity. However, it is restored when the pulse completes a round trip.

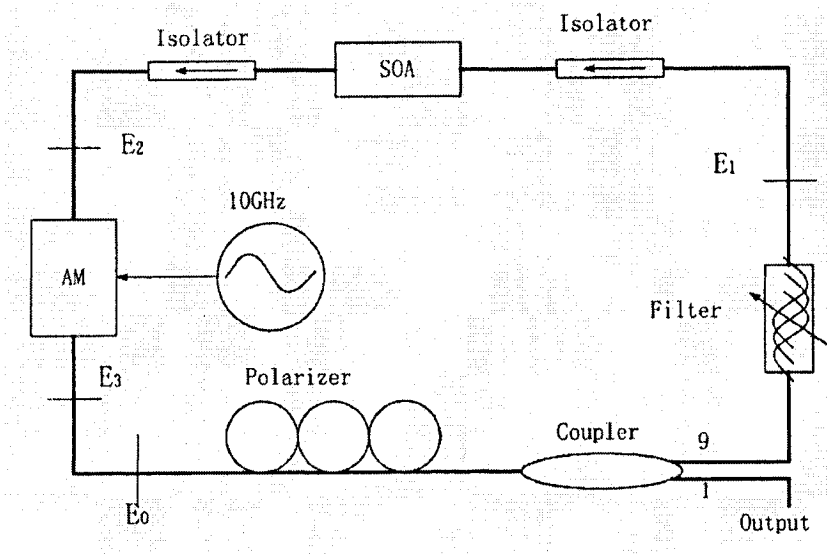


Fig. 3.5 General structure of fiber ring laser. [3.10]

### 3.2.1.2 SFRL by intracavity modulation

A 10 GHz actively mode-locked SFRL using an electro-absorption (EA) modulator was demonstrated in [3.13], see Fig. 3.6. The SOA was used as the gain medium and the EA modulator driven by 10 GHz RF electrical signals functioned as the amplitude modulator in the ring cavity. The laser cavity was composed entirely from fiber-pigtailed devices. The EA modulator had a 3 dB electrical bandwidth of 10 GHz and a fiber-to-fiber insertion loss of 10 dB. The SOA had a fiber-to-fiber gain of 26 dB at the maximum current of 200 mA. Two isolators were placed on either side of the SOA to prevent internal reflections and enable unidirectional operation. A tunable optical filter was used to define the lasing wavelength and had a 3 dB bandwidth of 1.5 nm.

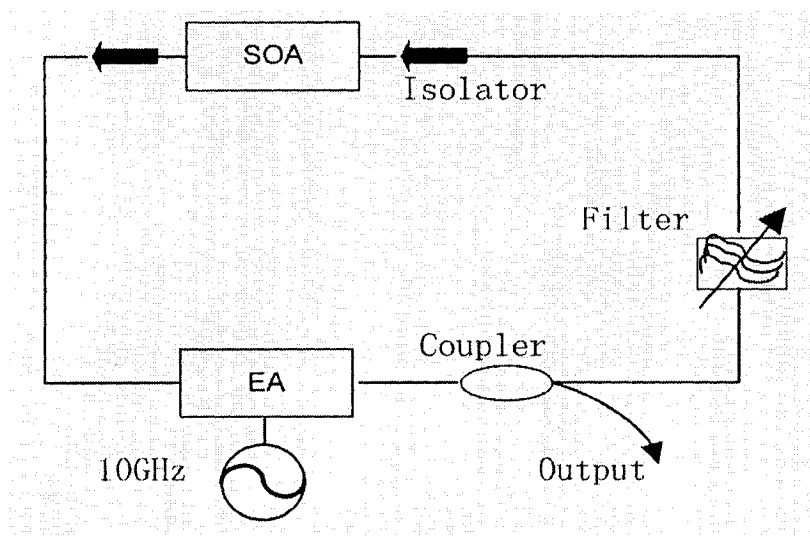


Fig. 3.6 Schematic diagram of laser configuration. [3.13]

Due to its compactness, robustness and other merits, the EA modulator is very attractive for use in mode-locked SFRLs. Fig.3.7 shows the spectrum of the output pulses. Fig. 3.8 displays the optical waveform of the pulse train. In the experiment, the output pulse train is stable with a 10 ps FWHM and 30 nm wavelength tuning range.

Both the injection current of SOA and modulation voltage of the EA modulator were finely adjusted. The RF frequency was also correspondingly tuned around 10 GHz to achieve the mode locking.

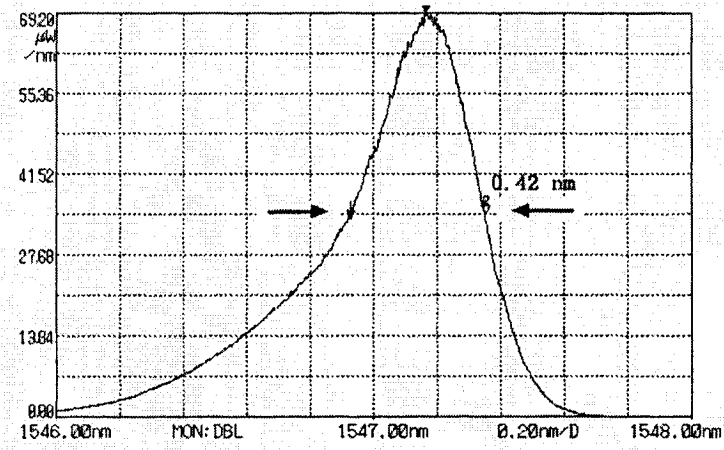


Fig. 3.7 Optical spectrum of output pulses. [3.13]

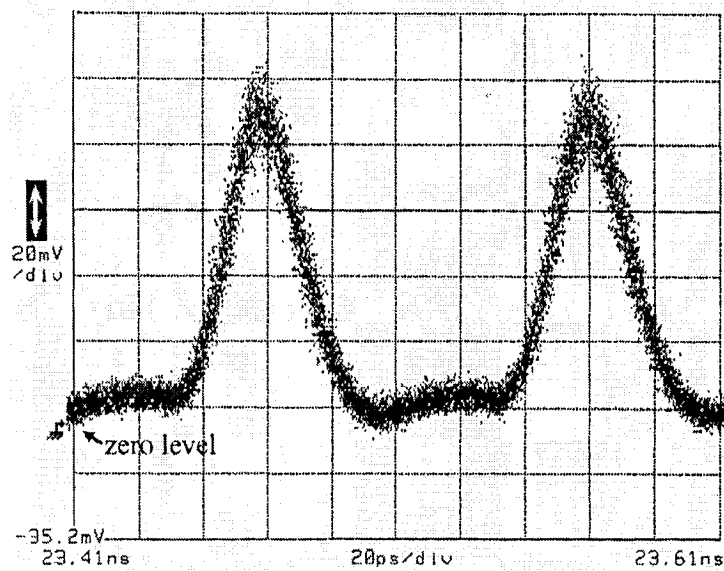


Fig. 3.8 Optical waveform of output pulses. [3.13]

### 3.2.1.3 Multi-wavelength SFRL by using sampled fiber grating

The multi-wavelength pulse train generation in SFRL using sampled fiber grating was demonstrated in [3.14]. The schematic of the laser is shown in Fig.3.9 and consists of a variable fiber coupler, polarization controller, LiNbO<sub>3</sub> Mach-Zehnder intensity modulator, optical isolator, SOA, optical circulator, and a sampled fiber Bragg grating (SFBG) [see Appendix A for further details on FBGs].

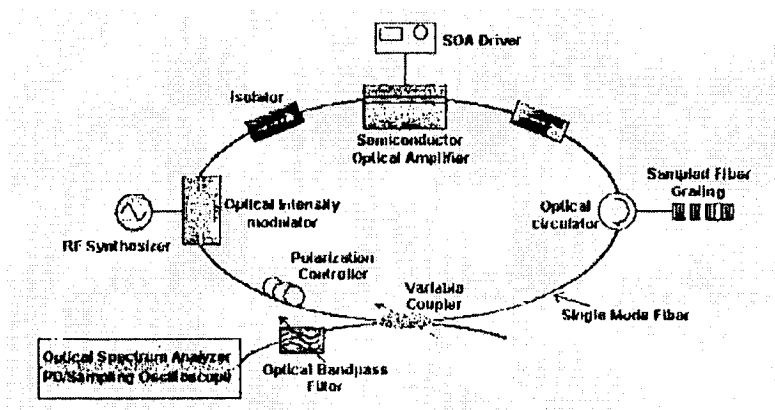


Fig. 3.9 Experimental setup for multiwavelength pulse train generation. [3.14]

The SFBG is used as an in-fiber comb filter to define the lasing wavelengths. The filter has less loss and more design flexibility than usual comb filters such as FP etalons and WDM multiplexers. Moreover, they are designed to compensate the nonuniform gain spectrum for the equal power distribution among the lasing wavelengths.

In the experimental setup, the SOA had a carrier lifetime of 2 ns, fiber-to-fiber gain of 23 dB, and a saturation output power of 7.5 dBm at the maximum pumping current of 200 mA. The number and the power distribution of the lasing wavelengths were determined by the pumping current, the uniformity of gain spectrum and reflection spectrum of the SFBG, and the polarization state in the cavity. For this given configuration, the number of lasing wavelength channels can be selected from 1 to 4, by

adjusting the polarization controller. Fig. 3.10 shows the output spectrum of the multi-wavelength laser and each channel pulse wavelength selected by the tunable optical bandpass filter when 3 channels are simultaneously mode-locked at 10 GHz.

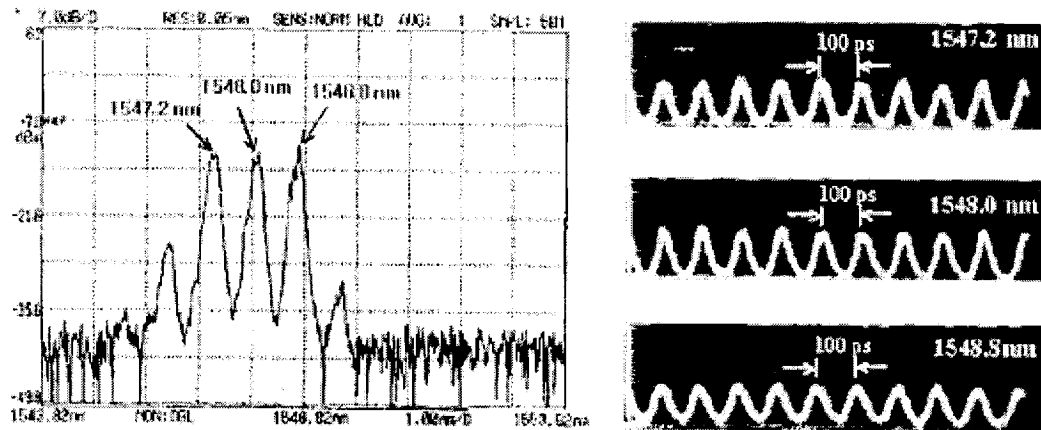


Fig. 3.10 Output spectrum and simultaneous pulse train for 3 channels at 10 GHz. [3.14]

### 3.2.1.4 Multi-wavelength SFRL

A 10 GHz SFRL (10 simultaneously synchronized wavelength channels mode-locked at 10 GHz, each producing 20 ps pulses) was demonstrated in [3.15], see Fig. 3.11.

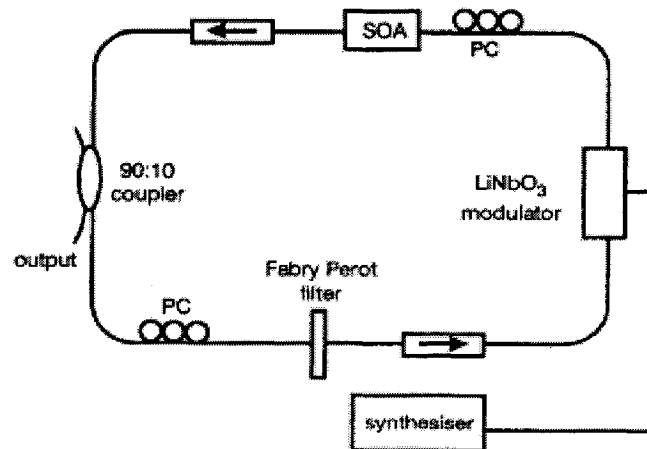


Fig. 3.11 Experimental setup. [3.15]

The laser cavity was composed entirely of fiber-pigtailed components. Gain was provided by an InGaAsP/InP ridge waveguide SOA whose waveguide facets were anti-reflection coated. Faraday isolators were used in the ring laser to ensure unidirectional operation and to eliminate back reflections. A 90:10 fused fiber coupler was used to tap the output signal from the laser. The wavelength selection element was a Fabry-Perot filter with a 3.1 nm FSR and 0.3 nm bandwidth, and was inserted in a fiber-pigtailed, free-space, beam expander. A 10 GHz LiNbO<sub>3</sub> Mach-Zehnder intensity modulator driven by sinusoidal signal from a signal generator was used to obtain the mode-locked pulse trains. Polarization controllers were used on the input ports of the LiNbO<sub>3</sub> modulator and the SOA for optimum performance. The total length of the cavity was about 24.9 m corresponding to a fundamental cavity frequency of 7.98 MHz.

The SOA had a small signal gain of 23 dB when driven with a 250 mA DC current at 1535 nm. During operation, the SOA was driven with a 240 mA DC current. With the RF signal turned off and the modulator biased on, the laser provides a CW, multi-wavelength output between 1507 and 1562nm. There was no special provision for power equalization between these oscillating modes in the cavity. The total output power of the multi-wavelength CW source was 67  $\mu$ W. With the LiNbO<sub>3</sub> modulator biased at -1 V and 24 dBm RF power at 10 GHz and fine adjustment of the frequency of the signal generator, the laser mode-locked.

Fig. 3.12 shows the optical spectrum of the mode-locked output from the laser. We can see 10 simultaneously mode-locked wavelengths at 10 GHz. Fig. 3.13 displays the variation of the pulsewidth monitored on the autocorrelator and the output power for different simultaneously mode-locked wavelengths. The maximum power variation

between the oscillation modes was less than 2 dB and the total output power of the source was  $40 \mu\text{W}$ . Fine adjustment of the F-P filter allowed tuning across its 3.1 nm FSR. The laser performance may be extended to higher rates and more channels with the simple substitution of the modulator and the F-P filter elements.

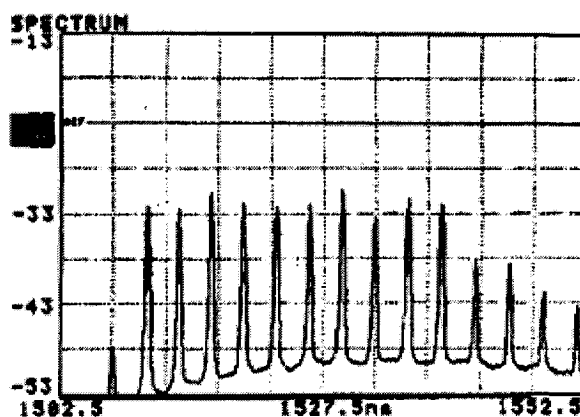


Fig. 3.12 Spectrum of multi-wavelength laser in mode-locked operation at 10 GHz. [3.15]

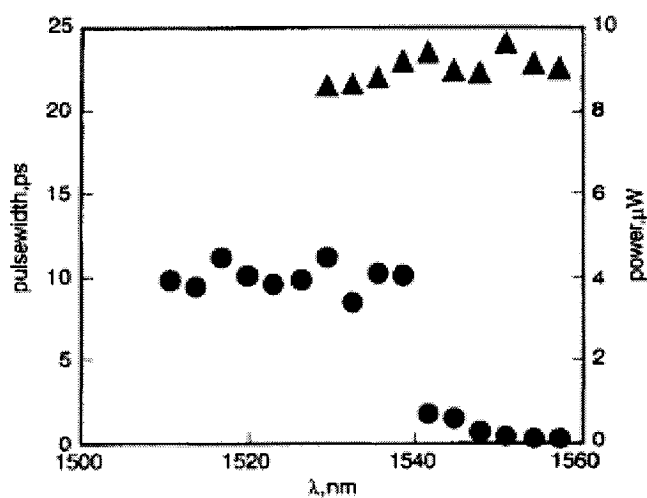


Fig. 3.13 Pulse width and output power against wavelength. [3.15]

### 3.2.2 All-optical mode-locked fiber ring laser configurations

#### 3.2.2.1 Pulse train generation from SOA based fiber ring laser

The pulse train generation from SFRL was demonstrated in [3.4]. Fig.3.14 shows the schematic of the laser.

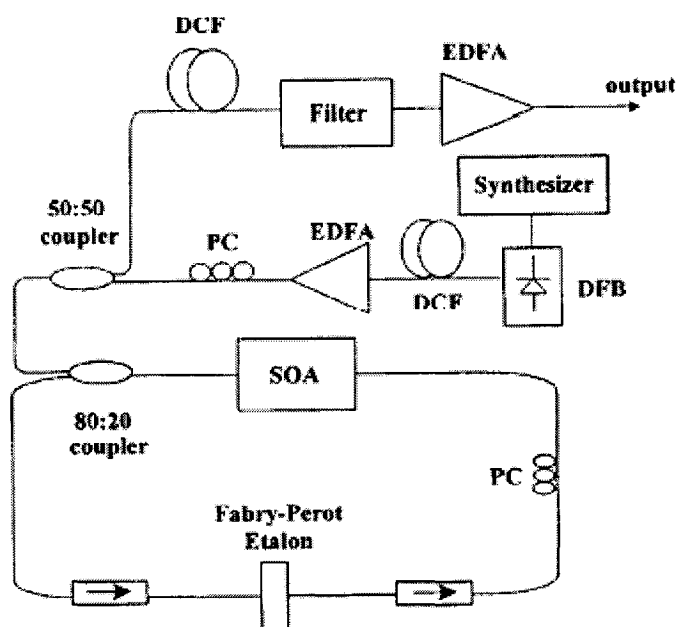


Fig. 3.14 The experimental setup. [3.4]

The laser ring cavity was constructed entirely from fiber-pigtailed devices. Gain was provided from a 500 mm InGaAsP–InP ridge waveguide SOA. The SOA had a peak gain at 1535 nm with a 20 nm bandwidth, providing 23 dB small signal gain with 250 mA DC drive current, and had 400 ps recovery time. Isolators were used at the input and output of the SOA to ensure unidirectional oscillation in the ring and to stop the externally introduced signal from circulating in the cavity. After the SOA, an 80:20 optical fiber coupler was used to insert the external control signal and to tap the output signal from the laser. The wavelength-selecting element was a Fabry–Perot (FP) etalon. The SOA exhibited 2 dB polarization gain dependence and a polarization controller (PC) was used

at its input port for optimization. The total length of the ring cavity was 24.25 m corresponding to a 7.98 MHz fundamental frequency. The external control pulse train was generated from a 5 GHz gain switched DFB laser diode operating at 1548.5 nm. These pulses were compressed to 7.5 ps with dispersion compensation fiber before amplification in an EDFA. Before injection into the ring laser cavity via the 80:20 controller, the polarization state of the pulses was adjusted to optimize the quality of the mode-locked pulses from the ring.

The principle of operation of the source relies on three key observations. The first is that the fast saturation of the gain of the SOA by an externally introduced picosecond optical pulse train pulse may be used for gain modulation in a ring cavity to obtain mode-locked picosecond pulse trains. Optical modulation of the gain of the SOA may be more easily performed at a higher rate than electrical gain modulation. In the present experiment, the externally introduced pulse train was obtained from a relatively low repetition rate, gain switched DFB diode laser.

The second observation is that the use of a heterogeneously broadened gain element such as the SOA, allows the simultaneous oscillation of a number of wavelengths in the same oscillator cavity. In the embodiment, the multi-wavelength oscillation in the laser source has been achieved with the use of a FP etalon.

The third observation is that repetition rate multiplication to  $nf_{\text{ext}}$  of the output pulse train may be achieved, by tuning the frequency  $f_{\text{ext}}$  of the externally introduced pulse trains to  $f_{\text{ext}} = (N+1/n) \delta f_{\text{ring}}$ . In this equation,  $N$  is the order of the harmonic mode-locking of the ring laser,  $\delta f_{\text{ring}}$  is the fundamental frequency of the ring laser oscillator and  $n$  is an integer. When the repetition rate of the external pulse train is adjusted to differ by

( $\delta f_{ring}/n$ ) from a harmonic of the fundamental of the ring cavity, it becomes temporally displaced by  $T_{ext}/n$  on each recirculation through the ring cavity with respect to its previous position.

Fig. 3.15 displays the mode-locked pulse trains after filtering at 1554.2 nm, 1559.8 nm, 1565.2 nm, and 1570.6 nm monitored on a 30 GHz-sampling oscilloscope and shows temporal synchronization between them.

Fig. 3.16(a) displays the variation of the pulsewidth and the pulsewidth-bandwidth product for each mode-locked wavelength. This figure shows that the pulsewidth–bandwidth products for all pulse trains are within 3% of 0.35, indicating that the pulses profiles are all close to squared hyperbolic secant. Fig. 3.16(b) shows the output power for each of the mode-locked wavelengths indicating less than 5% variation across them.

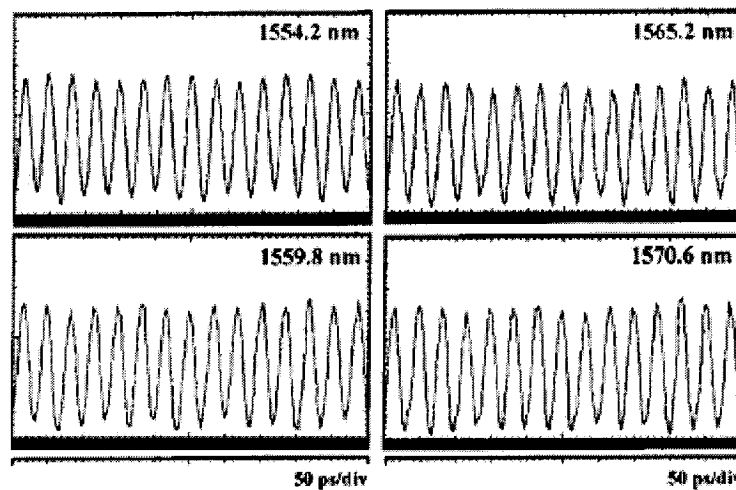


Fig.3.15 Simultaneous pulse train for four wavelengths. [3.4]

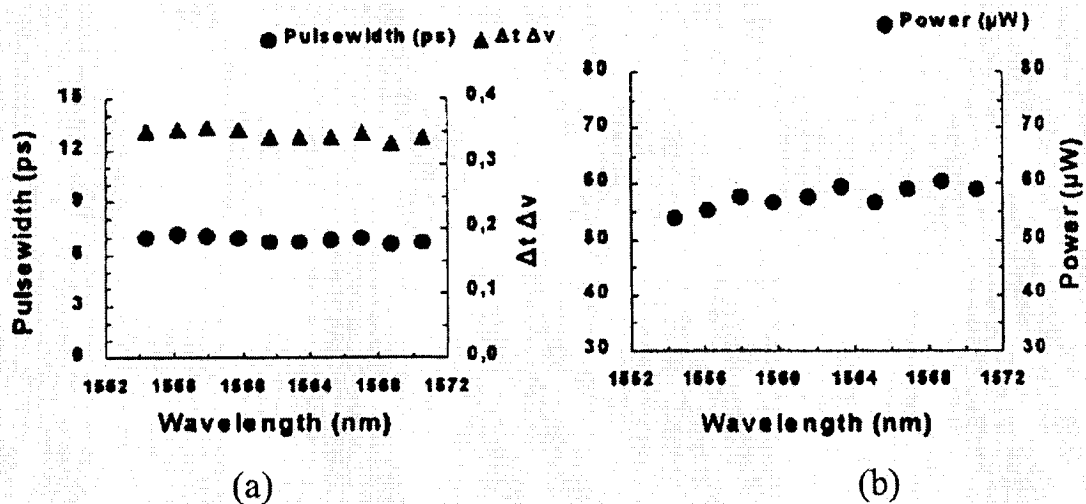


Fig. 3.16 (a) Variation of the pulsewidth and pulsewidth–bandwidth product versus wavelength. (b) Variation of the output power versus wavelength. [3.4]

In summary, the laser source is capable of generating 10 synchronized wavelength channels, each mode-locked at 30 GHz. The oscillator produces nearly transform limited, 7 ps pulses for all wavelengths with less than 5% power variation across them.

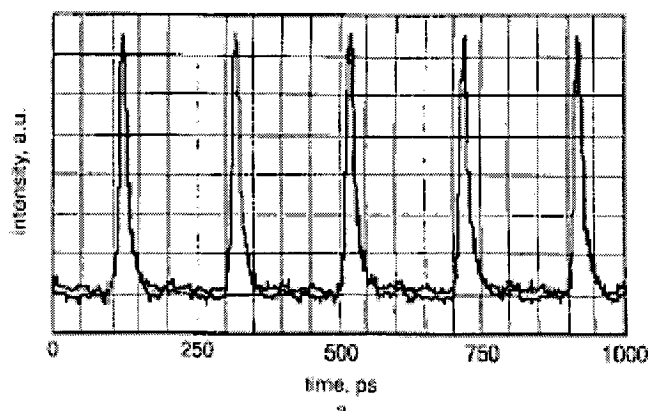
### 3.2.2.2 Wavelength-tunable mode-locked FRL based on XGM in SOA

A wavelength tunable mode-locked SFRL based on cross-gain modulation in an SOA was demonstrated in [3.5]. The experimental setup is shown in Fig 3.17. The SOA is used not only as the gain medium of the ring laser but also as an optically controlled mode-locker. The control signal was launched into the ring cavity through the optical circulator and was blocked by the optical circulator to ensure unidirectional operation of the laser.



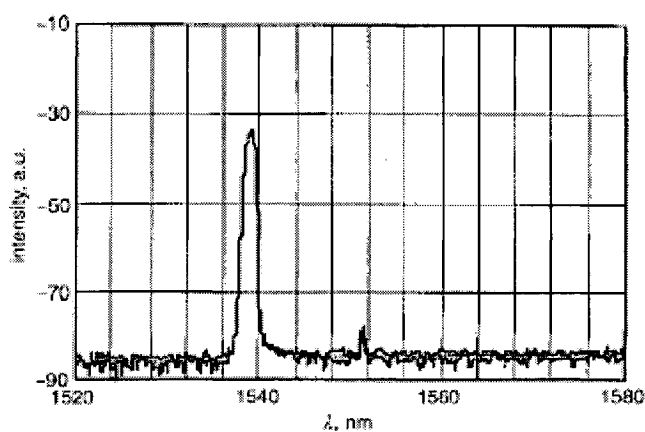
5.0GHz, which was the 276<sup>th</sup> harmonic frequency of the ring cavity. The behavior of mode-locking at the lower harmonic frequencies was similar.

Fig.3.18 shows a typical pulse train when the SOA was modulated by the control signal at 5.0 GHz.



**Fig.3.18** Pulse shape of the mode-locked output pulses at about 5 GHz. [3.5]

Fig. 3.19 shows the corresponding optical spectrum of the emission. The central wavelength was 1539.05 nm and the 3 dB spectrum width was about 0.7 nm. The average output power was about 900  $\mu$ W.



**Fig. 3.19** Spectrum of the mode-locked output pulses at about 5 GHz. [3.5]

In summary, it is one wavelength tunable mode-locked SFRL, the XGM serves to modulate SOA gain for the lasing wavelength. Continuous wavelength tuning with a

range of about 32 nm was achieved by tuning the filter and the tuning range can be extended to cover the entire gain bandwidth of the SOA.

### 3.2.2.3 Pulse train generation and wavelength switching from SFRL with Optical Delay Line

The generation and wavelength switching of picosecond pulses in an all-optically mode-locked SFRL with an optical delay line was proposed and demonstrated in [3.6]. The experimental setup is shown in Fig.3.20. The ring cavity is composed of a 1550 nm SOA, a polarization independent isolator, one polarization controller, eight cascaded FBGs, two optical circulators, one 10:90 coupler and the optical delay line.

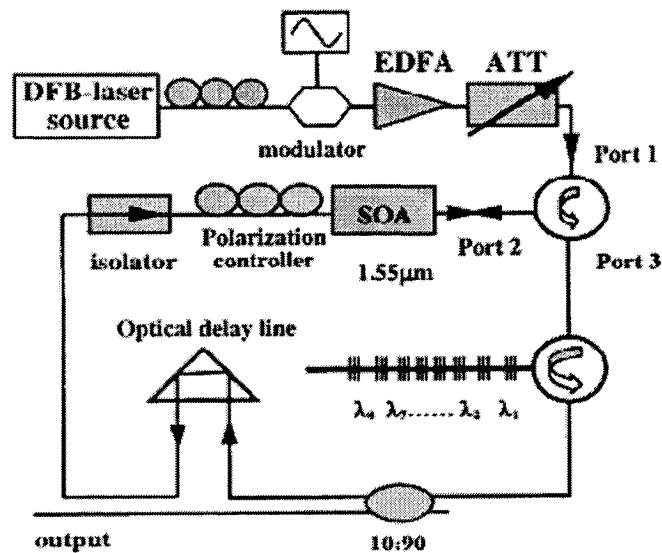


Fig. 3.20 The experimental setup of the fiber ring laser. [3.6]

The laser's gain medium is not the fiber itself, but the SOA in the fiber ring. Mode-locking is accomplished by modulating the gain of the amplifier at 2.5 GHz, the 119th harmonic of the fiber ring. The gain is modulated when it is saturated by the signal from

the amplified distributed feedback laser. The laser signal is coupled into the ring with a circulator and dumped at the isolator after a single pass through the SOA.

The radiation circulates clockwise in the fiber ring. A string of nested fiber Bragg gratings (FBGs) extends from the lower circulator into the center of the ring. Each reflects a different wavelength between 1549 nm and 1555 nm. By adjusting the power of the control light and the bias current of the SOA, stable pulse trains at each of the eight wavelengths at the repetition frequency set by the control signal have been obtained one after the other by carefully tuning the optical delay line. Regardless of the wavelength, each pulse has to make a single pass around the ring in 47.6 ns (119 times the reciprocal of 2.5 GHz) to remain in phase with the modulated gain of the SOA. Because different wavelengths must travel different distances into the string of FBGs, a given wavelength will oscillate in the ring only when the delay line is adjusted so that its transit time is 47.6 ns. The non-resonant wavelengths are suppressed by 30 dB. The pulse trains are all stable and no mode hopping can be observed when the laser has been mode-locked for two hours. The duration of the mode-locked pulses, which exit through the 10 percent coupler at the bottom of the figure, is approximately 43 ps.

The wavelength switching characteristics of the laser is shown in Fig.3.21. It was tuned just by adjusting the optical delay line. The switching rate is about 0.8 nm per delay change of 32 ps–35 ps. The figure shows clearly that the output wavelength can be switched among all those allowed by the FBGs. The pulsewidths and spectral widths of the output trains obtained are 41 ps–48.6 ps and 0.19 nm–0.23 nm, respectively.

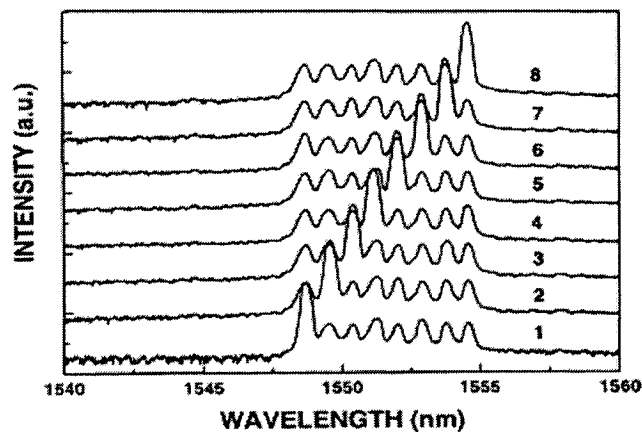


Fig. 3.21 The wavelength switching characteristics of the laser. [3.6]

Narrower and better quality output pulses can be further obtained by compensating the chirp produced in the SOA and by using FBGs with a broader and flatter wavelength response. The range of switched wavelengths of this laser can be extended to cover the whole gain region of the SOA by just adding more FBGs that reflect those wavelengths in the remaining gain region to the FBG string. The wavelength switching speed of the laser depends on the speed of the mechanical motion of the delay line and the speed of the pulse evolution in the cavity. The mechanical motion of the delay line dominates the wavelength switching speed. An RF spectrum analyzer with a fast photodetector measures the stability of the output pulse trains. Adjusting the length of the gratings and the separation between adjacent gratings can change the wavelength locking range.

In summary, an all-optically mode-locked SFRL having an SOA which plays the roles of both a gain element and an optically controlled mode-locker and eight cascaded FBGs which play the role of the wavelength selecting element has been proposed and demonstrated. Stable mode-locked pulses at the control signal repetition frequency have been obtained by injecting sinusoidal control light into the laser cavity. Wavelength

switching among wavelengths is achieved by merely tuning the delay time of the intracavity optical delay line while the without changing the rest of the experimental setup. The repetition frequency of the generated pulses remains unchanged during the wavelength switching process because the adjusted optical delay can compensate the dispersion-induced change of the cavity length.

### 3.2.2.4 Electrical wavelength tuning mode-locked fiber ring laser

One approach to generate switching-wavelength picosecond pulses is developed based on a dispersion-managed SOA fiber laser cavity [3.8]. Gain modulation on a 1550 nm SOA is used together with subharmonic gating of the pulses in the cavity. An 8 GHz, eight wavelengths output is obtained with a constant spacing of 0.91 nm between neighboring wavelengths. The wavelength channels have nearly identical peak powers. The total amplitude and time jitter of the output is measured to be smaller than 0.4 ps. The spacing and the number of output wavelengths can be easily tuned by changing the operating frequency and the subharmonic ratio without modifying the optical cavity.

The experimental setup of the SFRL is depicted in Fig. 3.22. An  $F$  GHz optical control signal is produced by externally modulating the output of a distributed-feedback (DFB) laser with an electrooptic modulator (EOM 1).

The control signal is used to optically modulate the gain of the SOA in the fiber ring laser. The laser cavity consists mainly of an SOA, an EOM (EOM 2), and two pieces of fiber providing equal and opposite group velocity dispersions. To prevent the control signal from oscillating inside the laser cavity, an isolator and an FBG are used to block its circulation.

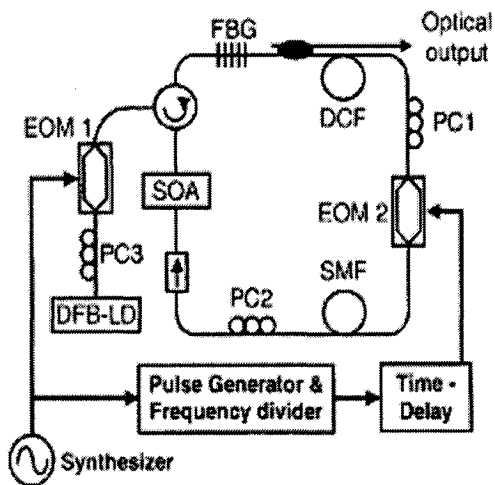
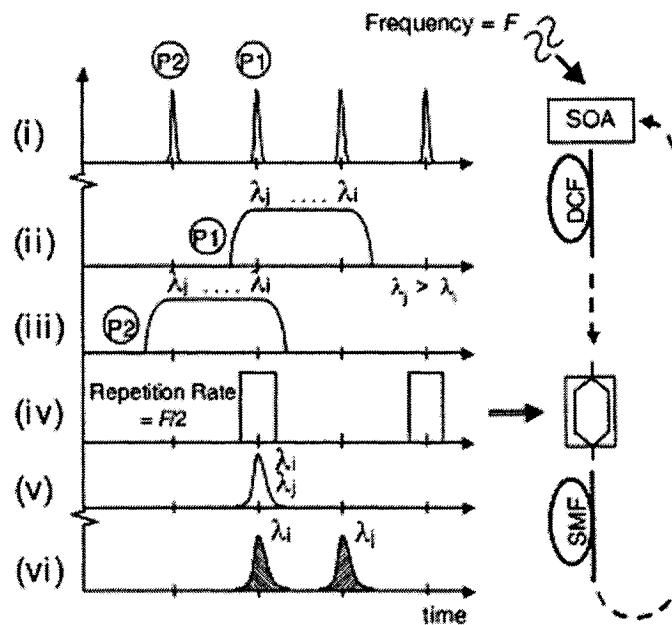


Fig. 3.22 Experimental setup of the SOA-based fiber ring laser. [3.8]

Fig. 3.23 illustrates the principle of pulse generation for the case of two-wavelength output. Multi-wavelength pulses generated from the SOA are dispersed and temporally separated by the dispersion compensating fiber (DCF). A subharmonic modulation signal is applied to EOM 2. At a given driving frequency, selected wavelengths satisfying the transmission window will successfully pass through the modulator. The transmitted pulse contains the two wavelength components simultaneously. Then the pulse is further directed into a piece of standard single mode fiber (SMF) with equal and opposite dispersion to that of the DCF. Finally, the two wavelength components will be temporally separated.



**Fig. 3.23** Operation principle of the pulse source (i) multiwavelength pulses generated from the SOA; (ii) pulse P1 after the DCF; (iii) pulse P2 after the DCF; (iv) subharmonic driving signal of EOM 2; (v) subharmonic gated optical pulse; (vi) optical pulse obtained after SMF. [3.8]

Thus, a pulse train with switching wavelengths is generated at  $F$  and is fed back to the SOA, resulting in the generation of time and wavelength-interleaved pulses in the ring cavity. The exact positions of the lasing wavelengths depend on the delay time between the electrical signals applied to EOM 1 and EOM 2. Only the wavelength components that successfully transmit through EOM 2 are selected for lasing.

### 3.3 Summary

In this chapter, we have provided an overview of SOA basics and several different configurations of mode-locked single and multi-wavelength SFRLs. Techniques used fall under of two classifications: using intracavity modulator or all-optical mode-locking.

A comparison between the main features of these configurations is given in Table 3.2.

Configuration	Multi- $\lambda$ operation	Tunability
Intracavity mode-locked SFRL using an EA modulator [3.13]	No	Yes
Intracavity mode-locked SFRL by using sampled FBG [3.14]	Yes	No
Intracavity mode-locked SFRL using a F-P filter [3.15]	Yes	No
Pulse train generation from all-optical mode-locked SFRL [3.4]	Yes	No
All-optical mode-locked SFRL with a tunable filter [3.5]	No	Yes
All-optical mode-locked SFRL with an optical delay line [3.6]	No	Yes
Electrical wavelength tuning mode-locked SFRL [3.8]	Yes	Yes

**Table 3.2** Comparison between different SFRL configurations

## References:

- [3.1] M. J. Connelly, Semiconductor optical amplifiers, Kluwer Academic, 2002.
- [3.2] J-J. Bernard and M. Renaud, "Semiconductor Optical Amplifier: A key technology for the all optical networks," Alcatel Research and Innovation, 2001
- [3.3] Y. Yamamoto, "Characteristics of AlGaAs Fabry-Perot cavity type laser amplifiers," IEEE J. Quantum Electron., 16, pp.1047-1052, 1980.
- [3.4] K. Vlachos, K. Zoiros, T. Houbavlis, and H. Avramopoulos, "10×30 GHz pulse train generation from semiconductor amplifier fiber ring laser," IEEE Photon. Technol. Lett., 12, 1, pp. 25-27, 2000.
- [3.5] J. He and K. T. Chan, "All-optical actively modelocked fiber ring laser based on cross-gain modulation in SOA," Electron. Lett., 38, 24, pp.1504-1505, 2002.
- [3.6] J. He and K. T. Chan, "Generation and wavelength switching of picosecond pulses by optically modulating a semiconductor optical amplifier in a fiber laser with optical delay line," IEEE Photon. Technol. Lett., 15, 6, pp.798-800, 2003.
- [3.7] K. Vlachos, C. Bintjas, N. Pleros, and H. Avramopoulos, "Ultrafast semiconductor-based fiber laser source," IEEE J. Sel. Topics in Quantum Electron., 10, 1, pp.147-154, 2004.

- [3.8] K. L. Lee and C. Shu, "Switching-wavelength pulse source constructed from a dispersion-managed SOA fiber ring laser," *IEEE Photon. Technol. Lett.*, 15, 4, pp.513-515, 2003.
- [3.9] M. J. Guy, J. R. Taylor, D. G. Moodie, and A. E. Kelly, "10 GHz 3 ps actively mode-locked ring laser incorporating a semiconductor laser amplifier and an electroabsorption modulator," *Electron. Lett.*, 32, 24, pp. 2240–2241, 1996.
- [3.10] C. Peng, M. Yao, J. Zhang, H. Zhang, Q. Xu, and Y. Gao, "Theoretical analysis of actively mode-locked fiber ring laser with semiconductor optical amplifier," *Opt. Commun.*, 209, pp.181–192, 2002.
- [3.11] H. Shi, G. A. Alphonse, J. C. Connolly, and P. J. Delfyett, "20×5 Gbit/s optical WDM transmitter using single-stripe multiwavelength modelocked semiconductor laser," *Electron. Lett.*, 34, 2, pp.179–181, 1998.
- [3.12] K. L. Hall, J. D. Moores, K. A. Rauschenbach, W. S. Wong, E. P. Ippen, and H. A. Haus, "All-optical storage of a 1.25 kb packet at 10 Gb/s," *IEEE Photon. Technol. Lett.*, 7, pp.1093–1095, 1995.
- [3.13] J. Zhang, M. Yao, and etc., "10 GHz actively mode-locked pulse generation employing a semiconductor optical amplifier and an electroabsorption modulator in a fiber ring," *Optics Communications*, 197, pp.385–391, 2001.
- [3.14] B.A. Yu, D.H. Kim and etc., "Multiwavelength pulse train generation in semiconductor fiber ring laser using sampled fiber grating," WR5, IEEE LEOS, 2000.
- [3.15] T. Papakyriakopoulos, A. Stavdas, and etc., "10×10 GHz simultaneously modelocked multiwavelength fiber ring laser," *Electronics Letters*, 35, 9, pp.717–718, 1999.

## **Chapter 4**

# **Electrically tunable single wavelength semiconductor fiber ring lasers**

From the above survey on different configurations and diversified applications of mode-locked semiconductor fiber ring lasers (SFRLs), we get to know their advantages and should direct more effect to their research. As is known, tunable optical pulse sources are of interest for applications in optical instrumentation, telecommunications, and sensing. Several groups have reported the mode-locked SFRLs where a SOA serves as both the gain medium and as the mode-locking element [4.1]-[4.5].

In some applications, it is important to be able to tune the output wavelength(s) of the optical pulse source. In addition to tunable optical filters, wavelength tuning can be achieved using dispersion tuning, i.e. using a cavity with high dispersion and by changing the modulation frequency of the mode-locking element [4.6]. The characteristics of dispersion-tuned mode-locked erbium doped fiber ring lasers (EDFRLs) have been investigated and electrically tuned, single and multi-wavelength EDFRLs with continuous wavelength tuning have been demonstrated [4.7] – [4.9].

In this chapter, we describe the design concept, experimental setup, and experimental results of mode-locked SFRLs with tunable single wavelength operation. We discuss multi-wavelength operation of the sources in chapter 5.

## 4.1 Brief description of dispersion tuning [4.10]

Ultrashort optical pulses have been generated in mode-locked fiber lasers with several configurations in which a number of optical filters were used to select wavelengths [4.11]-[4.13]. It is not always a straightforward proposition to design a multi-wavelength non-dispersive filter. If the filter is dispersive, i.e. a group delay exists between the different wavelengths, this then creates two main problems: (1) the cavity length of each wavelength needs to be precisely adjusted; (2) a number of feedback systems, equal to the number of wavelengths, are needed to stabilize the cavity lengths of such a laser. By using birefringent components, simultaneous generation of two or four wavelength optical pulses was demonstrated in an actively mode-locked fiber laser [4.14],[4.15]. Although this scheme overcomes the above-mentioned shortcomings, as the multiwavelength pulses were achieved by polarization dispersion in a number of birefringent components, the wavelengths could not be tuned and each birefringent component needed to be carefully adjusted. We can overcome the above-mentioned problems in an actively mode-locked fiber ring laser by using a cavity with high dispersion by changing the modulation frequency.

Fig. 4.1. shows the schematic of one laser, in which some dispersion compensation fiber (DCF) with large dispersion parameter is used in order to increase the dispersion of the laser cavity. The dispersion parameter  $D_d$  of the DCF is  $-95$  ps/nm km at  $\sim 1.5 \mu\text{m}$ .

The  $m$ th harmonic frequency of the laser cavity can be expressed as

$$f = \frac{mc}{n(\lambda)L + n_d(\lambda)L_d} \quad (4.1)$$

where  $\lambda$  is light wavelength,  $c$  is light velocity in vacuum, and  $L$  is the cavity length excluding the length of the DCF,  $L_d$  is the length of DCF, and  $n$  and  $n_d$  are the group indices of single mode fiber (SMF) and the DCF, respectively.

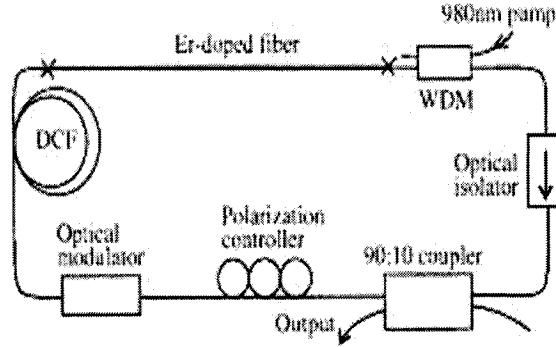


Fig. 4.1 Experimental setup. [4.10]

The derivative of  $f$  with respect to  $\lambda$  can be written as

$$\frac{df}{d\lambda} = -\frac{f^2}{m} [D(\lambda)L + D_d(\lambda)L_d] \quad (4.2)$$

where  $D(\lambda)$  and  $D_d(\lambda)$  are respectively the dispersion parameters of normal fiber and DCF in the laser cavity. (4.1) and (4.2) show that the fundamental and harmonic frequencies are all wavelength dependent. Thus, when the laser is modulated at the fundamental or one of the harmonics, the emission wavelength of the laser can be tuned continuously by changing the modulation frequency.

## 4.2 Mode-locking using an intracavity modulator

### 4.2.1 Operation description

Fig. 4.2 shows the schematic of our mode-locked SFRL using an intracavity modulator. We use an electro-optic modulator (JDS Uniphase 10 Gb/s modulator) driven

by a sinusoidal signal from an RF generator for mode-locking. A single linearly chirped fiber Bragg grating (LCFBG) is used to provide wavelength selection and dispersion (please refer to the Appendix A for more details about FBGs and the LCFBG).

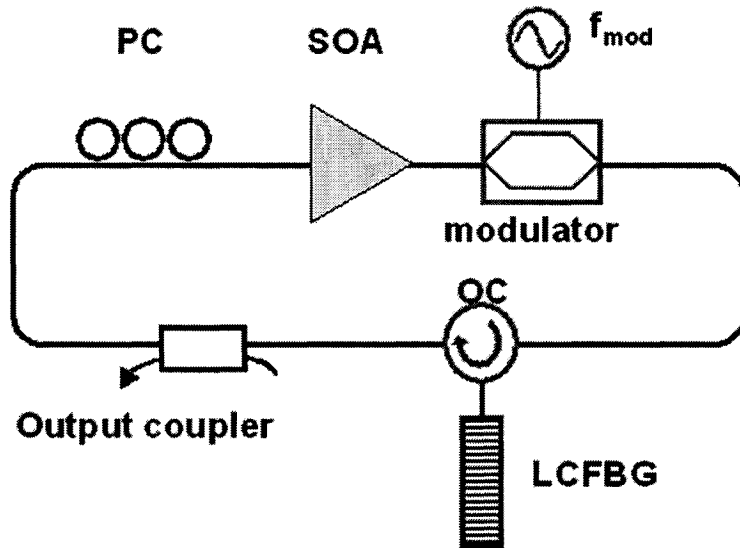


Fig. 4.2 Schematic of the mode-locked semiconductor fiber ring laser with intracavity modulator. OC: optical circulator, MOD: electro-optic modulator, PC: polarization controller.

The LCFBG used in this experiment is oriented with the reflections from longer wavelengths occurring closer to the optical circulator (OC). The OC is used to convert the reflective characteristic of the LCFBG to transmission type while also serving as an optical isolator. The  $m$ th harmonic frequency of the laser cavity can be expressed as

$$f = \frac{mc}{n(L_c + L_g)} \tag{4.4}$$

$$L_g = 2(\lambda - \lambda_{low}) / D \tag{4.5}$$

where  $D$  is the chirp constant of the grating,  $\lambda$  is light wavelength,  $\lambda_{low}$  is the shortest wavelength of the reflection bandwidth of the LCFBG,  $c$  is light velocity in vacuum,  $n$  is the refractive index of the fiber, and  $L_c$  is the cavity fiber length excluding the length of the fiber grating. (4.5) shows that the fundamental and harmonic frequencies are all

wavelength dependent. Thus, when the laser is modulated at the fundamental or one of the harmonics, the emission wavelength of the laser can be tuned continuously by changing the modulation frequency.

The reflectivity and group delay of the LCFBG used in this experiment is shown in Fig. 4.3. This single LCFBG has a 3 dB bandwidth of 2.7 nm, a peak reflectivity of 82%, and a dispersion of 68 ps/nm.

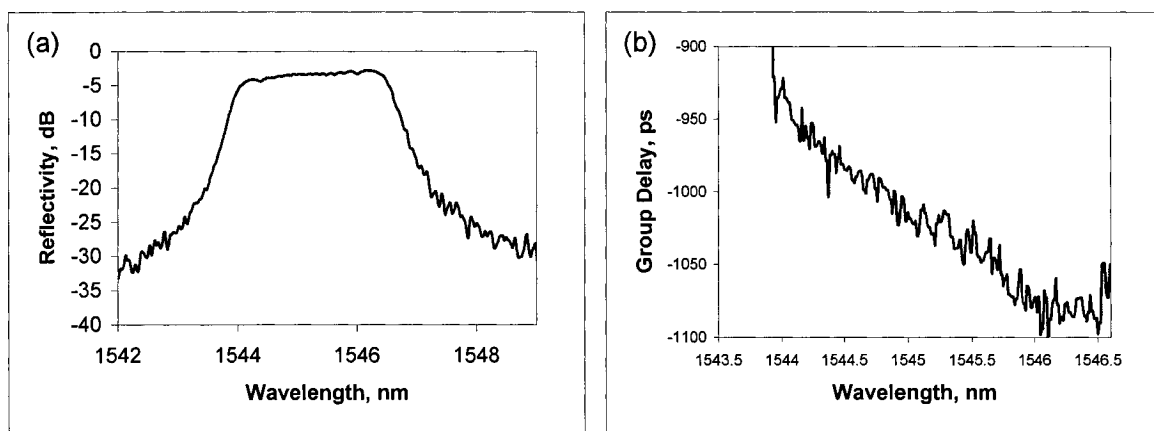


**Fig. 4.3** The characteristics of the single LCFBG (a) reflectivity, (b) group delay.

We use the Avanex 1901 SOA (Fig. 4.4), a Semiconductor Optical Amplifier module based on an InGaAsP chip, manufactured using Avanex's BRS (Buried Ridge Stripe) 2" wafer technology. The characteristics of the SOA module are given in Table 4.1.

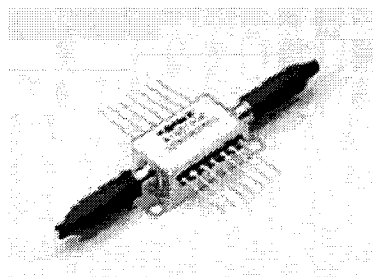


**Fig. 4.4** The Avanex A1901 SOA module [4.16]

<b>Electro-optical characteristics (25 °C )</b>	
Wavelength of max gain at 200 mA	1513 nm
Fiber to fiber gain at 2000mA Pin = -25 dBm	21.77 dB
Gain ripple at 200mA, over C band	0.2 dB
Polarization sensitivity at 200 mA, 1550 nm	1.31 dB
Noise figure	6.99 dB
Max output power at 200 mA	9.2 dB
Optical Bandwidth at -1 dB	37 nm
Optical Bandwidth at -3 dB	70 nm

**Table 4.1** Characteristics of the A1901 SOA module. [4.16]

## 4.2.2 Experiments and results

In this set of experiments, we began by investigating the impact of varying the operating conditions on the laser output characteristics for a fixed modulator bias voltage of 5.1 V. The laser output is observed using an optical spectrum analyzer (OSA) with 0.06 nm resolution and a high-speed photodetector connected to a sampling oscilloscope (CSA) with a combined impulse response time of  $\approx 16$  ps.

With a modulation frequency ( $f_{mod}$ ) of 5252.668 MHz, the corresponding output lasing wavelength is 1545.39 nm. Fig. 4.5 shows the output spectrum and temporal waveforms under different values of SOA bias current ( $I_{SOA}$ ). Fig. 4.6 shows the corresponding pulse widths, 3 dB bandwidths, and time bandwidth products. From the below pulse characteristics, we find that as  $I_{SOA}$  increases between 120 mA and 140 mA, the 3 dB bandwidth is approximately constant, and the pulse duration increases. The time

bandwidth products of the output pulses are  $\approx 0.86 - 0.88$ . As expected, the average output power from the laser also increases with increasing  $I_{SOA}$ .

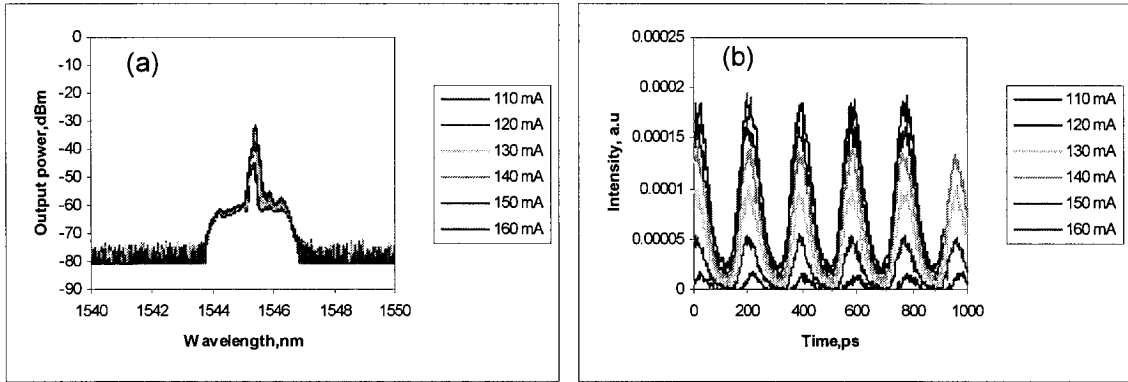


Fig. 4.5 Output spectral (a) and temporal (b) characteristics under different SOA bias currents.

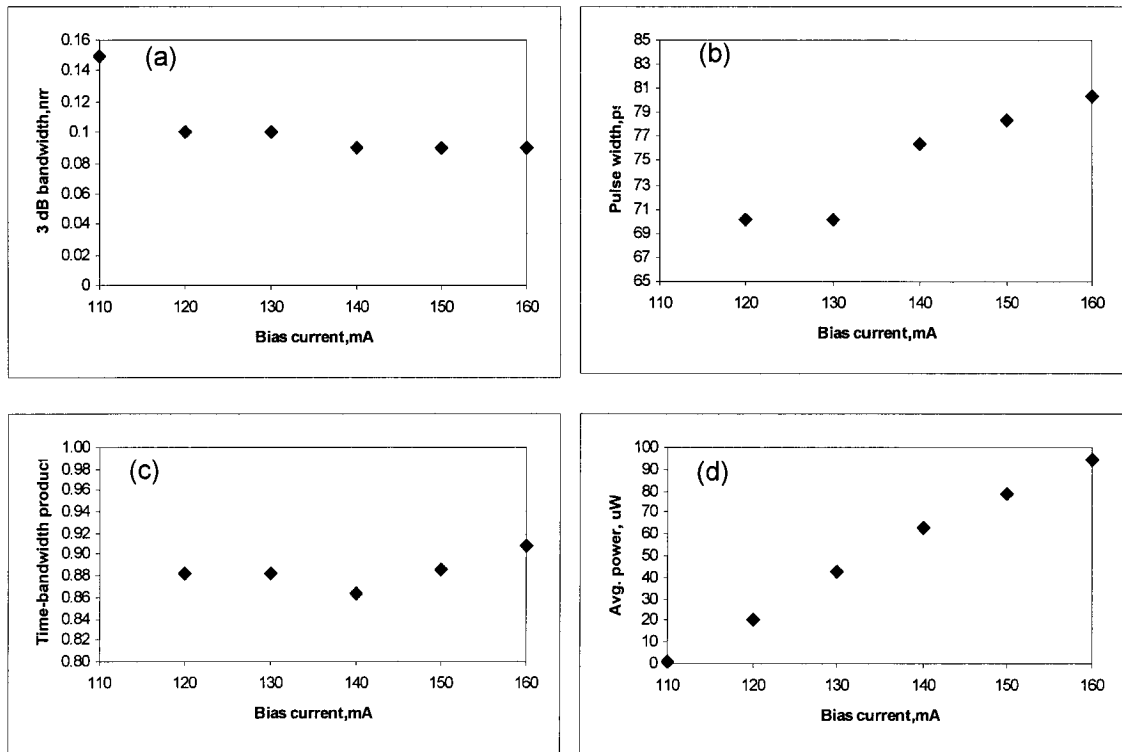


Fig. 4.6 Output pulse characteristics under different SOA bias currents: (a) 3 dB bandwidth; (b) pulse width; (c) time-bandwidth product; (d) average output power.

An optimum value of  $I_{SOA}$  is  $\approx 140$  mA where the time bandwidth product is  $\approx 0.86$  and reasonable average output power can be obtained (in this case,  $63 \mu\text{W}$ ).

Next, we fix the bias current  $I_{SOA} = 138$  mA. Fig. 4.7 shows the wavelength tuning characteristics as the modulation frequency is varied from 5245.911 MHz to 5254.795 MHz. During tuning, only  $f_{mod}$  is changed while all other settings are kept constant. The lasing wavelengths can be tuned over a range of 2.26 nm (from 1544.2 nm to 1546.45 nm) with a tuning rate of 0.63 nm/MHz. Note that the tuning is periodic with  $f_{mod}$  and the periodicity corresponds to the fundamental frequency of the laser cavity, which was determined to be  $\approx 5.0$  MHz.

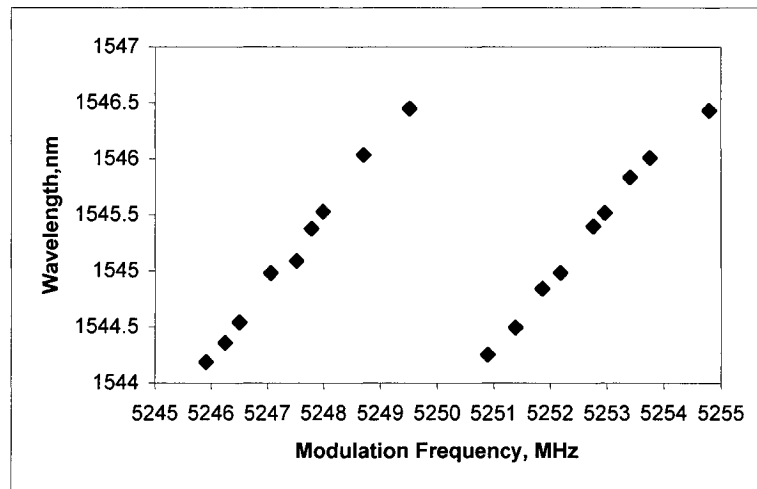
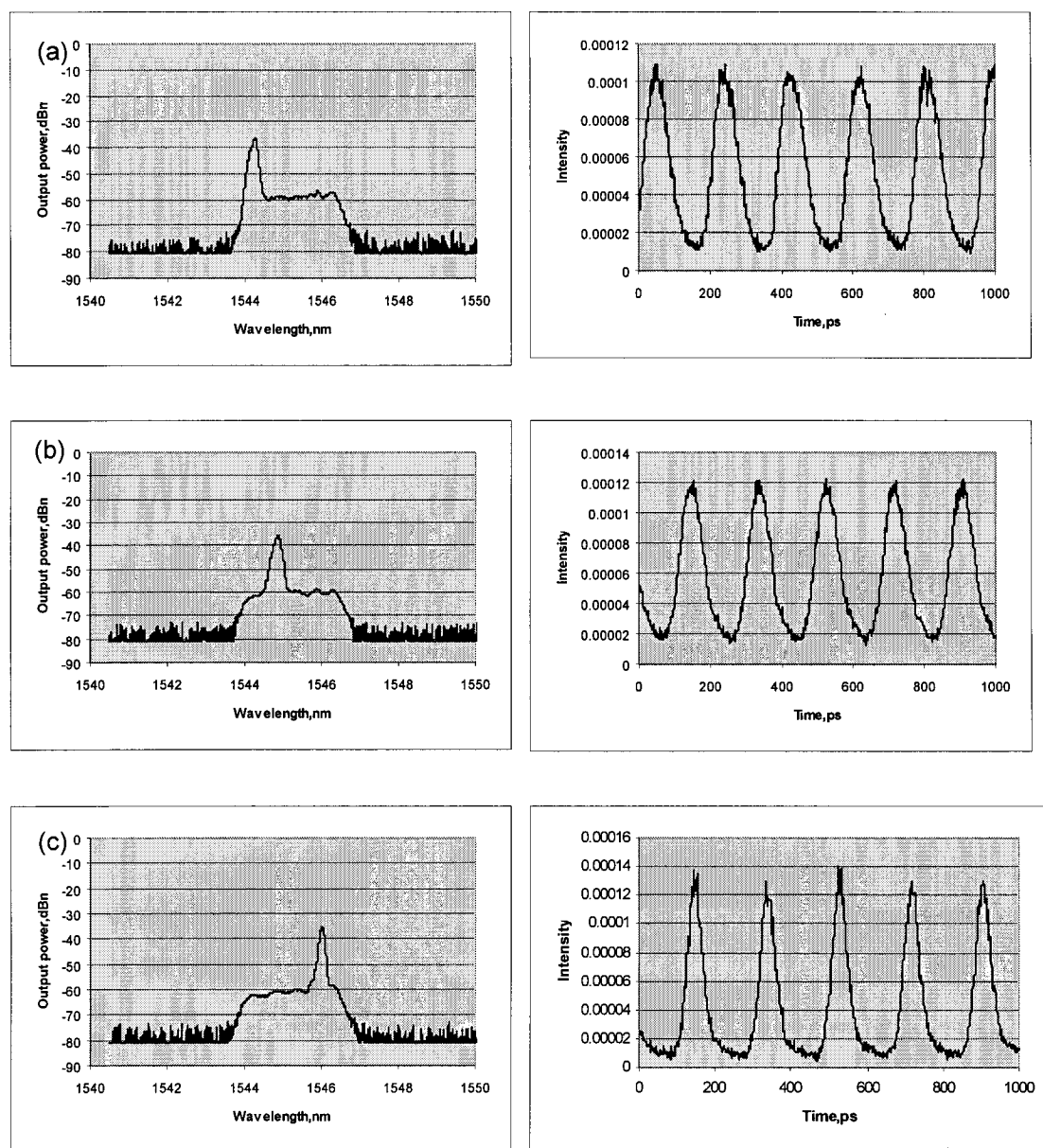


Fig. 4.7 Tuning characteristics of the SFRL using the single LCFBG.

Fig. 4.8 highlights sample traces of the output spectrum and waveforms of the laser for three different modulation frequencies.



**Fig. 4.8** Output spectral and temporal characteristics of the SFRL using the single LCFBG for  $f_{mod} =$  (a) 5250.894 MHz, (b) 5251.864 MHz, and (c) 5253.764 MHz.

Throughout the tuning range, the pulse widths, 3 dB bandwidths, and corresponding time bandwidth products range from 43 ps – 84 ps, 0.09 nm – 0.16 nm, and 0.69 – 1.32, respectively, indicating that the pulses are chirped. Fig. 4.9 summarizes the output pulse

characteristics. The average signal to noise ratio for each lasing wavelength is more than 24 dB and the average output power is typically greater than 30  $\mu\text{W}$ . When the RF signal was shut off, the laser output spectrum changed completely and the laser no longer emitted the wavelength.

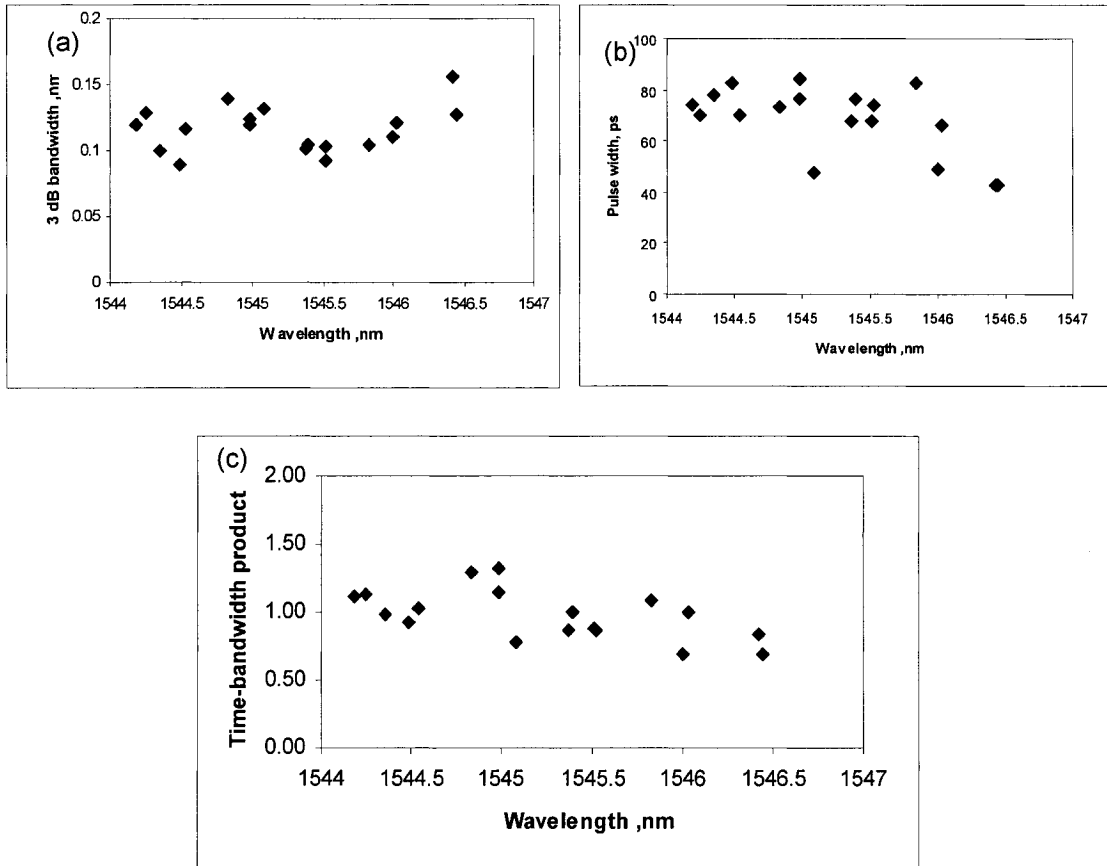


**Fig. 4.9** Output pulse characteristics of the SFRL: (a) 3 dB bandwidth, (b) pulse width, (c) time-bandwidth product.

In summary, we have successfully demonstrated a stable implementation for an electrically tuned actively mode-locked fiber ring laser with SOA and intracavity modulator where the key component is an LCFBG.

## 4.3 All-optical mode-locking

### 4.3.1 Design concept

In the laser configuration described in the previous section, the SOA is used as gain medium in the ring and an amplitude modulator (AM) is used to modulate the loss in the cavity to obtain an electrically tunable mode-locked SFRL. Recently, researchers have investigated more advanced mode-locked SFRLs [4.1]-[4.5]. In particular, as discussed in Section 3.2.2.2, injecting an external optical control signal will modulate the gain of the SOA such that mode-locking can be obtained via cross-gain modulation (XGM) [4.2]-[4.4], i.e. the SOA functions as an optically controlled intensity modulator. Indeed, short optical pulses at single or multiple wavelengths have been generated using such mode-locked SFRLs.

In our design, we combine the dispersion tuning technique with the use of an SOA as a gain and optically controlled intensity modulator to demonstrate an all-optically mode-locked, wavelength tunable SFRL. Again, an LCFBG is used to define the wavelength range of the laser output and to provide most of the cavity dispersion required for dispersion tuning. The output wavelength can be tuned continuously (within the grating bandwidth) by varying the frequency of the optical control signal with a tuning rate set by the grating chirp. The use of LCFBGs to provide the required dispersion results in a short cavity length, which reduces the output sensitivity to environmental perturbations. In addition to combining both gain and modulation functions in a single device, the use of SOA allows for stable operation at room temperature and any wavelength band. As a result, we are not constrained to the C- and L-bands as with EDFLs. In this section, we

demonstrate the single wavelength operation and obtain picosecond pulses with higher signal-to-noise ratio (compared with the results in the intracavity modulator approach).

### 4.3.2 Operation description

A schematic of our all-optically mode-locked SFRL is shown in Fig. 4.10. The laser cavity comprises a 1550 nm SOA, two polarization independent optical circulators (OCs), one of which is connected to the LCFBG, a polarization controller, and a 10:90 output coupler.

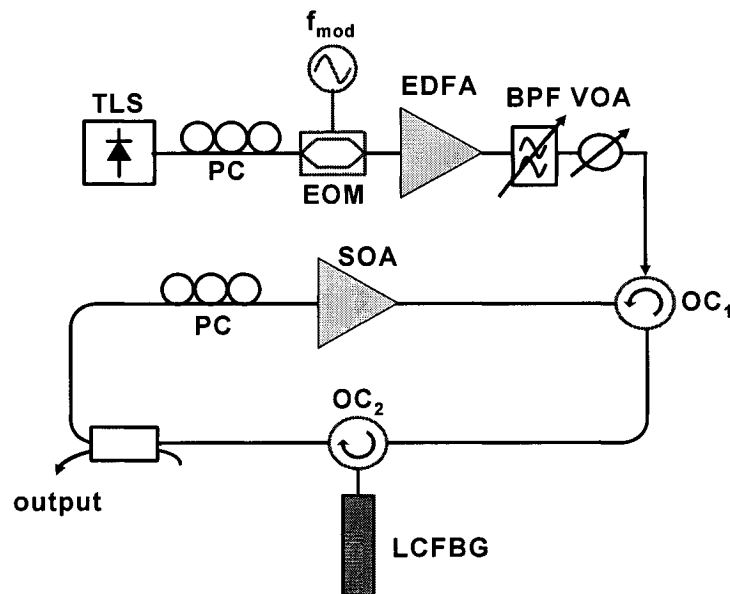


**Fig. 4.10** Schematic of all-optically mode-locked semiconductor fiber ring laser. TLS: tunable laser source, BPF: bandpass filter, EOM: electro-optic modulator, PC: polarization controller.

Again, we use the same SOA as in the intracavity modulator approach. The control signal is obtained by modulating the output from a tunable laser with a sinusoidal signal from an RF generator and amplified by an EDFA (ASE noise is reduced by using a tunable bandpass filter having a 3 dB bandwidth of 0.4 nm). The control signal, whose average power is adjusted using the variable optical attenuator (VOA), is injected into the cavity through OC1 in the opposite direction to the lasing signal; it is blocked

subsequently by OC2. The circulators ensure unidirectional operation of the ring laser. The grating bandwidth defines the wavelength range (tuning range) of the laser output; the chirp provides the cavity dispersion required for tuning and also sets the tuning rate. When the control signal is injected into the cavity, mode-locking is obtained via intensity modulation (due to XGM in the SOA) at a wavelength within the grating bandwidth that is self-tuned to the modulation frequency  $f_{mod}$  of the control signal. As before, the laser output is observed using an OSA, CSA, and also an autocorrelator.

### 4.3.3 Experiments and results

In this set of experiments, we use the same LCFBG as in Section 4.2 for the intracavity modulator approach. We begin by investigating the impact of varying different operating conditions on the laser output characteristics. Fig. 4.11 (a) and (b) show the pulse widths, 3 dB bandwidths, and time bandwidth products for different values of SOA bias current  $I_{SOA}$  and control signal average power  $P_{avg}^{control}$  respectively. The control signal wavelength is set at 1555 nm and  $f_{mod} = 5257.199$  MHz. The corresponding output lasing wavelength is 1545.3 nm. For a fixed  $P_{avg}^{control}$  of 2.9 mW, we find that for  $I_{SOA}$  between 120 mA and 135 mA, the time bandwidth products of the output pulses are  $\approx 0.5 - 0.55$ . Again, further increases in bias current result in larger bandwidth, but also longer pulse durations as well as increased output power. When we fix  $I_{SOA} = 135$  mA, we find that pulse widths and average output power decrease with increasing  $P_{avg}^{control}$ . An optimum value of  $P_{avg}^{control}$  is 2.9 mW where the time bandwidth product is also  $\approx 0.55$  and reasonable average output power can still be obtained (in this case, 70  $\mu$ W). When we use control signal wavelengths of 1540 nm and 1548 nm, we obtain similar output pulse characteristics

when  $P_{avg}^{control}$  are optimized for a given  $I_{SOA}$ . Thus, we conclude that all-optical mode-locking is equally effective using control signal wavelengths that are longer or shorter than the lasing wavelength, as shown in Fig. 4.12.

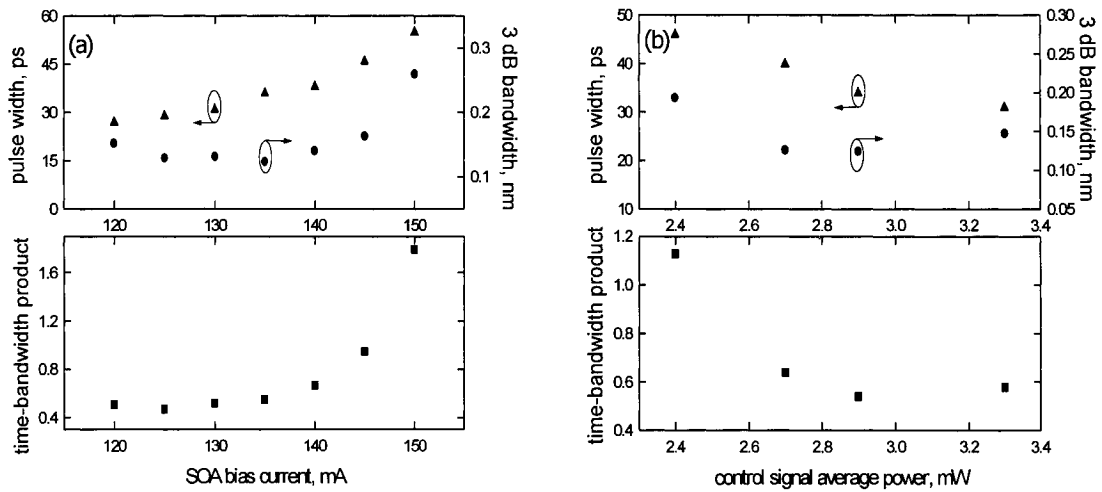


**Fig. 4.11** Output pulse characteristics as a function of (a) SOA bias current (with  $P_{avg}^{control} = 2.9$  mW) and (b) control signal average power (with  $I_{SOA} = 135$  mA). In all cases, the control signal wavelength is 1555 nm.

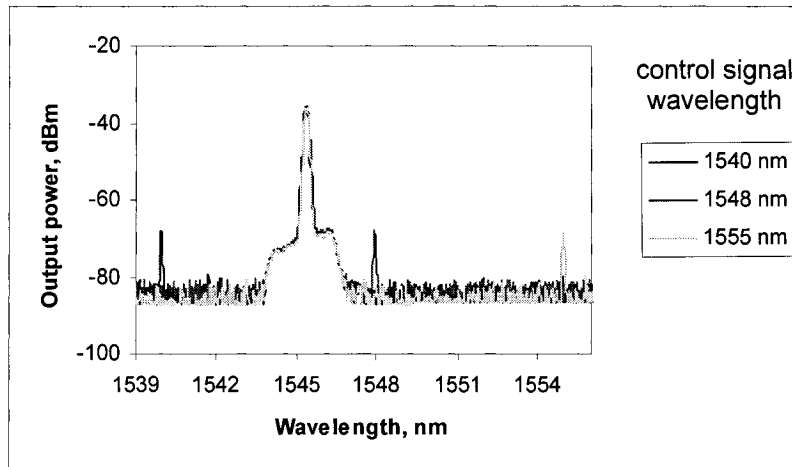


**Fig. 4.12** Output spectral characteristics using different control signal wavelengths.

Then, we fix  $I_{SOA} = 136$  mA and set the control signal at 1555 nm with  $P_{avg}^{control} = 2.9$  mW. Fig. 4.13 (a) depicts the wavelength tuning characteristics as the frequency  $f_{mod}$  of

the control signal is varied from 5248.8 MHz to 5259.4 MHz. During tuning, only  $f_{mod}$  is changed while all other settings are kept constant. The lasing wavelengths can be tuned over a range of 2.2 nm (from 1544.2 nm to 1546.4 nm) with a tuning rate of 0.51 nm/MHz. Note that the tuning is periodic with  $f_{mod}$  and the periodicity corresponds to the fundamental frequency of the laser cavity, which was determined to be  $\approx 6.16$  MHz.

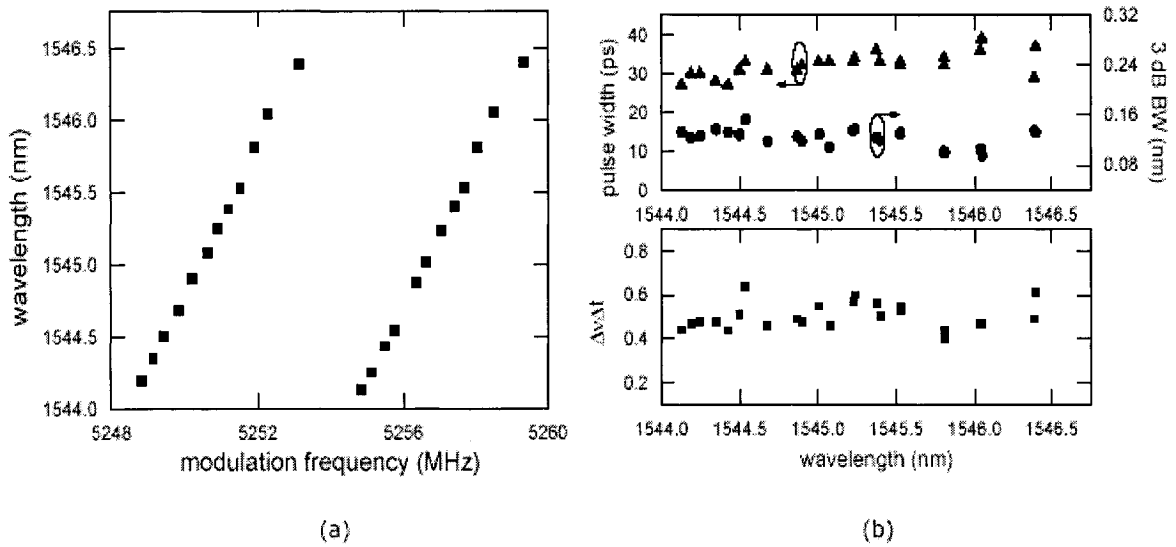


Fig. 4.13 (a) Tuning and (b) output pulse characteristics of the ML-SFRL using the single LCFBG.

Fig. 4.14 highlights sample traces of the output spectrum and waveforms of the laser for three different modulation frequencies. The inset shows a typical auto-correlation trace of the output pulses along with a  $\text{sech}^2$  fit. Throughout the tuning range, the pulse widths, 3 dB bandwidths, and corresponding time bandwidth products range from 27 ps – 39 ps, 0.1 nm – 0.16 nm, and 0.40 – 0.64, respectively, indicating that the pulses are slightly chirped. Fig. 4.13(b) summarizes the output pulse characteristics. The average signal-to-noise ratio for each lasing wavelength is more than 35 dB and the average output power is typically greater than 35  $\mu\text{W}$ . When no control signal was injected into the laser cavity, we did not obtain any output lasing signal, as shown in Fig. 4.15.

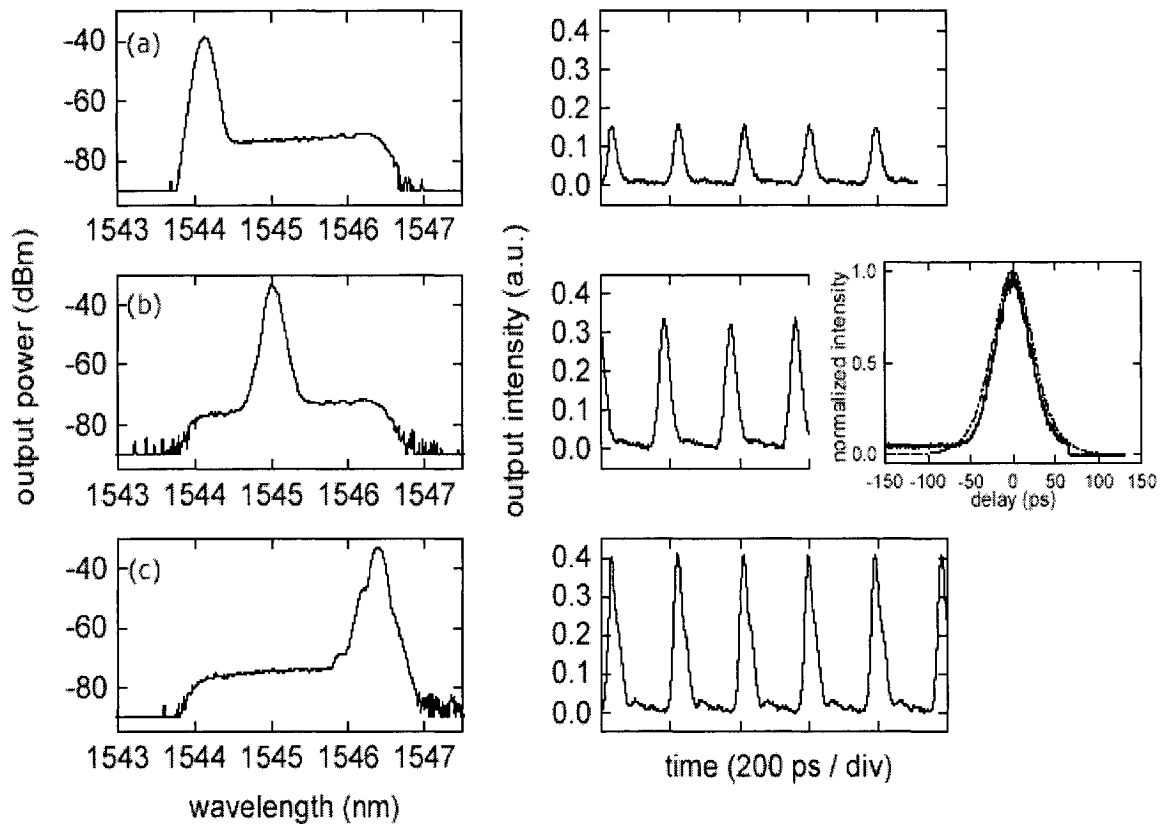


Fig. 4.14 Spectral and temporal characteristics of the output pulses for  $f_{mod}$  = (a) 5254.842 MHz, (b) 5256.641 MHz, and (c) 5259.335 MHz. Inset: typical auto-correlation trace with  $\text{sech}^2$  fit.

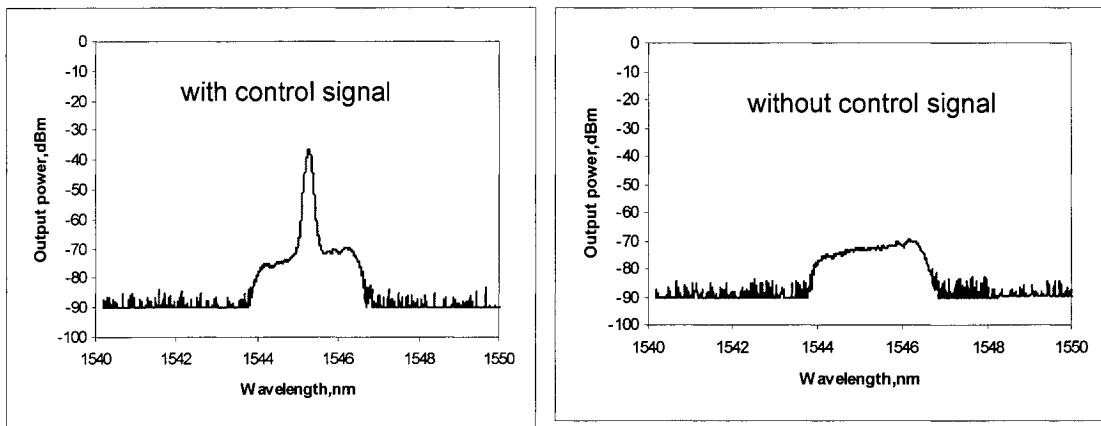


Fig. 4.15 Output spectral change under with and without the control signal.

## 4.4 Discussion and summary

We have successfully demonstrated the generation of wavelength tunable picosecond pulses from mode-locked SFRLs using an intracavity modulator and an external control optical signal. In both cases, the output wavelength can be tuned electrically by varying the frequency of the RF control signal. An LCFBG works as the key component. We use it to define the wavelength range of the laser output and to provide most of the cavity dispersion required for dispersion tuning. The output wavelength can be tuned continuously within the grating bandwidth by varying the frequency of the RF control signal with a tuning rate set largely by the grating chirp. Using LCFBG to provide the required dispersion results in a short cavity length that reduces the output sensitivity to environmental perturbations. In the experiments, the mode-locking behavior at different repetition frequencies is similar. Both spectra and pulse trains can be recorded simultaneously. Moreover, the output waveforms are all stable and no mode hopping can be observed when the laser has been mode-locked for four hours.

In contrast with EDFLs, the use of the SOAs allows for compact and relatively low-cost applications with stable room temperature operation. Compared with the intracavity modulator approach, the all-optically mode-locked approach uses the SOA as both the gain medium and the mode-locker. Furthermore, we have less cavity loss in this case, so that less gain is required to reach lasing threshold. In turn, the noise level is lower, and higher SNR can be obtained.

Based on our experimental results, we can generate close to transform-limited pulses with high SNR. Moreover, as the proposed scheme works all-optically, it can be useful in applications such as all-optical clock extraction and optical sensors.

## References:

- [4.1] K. Vlachos, K. Zoiros, T. Houbavlis, and H. Avramopoulos, "10×30 GHz pulse train generation from semiconductor amplifier fiber ring laser," *IEEE Photon. Technol. Lett.*, 12, 1, pp. 25-27, 2000.
- [4.2] J. He and K. T. Chan, "All-optical actively modelocked fiber ring laser based on cross-gain modulation in SOA," *Electron. Lett.*, 38, 24, pp. 1504-1505, 2002.
- [4.3] J. He and K. T. Chan, "Generation and wavelength switching of picosecond pulses by optically modulating a semiconductor optical amplifier in a fiber laser with optical delay line," *IEEE Photon. Technol. Lett.*, 15, 6, pp. 798-800, 2003.
- [4.4] K. Vlachos, C. Bintjas, N. Pleros, and H. Avramopoulos, "Ultrafast semiconductor-based fiber laser source," *IEEE J. Sel. Topics in Quantum Electron.*, 10, 1, pp. 147-154, 2004.
- [4.5] K. L. Lee and C. Shu, "Switching-wavelength pulse source constructed from a dispersion-managed SOA fiber ring laser," *IEEE Photon. Technol. Lett.*, 15, 4, pp. 513-515, 2003.
- [4.6] K. Tamura and N. Nakazawa, "Dispersion-tuned harmonically mode-locked fiber ring laser for self-stabilization to an external clock," *Opt. Lett.*, 21, pp. 1984-1986, 1996.
- [4.7] C. Shu and Y. Zhao, "Characteristics of dispersion-tuning in harmonically mode-locked fiber laser," *IEEE Photon. Technol. Lett.*, 10, 8, pp. 1106-1108, 1998.
- [4.8] G. E. Town, L. Chen, and P. W. E. Smith, "Dual wavelength modelocked fiber laser," *IEEE Photon. Technol. Lett.*, 12, pp. 1459-1461, 2000.
- [4.9] S. Li and K. T. Chan, "Electrical wavelength-tunable actively mode-locked fiber ring laser with a linearly chirped fiber Bragg grating," *IEEE Photon. Technol. Lett.*, 10, 6, pp. 799-801, 1998.
- [4.10] S. Li and K.T. Chan, "Electrical wavelength tunable and multiwavelength actively mode-locked fiber ring laser," *Applied physics letters*, 72, 16, pp.1954-1956, 1998.
- [4.11] D.A. Pattison, P.N. Kean, J.W. D. Gray, I. Bennion, and N.J. Doran, "Actively modelocked dual-wavelength fiber laser with ultra-low inter-pulse-stream timing jitter," *IEEE Photonics Technol. Lett.*, 7, 12, pp.1415-1417, 1995

[4.12] D.U. Noske, M. J. Guy, and K. Rottwitt, R. Kashyap, and J. R. Taylor, "Dual-wavelength operation of a passively mode-locked "figure-of-eight" ytterbium-erbium fibre soliton laser," *Opt. Commun.*, 108, 4-6, pp.297-301, 1994.

[4.13] S.P. Li, H. Ding, and K.T. Chan, "Dual-wavelength actively mode-locked Er-doped fibre ring laser with fibre gratings," *Electron. Lett.*, 33, 5, pp.390-392, 1997.

[4.14] J.B. Schlarger, S. Kawanishi, and M. Saruwatari, "Dual wavelength pulse generation using mode-locked erbium-doped fibre ring laser," *Electron. Lett.*, 27, 22, pp.2072-2073, 1991

[4.15] H.Takara, S.Kawanishi, M. Saruwatari, and J. B. Schlarger, "Multiwavelength birefringent-cavity mode-locked fibre laser," *Electron. Lett.*, 28, 25, pp. 2274-2275, 1992.

[4.16] Avanex 1901 SOA module measurement sheet, Avanex Corp., 2004.

## Chapter 5

# Electrically tunable multi-wavelength semiconductor fiber ring lasers

Based on the success of achieving single wavelength operation from SFRLs in chapter 4, in this chapter, we extend the results and consider mode-locked SFRLs with tunable multi-wavelength operation.

### 5.1 Brief description of multi-wavelength dispersion tuning [5.1]

As mentioned in Chapter 4, in dispersion-tuned lasers, the emission wavelength can be tuned continuously by changing the modulation frequency. Since the wavelength tuning range ( $\leq$  the gain bandwidth of the Er-doped fiber) is much smaller than the light wavelength as well as far it is away from the zero-dispersion wavelengths of the SMF and the DCF,  $D$  and  $D_d$  can be assumed to be constant in the tuning range. From (4.1), the frequency difference between the  $m$ th harmonic of the wavelength  $\lambda_l$  and the  $(m + N)$ th harmonic of wavelength  $\lambda_s$  ( $\lambda_l$  and  $\lambda_s$  are the longest and shortest wavelengths of the gain bandwidth of the Er-doped fiber,  $N$  is positive integer) is given by

$$\Delta f = \frac{mc}{n(\lambda_l)L + n_d(\lambda_l)L_d} - \frac{(m + N)c}{n(\lambda_l)L + n_d(\lambda_l)L_d + c(DL + D_dL_d)(\lambda_s - \lambda_l)} \quad (5.1)$$

If  $N = 1$  and  $\Delta f < 0$ , the laser can only work with one wavelength in the entire tuning range when laser is modulated at the  $m$ th or lower harmonic orders. If  $\Delta f \geq 0$ ,  $(N + 1)$  wavelengths may simultaneously be mode-locked when the laser is modulated at the  $m$ th

or higher harmonic orders. Therefore, dispersion-tuned lasers can produce not only single wavelength tunable pulses but also multi-wavelength tunable pulses if they are modulated at the proper harmonic orders. By analyzing (5.1), it is found that if we want to get single wavelength tunable pulses at higher repetition rates we can increase the ratio of the laser cavity length to the grating length; conversely, multi-wavelength tunable pulses can be obtained at lower modulation frequencies by decreasing this ratio. In other words, the laser could be tuned within the bandwidth of the LCFBG by changing the modulation frequency.

## 5.2 Mode-locking using an intracavity modulator

### 5.2.1 Operation description

Fig. 5.1 shows the schematic of our multi-wavelength dispersion-tuned SFRL using an intracavity modulator and SI-LCFBGs.

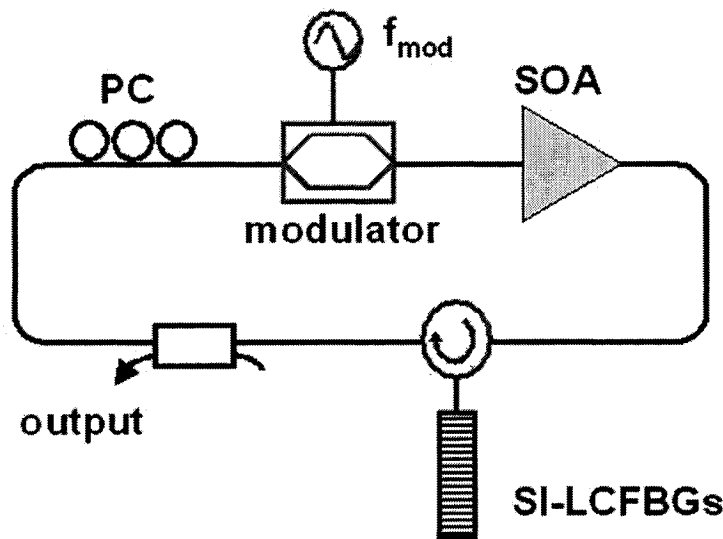


Fig. 5.1 Schematic of the SFRL using SI-LCFBGs.

The use of SI-LCFBGs ensures that the lasing wavelengths have the same cavity length and the grating chirp provides the dispersion required for tuning. This laser design

simplifies the requirements for multi-wavelength operation since for a given modulation frequency  $f_{mod}$ , each lasing wavelength (defined by each FBG) will be self-tuned, in other words, we do not require specific conditions between modulation frequency and the cavity dispersion as described above.

Again, we use the same SOA and electro-optic modulator (JDS Uniphase 10 Gb/s modulator) as before. The reflectivity and group delay of the two SI-LCFBGs are shown in Fig. 5.2. Other than their central wavelengths, the gratings were designed to have identical properties. However, slight deviations occurred during fabrication: the gratings have 3 dB bandwidths (BWs) of 4.4 nm and 4.9 nm, and the corresponding dispersions are 53.6 ps/nm and 46.7 ps/nm. Both gratings have a peak reflectivity about 80% and are spectrally separated by 5.8 nm.

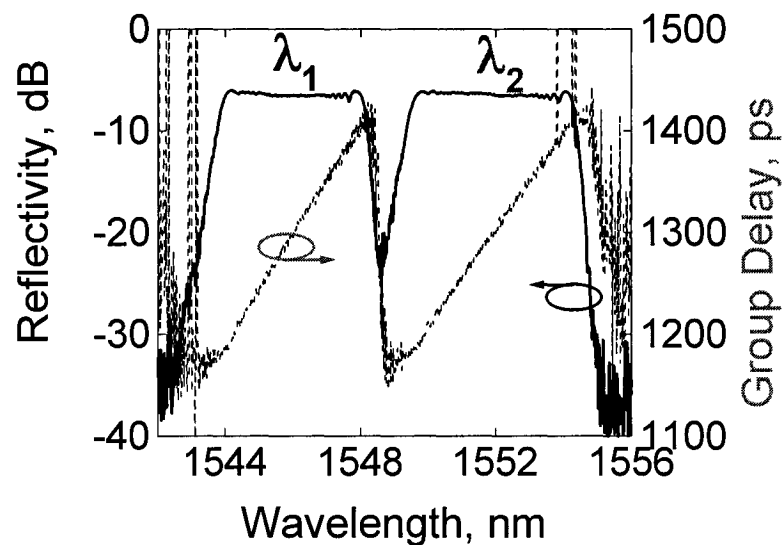


Fig. 5.2 SI-LCFBGs characteristics.

## 5.2.2 Experiments and results

In this set of experiments, we use a bias current  $I_{SOA} = 123$  mA. Fig. 5.3 shows the wavelength tuning characteristics as the modulation frequency is varied from 5403.375 MHz to 5411.702 MHz. During tuning, only  $f_{mod}$  was changed; all other settings were kept constant. Both wavelengths can be simultaneously tuned with a wavelength separation that varies from 5.8 nm to 6.2 nm (which corresponds approximately to the wavelength separation of the FBGs and is not constant since the tuning rates are not identical). The tuning range is set by the bandwidths of the FBGs; the tuning rate depends on the grating dispersion. Since the FBGs have slightly different BWs and dispersion, each wavelength has a slightly different tuning range and tuning rate. For this grating orientation, the wavelengths increase with increasing the  $f_{mod}$  (we obtain an opposite behavior when the grating orientation is reversed). Note also that the tuning is periodic with  $f_{mod}$ . The periodicity corresponds to the fundamental frequency of the laser cavity, which was determined to be about 4.8 MHz for both wavelengths. This indicates that both wavelengths are mode-locked at the same harmonic (in contrast with [5.1]).

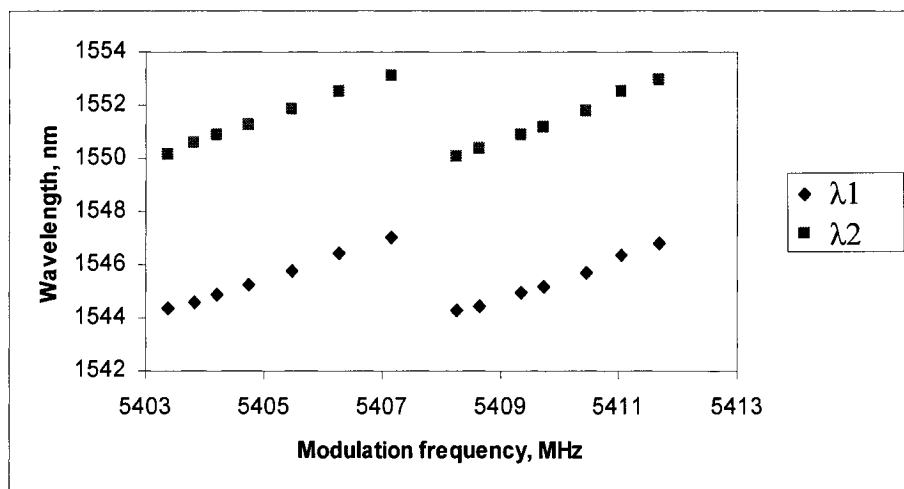
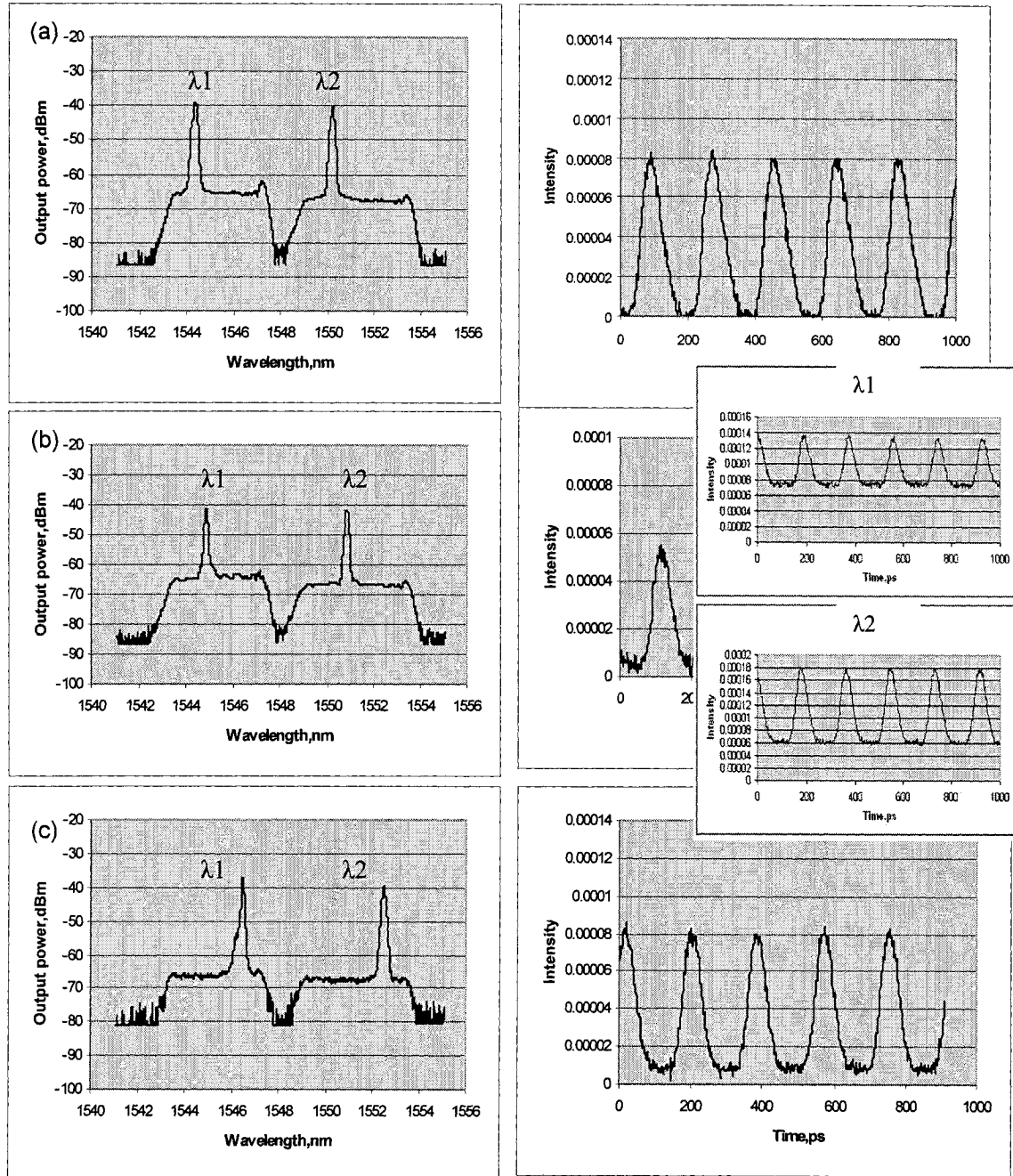


Fig. 5.3 Tuning characteristics of the laser.

Fig. 5.4 shows examples of the output spectrum and waveforms of the laser for three different modulation frequencies. The inset shows the output pulses at each lasing



**Fig.5.4** Spectral and temporal characteristics of the laser for  $f_{mod} =$  (a) 5403.375 MHz, (b) 5404.217 MHz, and (c) 5406.270 MHz. The inset shows the output pulses at each lasing wavelength obtained using a bandpass filter external to the laser.

wavelength obtained using a bandpass filter external to the laser. Throughout the tuning range, the average signal-to-noise ratio for each wavelength was greater than 24 dB and the total average output power of both wavelengths ranges from 23  $\mu\text{W}$  – 41  $\mu\text{W}$ . When the RF signal was shut off, the laser output spectrum changed completely and the laser no longer emitted the same two wavelengths.

In order to further characterize the pulses, the lasing wavelengths were filtered using a tunable bandpass filter (3 dB bandwidth about 0.4 nm) external to the laser. The characteristics of the output pulses are summarized in Fig. 5.5: the pulse widths vary from 35 ps to 61 ps, the 3 dB bandwidths from 0.08 nm – 0.16 nm, and the time bandwidth products range from 0.5 to 1.0 indicating that the pulses are chirped.

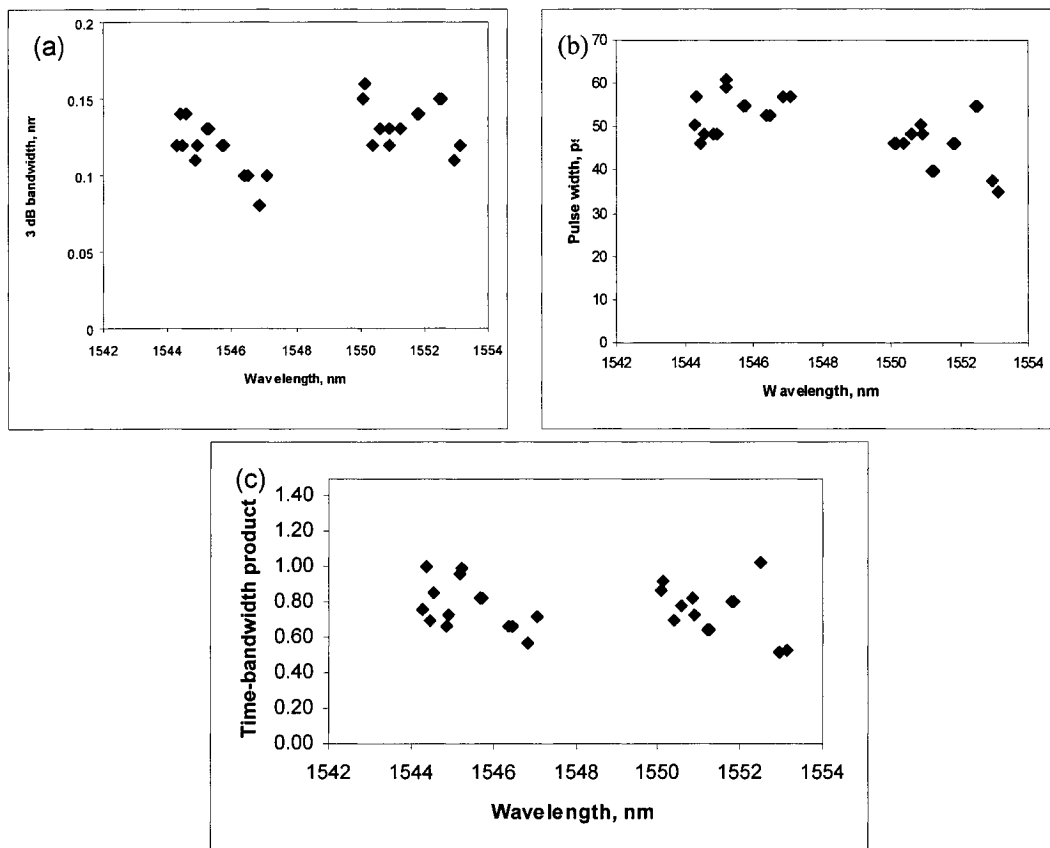


Fig. 5.5 Output pulse characteristics of the laser: (a) 3 dB bandwidth, (b) pulse width, (c) time-bandwidth product.

In this section, we have successfully demonstrated a simple implementation for an electrically tunable, dual-wavelength actively mode-locked fiber ring laser with SOA and intracavity modulator where the key component is a superimposed linearly chirped FBG. The gratings offer the flexibility for achieving a specific separation between the lasing wavelengths as well as a given tuning range and rate.

## 5.3 All-optical mode-locking

### 5.3.1 Operation description

Based on success of all-optically mode-locked for single wavelength operation, we can try the multi-wavelength operation. The schematic of our all-optically mode-locked SFRL is the same as that shown in Fig. 4.10 except that the SI-LCFBGs in Fig. 5.2 is used.

### 5.3.2 Experiments and results

Again using superimposed gratings allows us to define multiple (in this case 2) lasing wavelengths (one from each grating). The nature of the gratings ensures that the two lasing wavelengths nominally have the same cavity length which simplifies the requirements for multi-wavelength operation since for a given modulation frequency  $f_{mod}$ , each lasing wavelength will be self-tuned.

We first fix the modulation frequency at  $f_{mod} = 5259.835$  MHz and investigate the output pulse characteristics at both lasing wavelengths (1545.1 nm and 1551.1 nm) as a function of SOA bias current, control signal power, and control signal wavelength, as shown in Fig. 5.6.

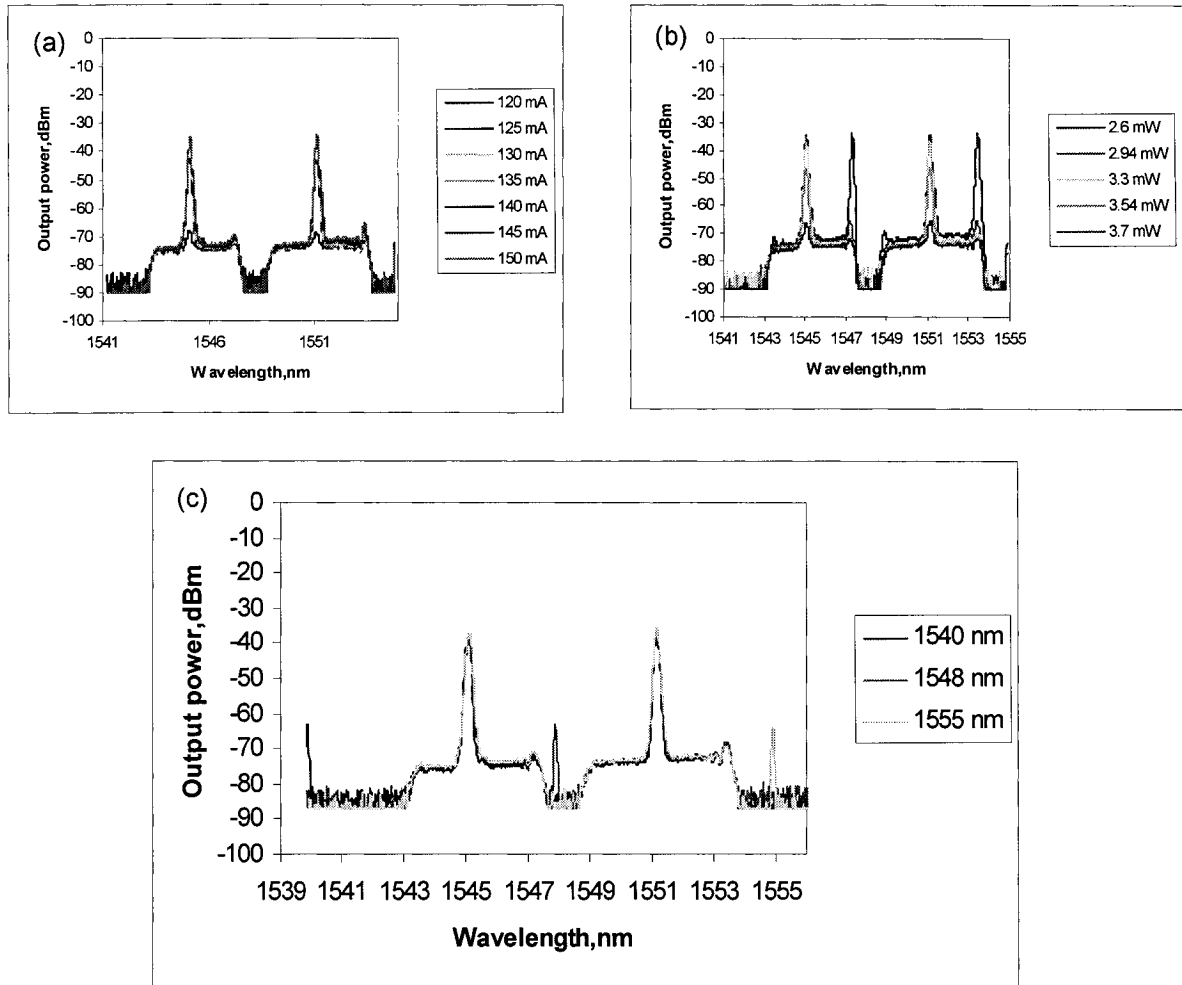


**Fig. 5.6** Output spectral characteristics under (a) different bias currents, (b) different control signal powers, and (c) different control signal wavelengths.

As we vary the parameters, we find that the output pulses at both wavelengths have similar characteristics. The optimum operating conditions which yield the best time bandwidth products are  $I_{SOA} = 135$  mA, a control signal wavelength of 1555 nm, and  $P_{avg}^{control} = 3.3$  mW. For these parameters, Fig. 5.7 (a) shows the wavelength tuning characteristics as  $f_{mod}$  is varied from 5257.4 MHz to 5270.7 MHz.

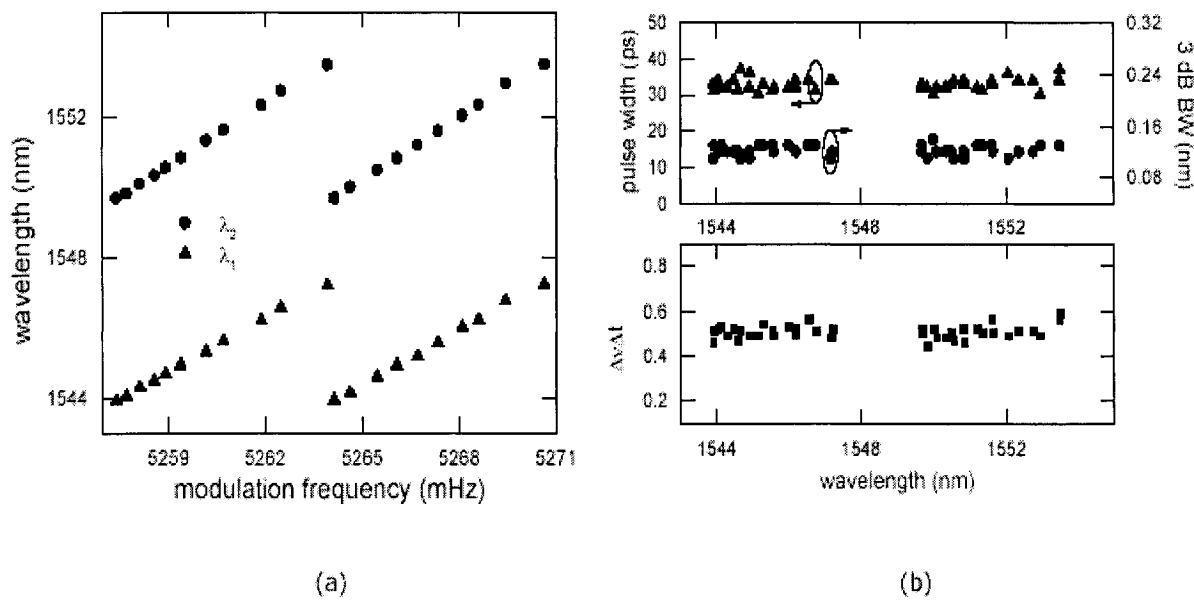
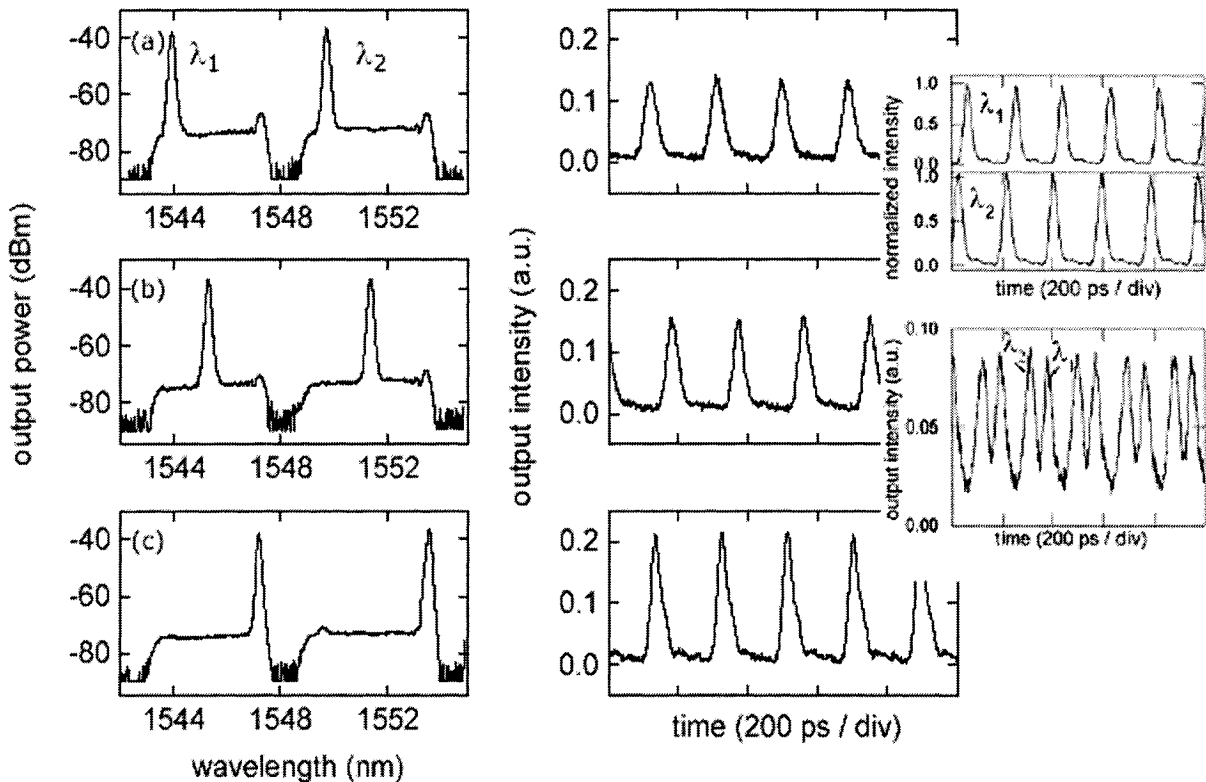


Fig. 5.7 (a) Tuning and (b) output pulse characteristics of the mode-locked SFRL using SI-LCFBGs.

Again during tuning, only modulation frequency ( $f_{mod}$ ) was changed while all other settings were kept constant. The tuning ranges are 3.3 nm and 3.8 nm  $\lambda_1$  and  $\lambda_2$ , respectively, and the corresponding tuning rates are 0.52 nm/MHz and 0.6 nm/MHz. Both wavelengths can be simultaneously tuned with a wavelength separation that varies from 5.8 nm to 6.3 nm (which corresponds approximately to the wavelength separation of the FBGs and is not constant since the tuning rates are not identical). The fundamental frequency of the laser cavity was determined to be  $\approx 6.7$  MHz for both wavelengths.

Fig. 5.8 shows sample traces of the output spectrum and output pulse envelope corresponding to both wavelengths for different modulation frequencies. The insets show the output pulses after a tunable bandpass filter is used external to the laser to isolate each wavelength as well as the waveform after propagation through 7.44 km of SMF. As before, to character further the pulses at each wavelength, we use a tunable BPF external to the laser cavity. The pulse widths vary from 30 ps – 37 ps, the 3 dB bandwidths from

0.11 nm – 0.14 nm, and the time bandwidth products range from 0.44 – 0.59, again indicating that the pulses are slightly chirped, see Fig. 5.7 (b). Over the tuning range, the average signal-to-noise ratio for each lasing wavelength is above 35 dB and the total average output power of both wavelengths ranges from 33  $\mu$ W – 51  $\mu$ W. Note that by reversing the grating orientation, similar output pulse characteristics are obtained, but with an opposite tuning rate. In this case, the tuning rates for  $\lambda_1$  and  $\lambda_2$  are -0.57 nm/MHz and -0.67 nm/MHz, respectively. When no control signal was injected into the laser cavity, we did not obtain any output lasing signal, as shown in Fig. 5.9.



**Fig. 5.8** Typical spectral and temporal characteristics of laser output with dual-wavelength operation for  $f_{mod}$  = (a) 5257.426 MHz, (b) 5260.166 MHz, and (c) 5263.939 MHz. The insets show the output pulses at each lasing wavelength obtained using a bandpass filter external to the laser and the output waveform after propagation through 7.44 km of SMF.

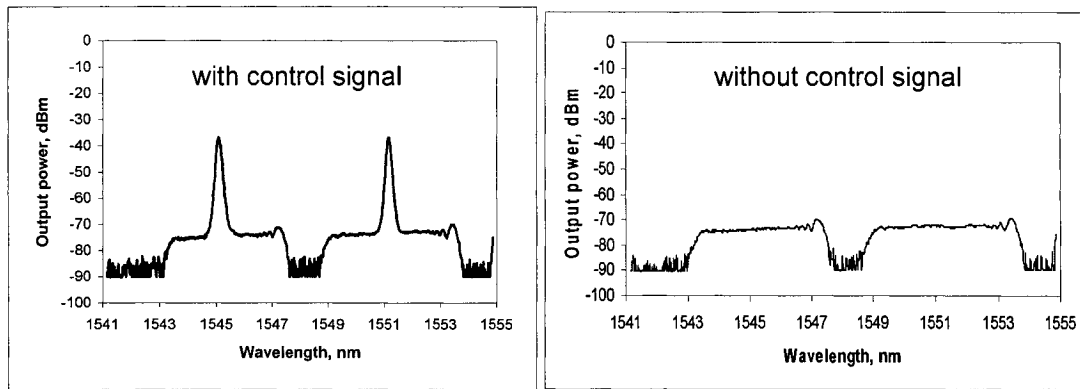


Fig. 5.9 Output spectral change under with and without the control signal.

## 5.4 Discussion and summary

We have successfully demonstrated the generation of picosecond pulses in both intracavity modulator and an all-optically mode-locked. We obtain multi-wavelength output using SI-LCFBGs. In both approaches, the output wavelengths can be tuned electrically by varying the frequency of the RF control signal. Both spectra and output waveforms can be recorded simultaneously. Moreover, the pulse trains are all stable and no mode hopping can be observed when the laser has been mode-locked for four hours. The use of SI-LCFBGs offers the flexibility for achieving a specific separation between the lasing wavelengths as well as the tuning range and rate. We provide a simple means for achieving multi-wavelength, dispersion-tuned operation. In contrast with multi-wavelength EDFLs [5.1], we have obtained dual-wavelength operation with narrower wavelength spacing and using a more compact and simpler implementation. The use of compact SOA modules allows for stable, multi-wavelength emission at room temperature and for operation at any wavelength band. As a result, we are not constrained to the C- and L-bands as with EDFLs. Furthermore, operation at multiple wavelengths with narrow

wavelength separation can be achieved, i.e. we are not constrained by the homogenous broadened linewidth of the EDF gain medium.

When compared with the intracavity modulator approach, the all-optically mode-locked approach uses the SOA as both the gain medium and the mode-locker. Again as in the single-wavelength instance, the all-optical mode-locking approach results in shorter pulses that are closer to the transform-limit and exhibit higher SNR.

## **References:**

[5.1] S. Li and K. T. Chan, "Electrical wavelength tunable and multiwavelength actively mode-locked fiber ring laser," *Appl. Phys. Lett.*, 72, 16, pp.1954-1956, 1998.

## Chapter 6

### Conclusion and future work

In this thesis, we focus on demonstrating novel designs of high performance optical sources that generate short pulses at multiple wavelengths with wavelength tunable capacity. We have presented systematic studies of semiconductor fiber ring lasers (SFRLs). The two types of mode-locked SFRLs structures are investigated, while approaches involving intracavity modulator and all-optical control technique have been designed and measured. In both cases, linearly chirped fiber Bragg gratings (LCFBGs) work as the key component to sustain operation.

We first introduce some basic properties of fiber lasers and details on mode-locking operation and then describe and compare SFRLs and EDFLs. Then we discuss the basic properties of SOAs and render an up-to-date survey on various mode-locked SFRLs.

Based on the mode-locked SFRL single wavelength operation, two approaches of electrically tunable mode-locked SFRLs, one using an intracavity electro-optic modulator and the other an injected optical control signal, are proposed and experimentally characterized. In contrast with EDFLs, the use of the SOAs in FRL allows for compact and relatively low-cost applications with stable room temperature operation. We design and successfully demonstrate of a novel tunable all-optically mode-locked SFRL. Compared with the intracavity modulator approach, this approach uses the SOA as both the gain medium and the mode-locker. The output wavelength can be tuned electrically by varying the frequency of the injected control signal. Moreover, the tuning range and rate are determined by the grating bandwidth and chirp respectively. In our experiments, the tuning range was limited only by the available grating. Based on our experimental results,

it can generate close to the transform-limit pulses with high SNR and reasonable average output power.

We also investigate the multi-wavelength operation of mode-locked SFRLs in both the intracavity modulator and the all-optical control modes. We successfully demonstrate the first tunable, multi-wavelength all-optically mode-locked SFRL using SI-LCFBGs. In addition to the merits of the single-wavelength operation, the key component is the superimposed grating that ensures that the lasing wavelengths nominally have the same cavity length so that specific conditions between modulation frequency and cavity dispersion do not need to be satisfied to ensure proper multi-wavelength operation. Moreover, the wavelength spacing is set by the spectral separation of the superimposed gratings. Again, as in the single-wavelength operation case, the all-optical mode-locking approach results in short pulses that are near the transform-limit and exhibit better performance than some previously reported results.

As the above proposed schemes work all-optically, they are promising in applications such as all-optical sources for next generation all-optical network and photonic devices testing and characterization, as well as in optical instrumentation, time-resolved spectroscopy, and optical sensors, etc.

In the future, the numerical modeling and simulation on mode-locked SFRLs operations and a more thorough study on impacts of environmental parameters are needed. Other issues that need to be explored include the maximum output power that such configurations could support and the number of wavelengths that the structure could stably generate. Furthermore, we will develop more designs of all-optical multi-wavelength SFRLs by using sampled FBGs and programmable high-birefringence fiber

loop mirrors. The results presented herein provide the basis for these further investigations.

## Appendix A

### 1. Fiber Bragg grating basic [A.1]

An FBG consists of a periodic modulation of the refractive index in the longitudinal direction of the core of an optical fiber [A.2] –[A.6]. If we consider a single-mode fiber, then light guided in the fundamental  $LP_{01}$  mode will be reflected by the refractive index variation. Under the Bragg condition, the reflected light will add coherently, otherwise, it will become progressively out of phase with each reflection and eventually cancel out. In other words, if the Bragg condition is satisfied, there is a coherent reflection otherwise light is mostly transmitted. Fig. A.1 illustrates the principle of operation of an FBG.

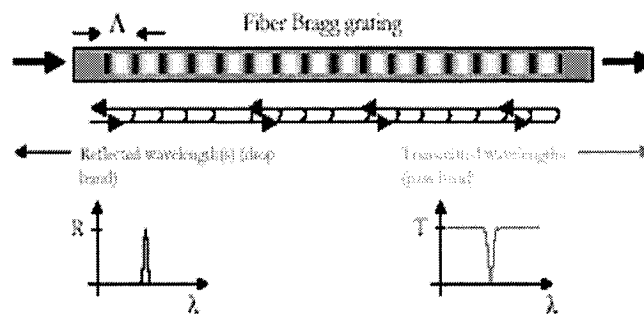


Fig. A.1 Schematic representation and principle of operation of a fiber Bragg grating. [A.1]

An FBG is a diffraction grating. Light comprising distinct wavelengths incident at an arbitrary angle on a diffraction grating, assumed to have a sinusoidal profile with period  $\Lambda$ , will be diffracted into wavelength specific angles (see Fig. A.2) according to the relation [A.7] where  $\theta_1$  is the angle of the incident wave,  $\theta_2$  is the angle of the diffracted wave,  $m$  is the order of diffraction,  $n$  is the refractive index of medium light is propagating in, and  $\lambda$  is the wavelength. Bragg gratings are those that couple modes

traveling in opposite directions; in contrast, long-period gratings that couple modes traveling in the same direction [A.8]. If the Bragg grating couples counter-propagating waves have the same mode, then  $\theta_1 = \theta_2$ . Since the propagation constant of a wave in the fiber is given by  $\beta = \frac{2\pi}{\lambda} n_{eff} = \frac{2\pi}{\lambda} n_{co} \sin \theta$  ( $n_{eff}$  and  $n_{co}$  are respectively the effective refractive index of the propagating mode and the fiber core), the diffraction equation (1) becomes

$$\beta_2 = \beta_1 + m \frac{2\pi}{\Lambda} \quad (2)$$

Although higher order diffraction orders can exist, the dominant contributions for an FBG arise from first order diffraction, say  $m=-1$ . Therefore,

$$\beta_2 = \beta_1 - \frac{2\pi}{\Lambda} \quad (3)$$

If we identify negative values of  $\beta$  as those that propagate in the negative  $z$ -direction, then for  $\beta_2 = -\beta_1$  so that the resonant wavelength of a grating having a period  $\Lambda$  is

$$\lambda_{Bragg} = 2n_{eff} \Lambda \quad (4)$$

the well-known result for Bragg reflection. In short, the Bragg reflection condition is a statement of conservation of momentum as illustrated in Fig. A.3.

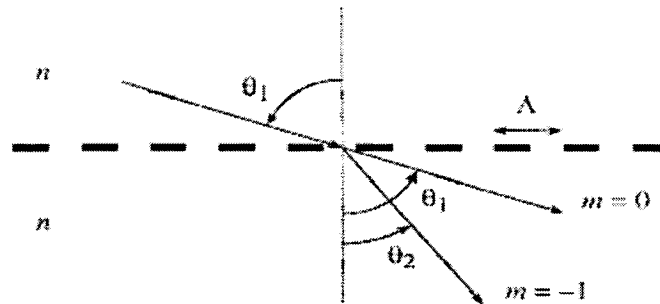


Fig. A.2 Diffraction of a light wave by a grating. [A.7]

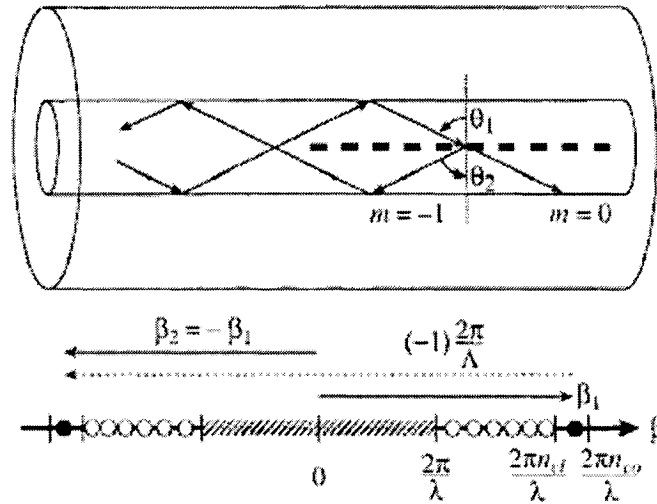


Fig.A.3 Ray-optic illustration of core-mode Bragg reflection by a fiber Bragg grating. [A.7]

## 2. Chirped Bragg gratings [A.9]

One of the most promising Bragg grating structures is the chirped Bragg grating. As shown schematically in Fig. A.4, this grating has a monotonically varying period.

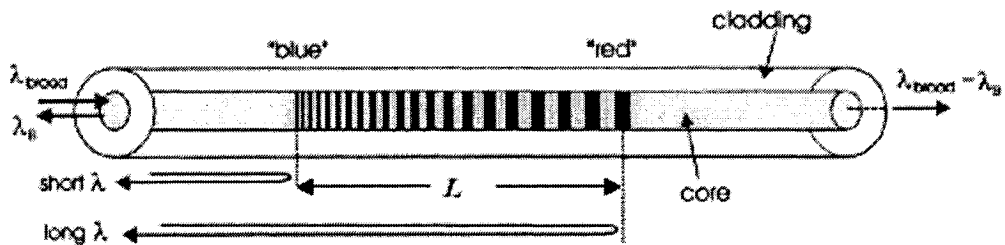


Fig. A.4 A schematic diagram of a chirped grating with an aperiodic pitch. For forward-propagating light as shown, long wavelengths travel further into gratings before being reflected. [A.9]

There are some characteristic properties offered by monotonically varying the period of gratings that are considered advantages for specific applications in telecommunications and sensor technology, such as dispersion compensation and the stable synthesis of multi-wavelength sources [A.10],[A.11]. These types of gratings can be realized by axially

varying either the period of the grating  $\Lambda$  or the refraction index of the core or both. From (4) we have

$$\lambda_{Bragg}(z) = 2n_{eff}(z)\Lambda(z) \quad (5)$$

The simplest type of chirped grating structure is one where the variation in the grating period is linear:

$$\Lambda(z) = \Lambda_0 + \Lambda_1 z \quad (6)$$

where  $\Lambda_0$  is the starting period and  $\Lambda_1$  is the linear change along the length of the grating.

Thus, one may consider such a grating structure made up of a series of smaller length uniform Bragg gratings increasing in period. If such a structure is designed properly, one may realize a broadband reflector. Typically, the linear chirped grating has associated with it a chirped value/unit length ( $\Lambda_1$ ) and the starting period. Chirped gratings have been written in optical fibers using various methods.

In today's optical long-haul telecommunication systems, the main limitation to data transmission is pulse broadening caused by chromatic dispersion. The pulse broadening can be eliminated by incorporating an element have a dispersion of opposite sign and equal magnitude to that of the optical fiber link. Traditionally, optical fibers displaying the correct negative dispersion characteristics have been incorporated into telecom lines. However, the modal field diameter of the compensating fiber rarely matches that of the standard guide; therefore, splicing between different fiber sections requires pre-fusion preparation. This can be achieved with a single fusion-splicing device; however, it is advantageous if this can be avoided. In a chirped grating the resonant frequency is a linear function of the axial position along the grating, so that different frequencies present in the pulse are reflected at different points and thus acquire different delay times (Fig.

A.4). It is now possible to compress temporally broadened pulses. Fig. A.5 (a) gives examples of the chirped grating transmission and reflection profiles [A.12]; an example of the group delay as a function of wavelength for a chirped grating is shown in Fig. A.5 (b) [A.13].

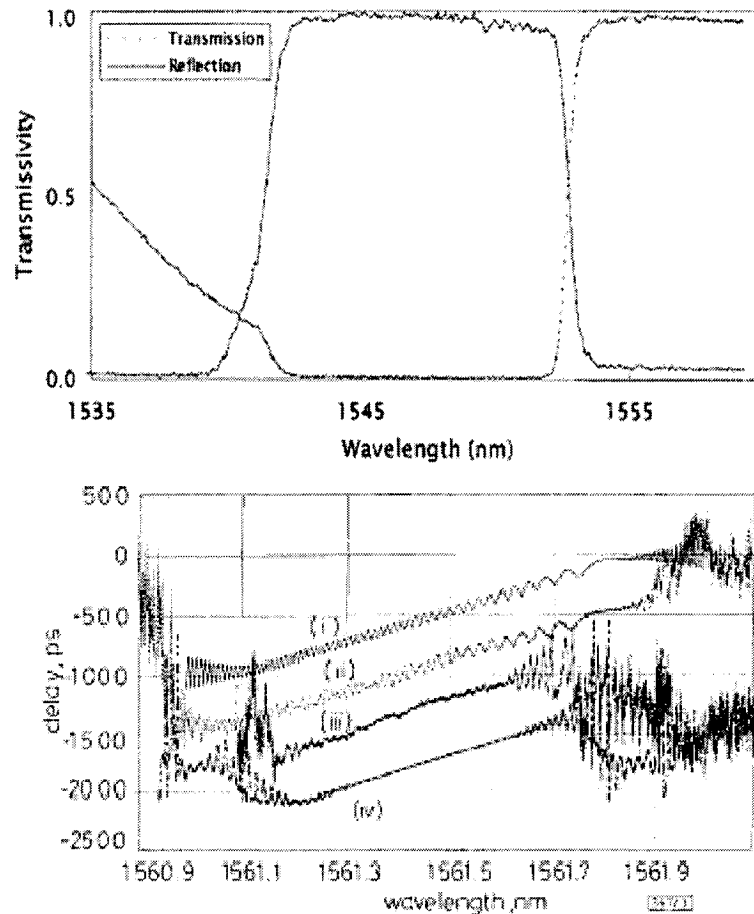
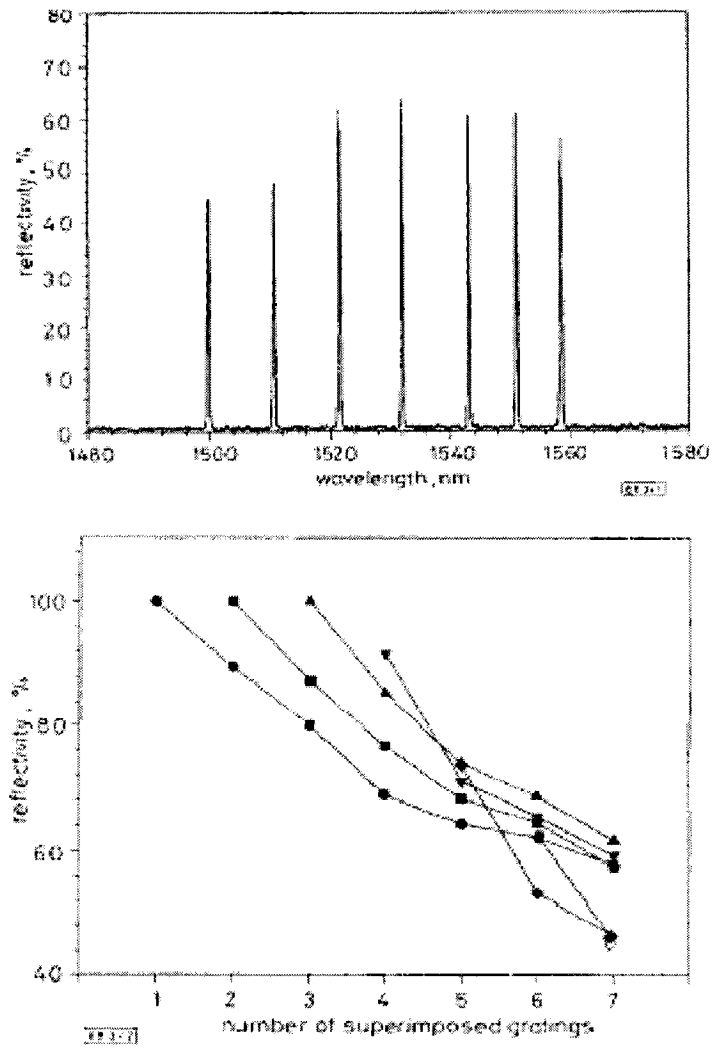


Fig. A.5 (a) Typical transmission and reflection profiles of a chirped Bragg grating [A.12]; (b) Group delay for unapodized and apodized chirped grating [A.13]

### 3. Superimposed Bragg gratings [A.9]

It was in 1994 that researchers demonstrated the writing of several Bragg gratings at the same location on an optical fiber [A.14]. This is of interest as a device in fiber communications and sensor systems, because multiple Bragg gratings at the same

location basically perform a comb function that is ideally suited for multiplexing and demultiplexing signals. All the gratings are written at the same location of the fiber, which makes this approach well suited to the optical integrated technology, where the issues of size is always a concern. This can also be used for material detection where the multiple Bragg lines can be designed to match the signature frequencies of a given material. A narrow linewidth KrF excimer laser was used in an interferometric setup to inscribe the different Bragg gratings on the same fiber location (Fig. A.6). The fiber was first hydrogen loaded to enhance its photosensitivity. Fig. A.6 shows the reflectivity for seven superimposed Bragg gratings. The first grating was written at 1550.05 nm and reached a reflectivity of : 100% within 15 seconds of UV exposure and had a linewidth of 0.25nm. After adjusting the interferometer to write at a different Bragg wavelength, the second grating was written at 1542.6 nm with approximately the same characteristics. Each time a new grating was inscribed, the reflectivity of the existing gratings was reduced. Nevertheless, even after superimposing five gratings, the individual grating reflectivities were higher than 60%. Additionally, the center wavelength of the existing Bragg gratings shifted to longer wavelengths each time a new grating was inscribes because of the change of the effective index of refraction. The shift in wavelength of the first grating after writing all seven corresponds to an effective index of refraction increase of  $0.86 \times 10^{-3}$ .



**Fig. A.6** Superimposed multiple Bragg gratings at the same location on photosensitive optical fiber. The plot on the lower shows reflectivities for each of the Bragg gratings, as a function of the number of gratings, superimposed on the same location [A.14].

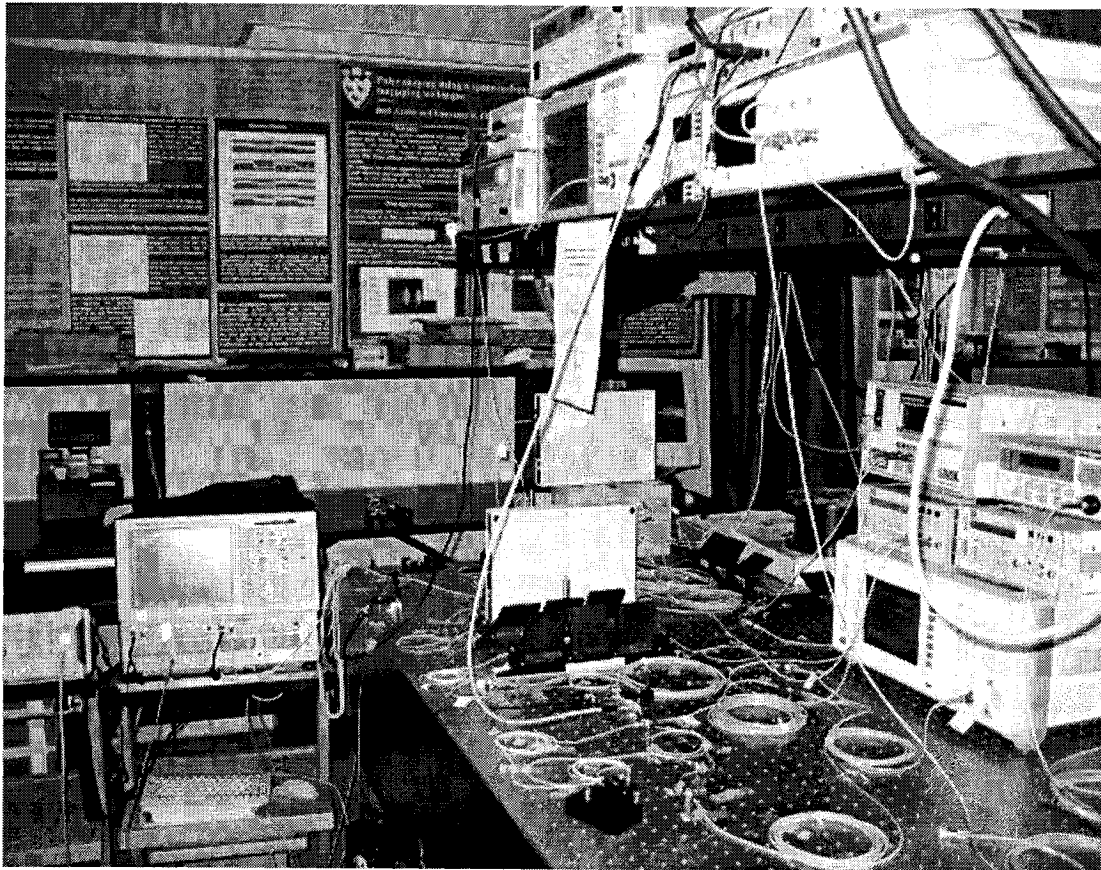
## References:

- [A.1] L.R. Chen, "Application of compound fiber Bragg grating structures in lightwave communications," Ph.D. Thesis, 2000.
- [A.2] K.O.Hill, B. Malo, F. Bilodeau, and D.C. Johnson, "Photosensitivity in optical fibers," *Annu. Rev. Materi. Sci.*, 23, pp. 125-157, 1993.
- [A.3] K.O.Hill, Y.Fujii, D.C. Johnson, and B.S. Kawasaki, "Photosensitivity in optical waveguides: application to reflection filter fabrication," *Appl. Phys. Lett.*, 32, 10, pp. 647-649, 1978.
- [A.4] B.S. Kawasaki, K.O. Hill, D.C. Johnson, and Y. Fuji, "Narrow-band Bragg reflectors in optical fibers," *Opt. Lett.*, 3, 2, pp.66-68, 1978.
- [A.5] A. Otonous, "Fiber Bragg gratings," *Rev. Sci. Instrum.*, 68, 12, pp.4309-4340, 1997.
- [A.6] I. Bennion, J.A.R. Williams, L.Zhang, K.sugden, and N.J. Doran, "UV-written in-fiber Bragg gratings," *Opt. Quantum Electron.*, 28, pp.93-135, 1996.
- [A.7] T.Erdogan, "Fiber grating spectra," *IEEE/OSA J. Lightwave Technol.*, 15, 8, pp.1277-1294, 1997.
- [A.8] A.M. Vengsarkar, P.J.Lemaire, J.B. Judkins, V. Bhatia, T.Erdogan, and J.E. Sipe, "Long-period fiber gratings as band-rejection filters," *IEEE/OSA J. Lightwave Technol.*, 14, 1, pp.58-65, 1996.
- [A.9] A. Othonos, Fiber Bragg Gratings: Fundamentals and Applications in Telecommunications and Sensing, Artech House, 1999.
- [A.10] Ouellette, F., "Dispersion cancellation using linearly chirped Bragg grating filters in optical waveguides," *Optics Letters*, 12, pp. 847-849, 1987.
- [A.11] Brady, G.P., et al. "Extended range coherence tuned, dual wavelength interferometry using a superfluorescent fiber source and chirped fiber Bragg gratings," *Optics Communications*, 134, pp.341-346, 1997.
- [A.12] Sugden, K., et al. "Fabrication and characterization of bandpass filters based on concatenated chirped fiber gratings," *IEEE/OSA J. Lightwave Technol.*, 15, 8, pp.1424-1432, 1997.
- [A.13] Kashyap, R., A. Shwanton, and D.J. Armes, "Simple technique for apodising chirped and unchirped fiber Bragg gratings," *Electron. Letters*, 32, pp.1226-1228, 1996.

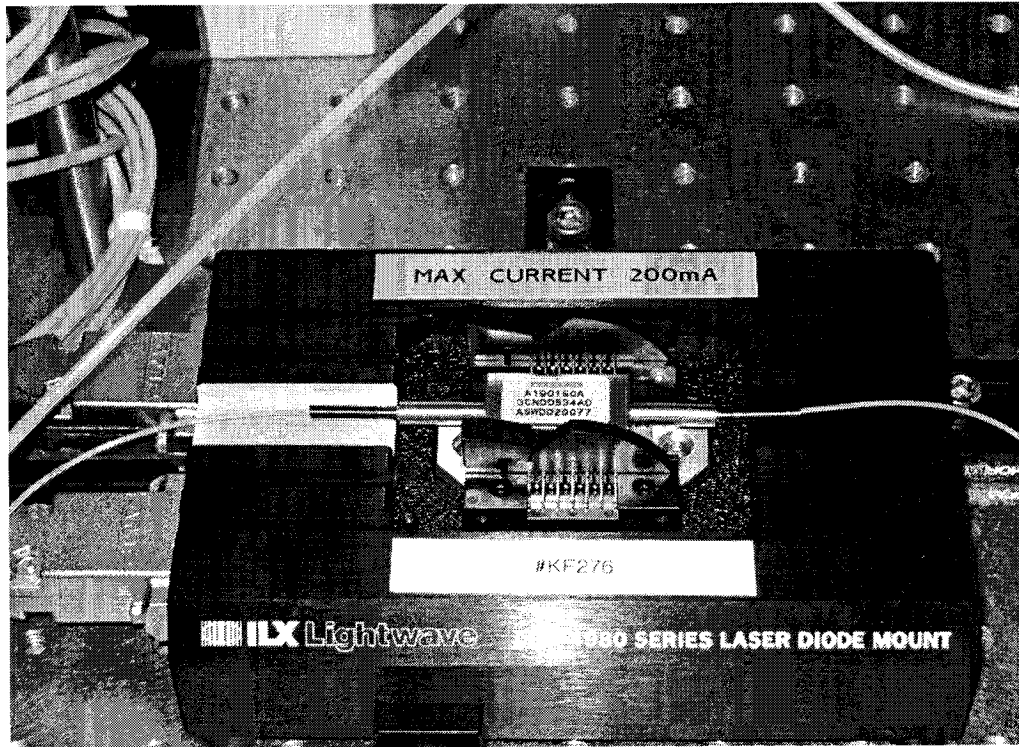
[A.14] Othonos, A., X. Lee, and R.M. Measures, "Superimposed multiple Bragg gratings," *Electronics Letters*, 30, pp.1972-1973, 1994.

## Appendix B

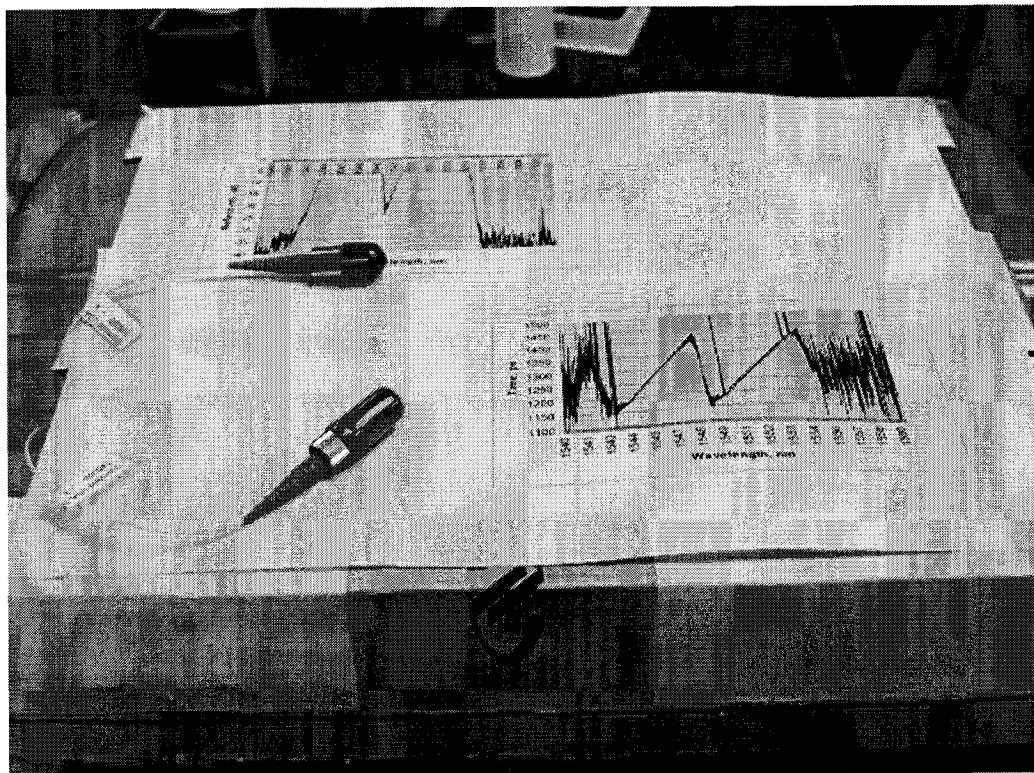
### Photographs of the experimental setup



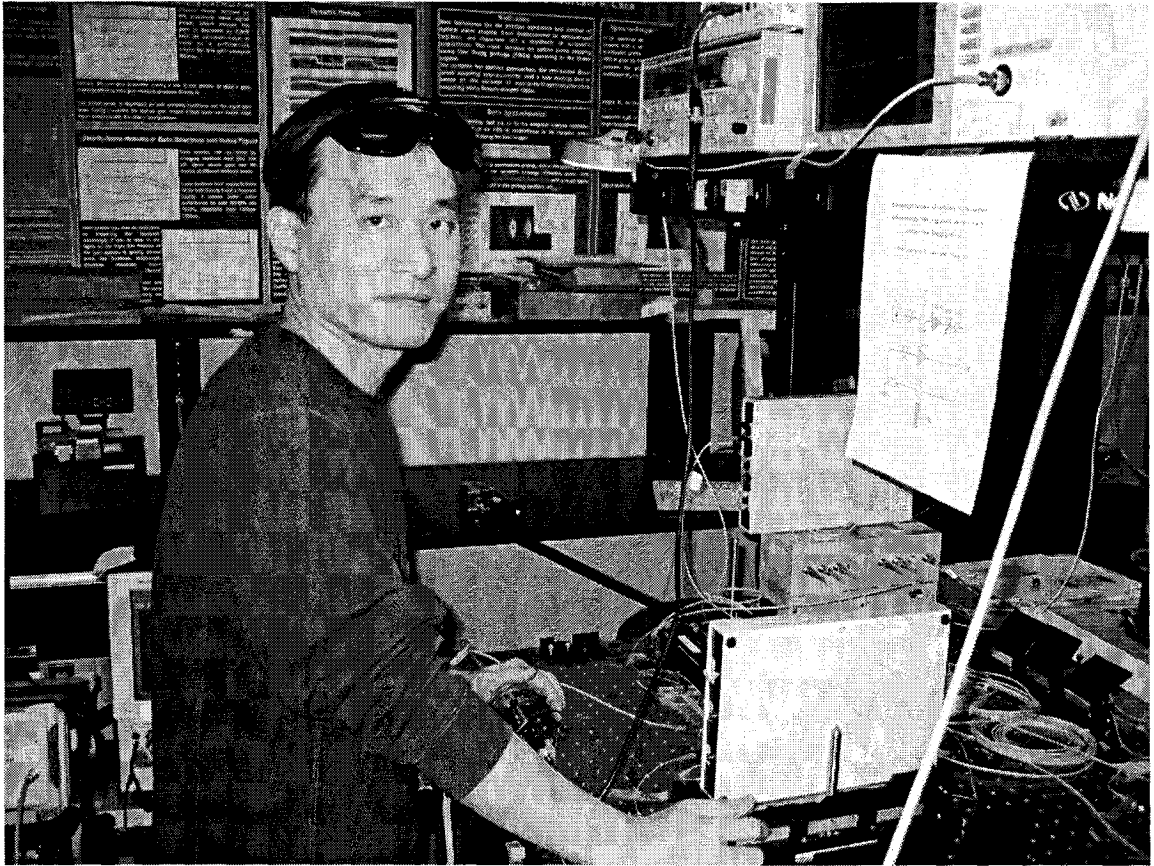
The mode-locked SFRLs experimental setup.



The A1901 SOA module.



The SI-LCFBGs.



The author tweaking his setup.